ISSN 1948-5182 (online)

World Journal of *Hepatology*

World J Hepatol 2024 April 27; 16(4): 490-660

Published by Baishideng Publishing Group Inc

World Journal of Hepatology

Contents

Monthly Volume 16 Number 4 April 27, 2024

EDITORIAL

REVIEW

ORIGINAL ARTICLE

Case Control Study

Retrospective Cohort Study

World Journal of Hepatology

Monthly Volume 16 Number 4 April 27, 2024

Contents

World Journal of Hepatology

Monthly Volume 16 Number 4 April 27, 2024

Contents

ABOUT COVER

Peer Reviewer of *World Journal of Hepatology*, Somchai Amornyotin, MD, Professor, Staff Physician, Department of Anesthesiology and Siriraj Gastrointestinal Endoscopy Center, Faculty of Medicine, Siriraj Hospital, Mahidol University, Bangkok 10700, Thailand. somchai.amo@mahidol.ac.th

AIMS AND SCOPE

The primary aim of *World Journal of Hepatology* (*WJH*, *World J Hepatol*) is to provide scholars and readers from various fields of hepatology with a platform to publish high-quality basic and clinical research articles and communicate their research findings online.

WJH mainly publishes articles reporting research results and findings obtained in the field of hepatology and covering a wide range of topics including chronic cholestatic liver diseases, cirrhosis and its complications, clinical alcoholic liver disease, drug induced liver disease autoimmune, fatty liver disease, genetic and pediatric liver diseases, hepatocellular carcinoma, hepatic stellate cells and fibrosis, liver immunology, liver regeneration, hepatic surgery, liver transplantation, biliary tract pathophysiology, non-invasive markers of liver fibrosis, viral hepatitis.

INDEXING/ABSTRACTING

The *WJH* is now abstracted and indexed in PubMed, PubMed Central, Emerging Sources Citation Index (ESCI), Scopus, Reference Citation Analysis, China Science and Technology Journal Database, and Superstar Journals Database. The 2023 Edition of Journal Citation Reports® cites the 2022 impact factor (IF) for *WJH* as 2.4.

RESPONSIBLE EDITORS FOR THIS ISSUE

Production Editor: *Yi-Xuan Cai*; **Production Department Director:** *Xiang Li*; **Cover Editor:** *Xiang Li*.

NAME OF JOURNAL
World Journal of Hepatology

ISSN
ISSN 1948-5182 (online)

LAUNCH DATE
October 31, 2009

FREQUENCY
Monthly

EDITORS-IN-CHIEF
Nikolaos Pyrsopoulos, Ke-Qin Hu, Koo Jeong Kang

EXECUTIVE ASSOCIATE EDITORS-IN-CHIEF
Shuang-Suo Dang

EDITORIAL BOARD MEMBERS
https://www.wjgnet.com/1948-5182/editorialboard.htm

PUBLICATION DATE
April 27, 2024

COPYRIGHT
© 2024 Baishideng Publishing Group Inc

PUBLISHING PARTNER
Department of Infectious Diseases, the Second Affiliated Hospital of Xi'an Jiaotong University

INSTRUCTIONS TO AUTHORS
https://www.wjgnet.com/bpg/gerinfo/204

GUIDELINES FOR ETHICS DOCUMENTS
https://www.wjgnet.com/bpg/GerInfo/287

GUIDELINES FOR NON-NATIVE SPEAKERS OF ENGLISH
https://www.wjgnet.com/bpg/gerinfo/240

PUBLICATION ETHICS
https://www.wjgnet.com/bpg/GerInfo/288

PUBLICATION MISCONDUCT
https://www.wjgnet.com/bpg/gerinfo/208

POLICY OF CO-AUTHORS
https://www.wjgnet.com/bpg/GerInfo/310

ARTICLE PROCESSING CHARGE
https://www.wjgnet.com/bpg/gerinfo/242

STEPS FOR SUBMITTING MANUSCRIPTS
https://www.wjgnet.com/bpg/GerInfo/239

ONLINE SUBMISSION
https://www.f6publishing.com

PUBLISHING PARTNER's OFFICIAL WEBSITE
http://2yuan.xjtu.edu.cn/Html/Departments/Main/Index_21148.html

© 2024 Baishideng Publishing Group Inc. All rights reserved. 7041 Koll Center Parkway, Suite 160, Pleasanton, CA 94566, USA
E-mail: office@baishideng.com https://www.wjgnet.com

World Journal of Hepatology

Submit a Manuscript: https://www.f6publishing.com

World J Hepatol 2024 April 27; 16(4): 566-600

DOI: 10.4254/wjh.v16.i4.566

ISSN 1948-5182 (online)

REVIEW

Molecular mechanism of nanomaterials induced liver injury: A review

Sanjib Kumar Das, Koushik Sen, Biswatosh Ghosh, Nabanita Ghosh, Krishnendu Sinha, Parames C Sil

Specialty type: Toxicology

Provenance and peer review: Invited article; Externally peer reviewed.

Peer-review model: Single blind

Peer-review report's scientific quality classification
Grade A (Excellent): A
Grade B (Very good): B
Grade C (Good): C
Grade D (Fair): 0
Grade E (Poor): 0

P-Reviewer: Qu S, China; Rasool A, Pakistan; Tao M, China

Received: December 28, 2023
Peer-review started: December 28, 2023
First decision: January 30, 2024
Revised: February 5, 2024
Accepted: March 19, 2024
Article in press: March 19, 2024
Published online: April 27, 2024

Sanjib Kumar Das, Koushik Sen, Krishnendu Sinha, Department of Zoology, Jhargram Raj College, Jhargram 721507, India

Biswatosh Ghosh, Department of Zoology, Bidhannagar College, Kolkata 700064, India

Nabanita Ghosh, Department of Zoology, Maulana Azad College, Kolkata 700013, India

Parames C Sil, Department of Molecular Medicine, Bose Institute, Calcutta 700054, India

Corresponding author: Krishnendu Sinha, PhD, Assistant Professor, Department of Zoology, Jhargram Raj College, Raj College Road, Jhargram 721507, India.
dr.krishnendusinha@gmail.com

Abstract

The unique physicochemical properties inherent to nanoscale materials have unveiled numerous potential applications, spanning beyond the pharmaceutical and medical sectors into various consumer industries like food and cosmetics. Consequently, humans encounter nanomaterials through diverse exposure routes, giving rise to potential health considerations. Noteworthy among these materials are silica and specific metallic nanoparticles, extensively utilized in consumer products, which have garnered substantial attention due to their propensity to accumulate and induce adverse effects in the liver. This review paper aims to provide an exhaustive examination of the molecular mechanisms underpinning nanomaterial-induced hepatotoxicity, drawing insights from both *in vitro* and *in vivo* studies. Primarily, the most frequently observed manifestations of toxicity following the exposure of cells or animal models to various nanomaterials involve the initiation of oxidative stress and inflammation. Additionally, we delve into the existing *in vitro* models employed for evaluating the hepatotoxic effects of nanomaterials, emphasizing the persistent endeavors to advance and bolster the reliability of these models for nanotoxicology research.

Key Words: Nanoparticles; Hepatotoxicity; Oxidative stress; Inflammation; Autophagy

©The Author(s) 2024. Published by Baishideng Publishing Group Inc. All rights reserved.

Core Tip: This comprehensive review explores nanoparticle-induced hepatotoxicity, focusing on diverse nanomaterials (*e.g.*, silver nanoparticles, carbon nanotubes) and their impacts on hepatic function. It categorizes nanoparticles, discusses exposure routes, and highlights hepatotoxic mechanisms. The review emphasizes the need for comprehensive assessments, understanding, and responsible practices in nanotechnology to guide future research for the development of safer nanomaterials.

Citation: Das SK, Sen K, Ghosh B, Ghosh N, Sinha K, Sil PC. Molecular mechanism of nanomaterials induced liver injury: A review. *World J Hepatol* 2024; 16(4): 566-600
URL: https://www.wjgnet.com/1948-5182/full/v16/i4/566.htm
DOI: https://dx.doi.org/10.4254/wjh.v16.i4.566

INTRODUCTION

In the rapidly advancing field of nanotechnology, the utilization of nanomaterials has become widespread across various industries, promising groundbreaking applications in medicine, electronics, and environmental science. Among the myriad potential benefits, the unique physicochemical properties of nanoparticles (NPs) have enabled remarkable achievements, from targeted drug delivery systems to innovative diagnostic tools. However, this surge in nanomaterial applications has brought forth concerns regarding their safety, particularly in the context of hepatotoxicity[1]. This comprehensive review aims to delve into the intricate landscape of nanoparticle-induced hepatotoxicity, exploring the diverse range of nanomaterials and their impacts on hepatic function. We will navigate through recent findings on prominent nanomaterials, including silver nanoparticles, carbon nanotubes, quantum dots, and gold nanoparticles, shedding light on the complex mechanisms underlying their hepatotoxic effects[2-4]. By examining the interplay between nanoparticles and liver cells, such as hepatocytes and Kupffer cells, this review seeks to provide a nuanced understanding of the potential risks associated with nanomaterial exposure.

NPs are classified into four main groups based on structural morphology: organic, inorganic, carbon-based, and composite[1,5]. Organic nanoparticles, derived from compounds like proteins and lipids, exhibit non-toxic and biodegradable properties, making them suitable for drug delivery, imaging, biosensors, and cancer treatment[5,6]. Inorganic nanoparticles, including metal-based, metal oxide-based, ceramic, and semiconductor nanoparticles, offer tailored electrical, optical, and magnetic properties for applications in biomedical science, catalysis, and imaging[5,7]. Quantum dots, semiconductor nanoparticles with size-dependent optoelectronic properties, find applications in electronic and biomedical industries[8,9]. Carbon-based nanoparticles, such as graphene, fullerenes, and carbon nanotubes, demonstrate unique structural configurations and are utilized in electrical and photonic devices, biomedical sciences, and nanocomposites[10,11]. Composite nanoparticles integrate different components, leading to unique physical and chemical properties, with three main categories: simple hybrid, core or shell structured, and multifunctional quantum nanoparticles, applied in electronics, optoelectronics, and biomedical sciences[12].

To ensure the safety of NPs within the human body, understanding their exposure route is crucial[13-15]. NPs can be orally exposed through food, drinks, supplements, or nanomedicines, with absorption occurring in organs like the stomach and small intestine. Factors like size, charge, and concentration influence absorption, with NPs under 100 nm diameter taken up directly through endocytosis in the small intestine. Inhalation is another exposure route, with NPs deposited in different regions of the respiratory tract, potentially translocating to other organs. Elimination of NPs from the lungs is complex and depends on physicochemical properties. Dermal exposure, through cosmetics and medications, is facilitated by the skin's permeability to nanoscale particles. Skin penetration varies based on factors like particle size and skin condition. Overall, understanding exposure routes is vital for assessing NP-induced toxicity and ensuring their safe utilization.

Various NPs exert hepatotoxic effects, with silica nanoparticles (SiNPs) showing size-dependent liver injury, synergies with other toxins, and impacts on cholesterol biosynthesis. Nickel oxide nanoparticles (NiO-NPs), tungsten trioxide nanoparticles (WO3 NPs), and copper oxide nanoparticles (Nano-CuO) induce oxidative stress-related liver damage, apoptosis, and genotoxicity[2,16-18]. Integrative omics analyses identify key proteins and disrupted metabolic pathways in SiNP-induced hepatotoxicity[19]. Zinc oxide (ZnO-NPs), titanium dioxide (TiO2NPs), magnesium oxide (MgO-NPs), aluminum oxide (Al_2O_3NPs), chromium oxide (Cr_2O_3-NPs), and iron oxides (IONPs) exhibit diverse hepatotoxic mechanisms, including oxidative stress, endoplasmic reticulum (ER) stress, inflammation, and disruptions in metabolism [20-24] (Figures 1 and 2). Carbon nanotubes (CNTs) induce hepatotoxicity through inflammatory responses and oxidative stress, with variations in toxicity based on type and administration method[4]. Copper sulfide/cadmium sulfide nanoparticles (CuS/CdS-NPs), cobalt nanoparticles, and nanoclay particles also induce oxidative stress-mediated apoptosis and acute hepatotoxicity[25,26]. Various nanomaterials, such as nanocellulos, polystyrene nanoparticles, chitosan nanoparticles, hydroxyapatite nanoparticles, quantum dots, and gold nanoparticles, display hepatotoxicity through disrupted redox balance, altered metabolism, necrotic cell death, and impaired mitochondrial function[8,9,27-29]. The complexity of nanoparticle-induced hepatotoxicity highlights the need for comprehensive assessments and understanding for safe use.

In conclusion, this review not only synthesizes existing knowledge but also highlights critical gaps in understanding nanoparticle-induced hepatotoxicity. By proposing recommendations for future research, we aim to guide the scientific

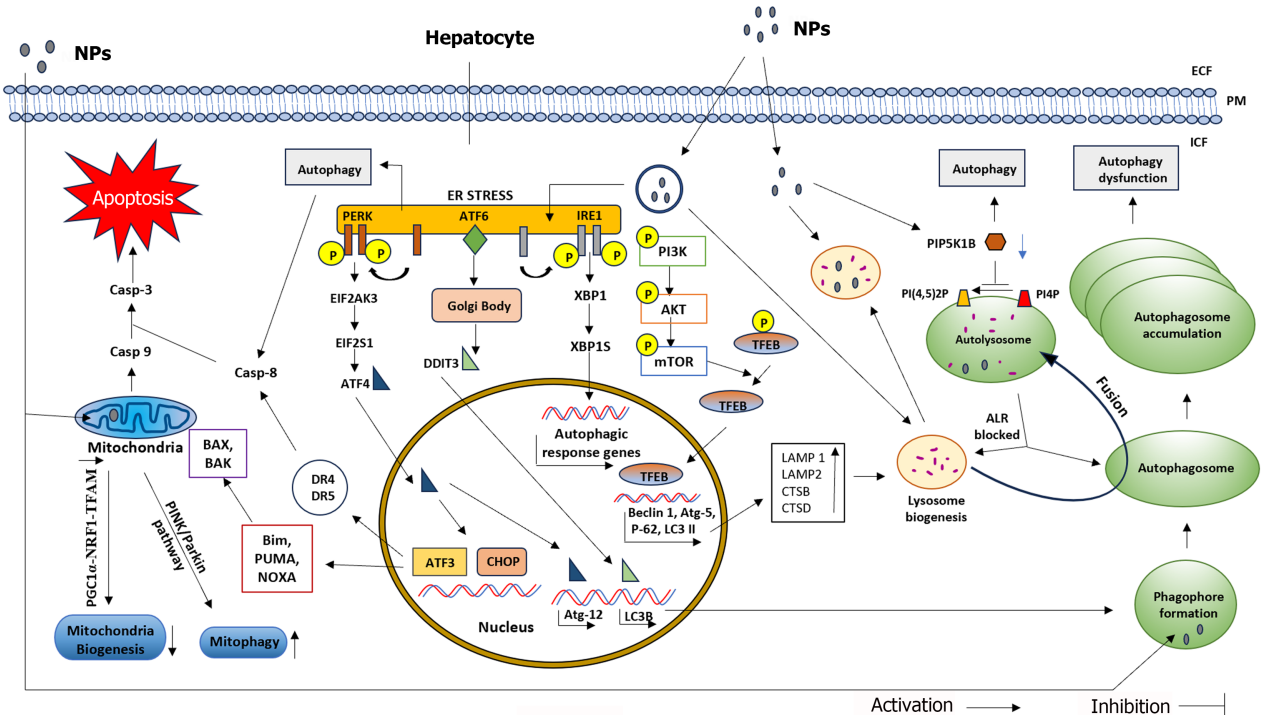

Figure 1 Diagram showing NPs induced hepatotoxicity through crosstalk between endoplasmic reticulum stress, oxidative stress, autophagic and apoptotic pathways. AKT: Protein kinase B; ALR: Autophagic lysosome reformation; ATF 3/4/6: Activating transcription factor 3/4/6; Atg 5/12: Autophagy related gene 5/12; BAK: Bcl-2 homologues antagonist/killer; Bax: Bcl-2-associated X-protein; Bim: Bcl-2 interacting mediator of cell death; Casp 3/8/9: Caspase 3/8/9; CHOP: C/EBP Homologous Protein; CTSB: Cathepsin B; CTSD: Cathepsin D; DDIT3: DNA damage inducible transcript 3; DR: Death receptor; ECF-Extra cellular fluid; EIF2AK3: Eukaryotic translation initiation factor 2-alpha kinase 3; EIF2S1: Eukaryotic translation initiation factor 2 subunit 1; ICF-Intra cellular fluid; IRE1: Inositol-requiring enzyme type-1; LAMP1/2: Lysosome-associated membrane protein 1/2; LC3B-Microtubule-associated proteins 1A/1B light chain 3B; LC3II: LC3-phosphatidylethanolamine conjugate; mTOR: Mammalian target of rapamycin; NOXA: Phorbol-12-myristate-13-acetate-induced protein 1; NPs- Nanoparticles; NRF1: Nuclear factor erythroid 2-related factor 1; P 62-Ubiquitin-binding protein p62; P: Phosphate; Parkin-Parkin RBR E3 ubiquitin-protein ligase; PERK: Protein kinase RNA like endoplasmic reticulum kinase; PGC1α: Peroxisome proliferator-activated receptor gamma coactivator 1 alpha; PI(4,5)2P: Phosphatidylinositol 4,5-bisphosphate; PI3K: Phosphatidylinositol 3-kinase; PI4P: Phosphatidylinositol 4-phosphate;PINK: PTEN induced kinase; PIP5K1B: Phosphatidylinositol-4-phosphate 5 kinase type 1 beta; PM: Plasma membrane; PUMA- p53 upregulated modulator of apoptosis; TFAM: Mitochondrial transcription factor A; TFEB: Transcription factor EB; XBP1/1S: X box binding protein-1/1S.

community toward developing safer nanomaterials and fostering responsible practices in nanotechnology. As the field continues to evolve, this exploration into nanotoxicology endeavors to contribute to the ethical and sustainable advancement of nanotechnology.

MAJOR TYPES AND APPLICATIONS OF NANOPARTICLES

Nanoparticles are categorized into four groups based on structural morphology: Organic, inorganic, carbon-based, and composite. Some of the most important types of nanoparticles are listed below:

Organic nanoparticles

Organic nanoparticles, derived from compounds like proteins, carbohydrates, lipids, and polymers, encompass micelles, dendrimers, liposomes, nanogels, polymeric NPs, and ferritin[6]. Generally non-toxic and biodegradable, they may have a hollow core, such as liposomes, and are sensitive to thermal and electromagnetic radiation. Formed through non-covalent interactions, these labile organic NPs are easily cleared from the body. Nanospheres or nano-capsules, common polymeric forms, collectively referred to as labeled polymorphic NPs, possess properties like a high surface area to volume ratio, stability, inertness, ease of functionalization, and unique optical, electrical, and magnetic behaviors, making them suitable for applications in drug delivery, imaging, biosensors, and cancer treatment[30].

Inorganic nanoparticles

Inorganic nanoparticles, devoid of carbon atoms, are hydrophilic, non-toxic, and biocompatible, providing high mechanical strength and stability. Precise control over size, shape, and composition allows researchers to design nanoparticles with tailored electrical, optical, and magnetic properties for targeted biomedical applications[5,7].

Metal-based nanoparticles: Metal-based nanoparticles, derived from various metals through disruptive or constructive methods and typically ranging in size from 10 to 100 nm, including aluminum (Al), cadmium (Cd), cobalt (Co), copper

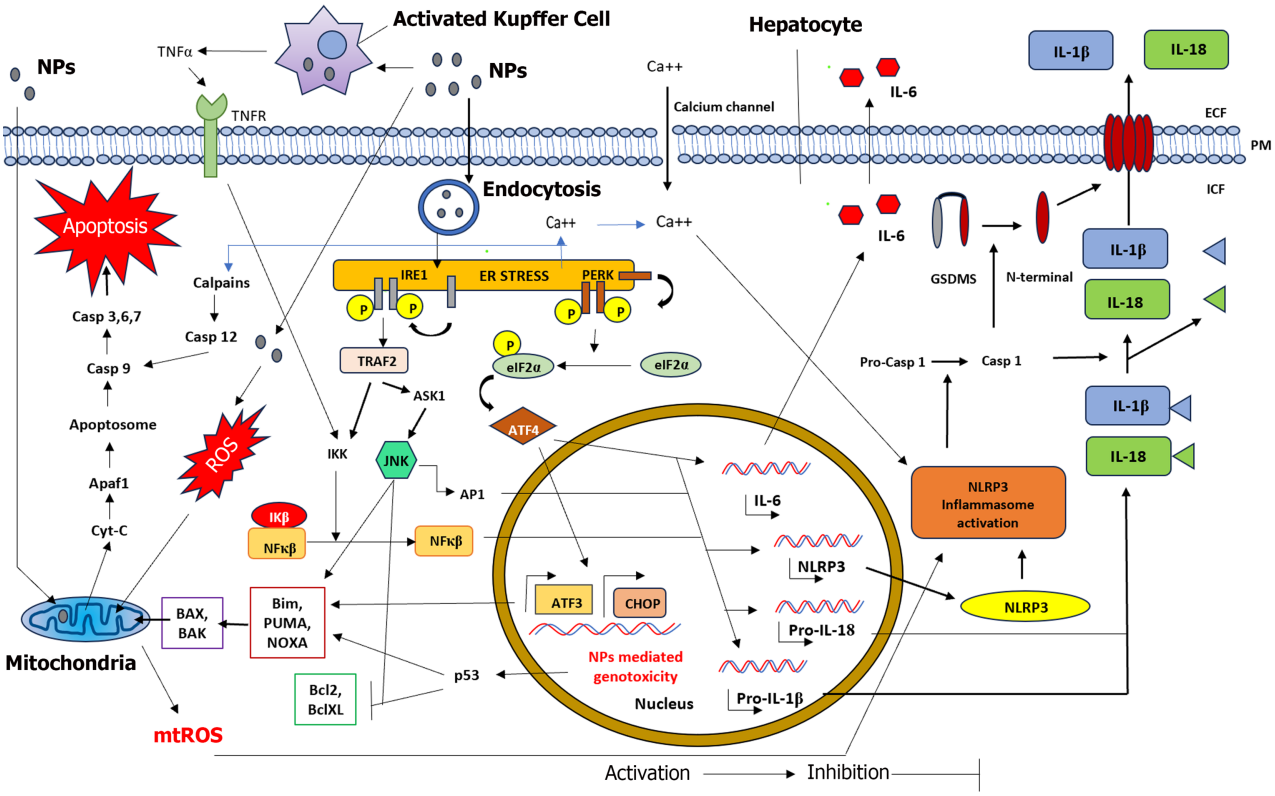

Figure 2 Diagram showing nanoparticles induced hepatotoxicity through inflammatory pathway and its crosstalk with oxidative stress, endoplasmic reticulum stress and apoptotic pathways. AP1: Activator protein 1; Apaf-1: Apoptotic peptidase activating factor 1; ASK1: Apoptosis signal-regulating kinase 1; ATF3/4: Activating transcription factor 3/4; BAK: Bcl-2 homologues antagonist/killer; Bax: Bcl-2-associated X-protein; Bcl2: B-cell lymphoma 2; BclXL: B-cell lymphoma-extra-large; Bim: Bcl-2 interacting mediator of cell death; Ca++: Calcium ion; Casp 1/3/6/7/9/12: Caspase 1/3/6/7/9/12; CHOP: C/EBP Homologous Protein; CytC: Cytochrome C; eIF2α: Eukaryotic initiation factor 2 alpha; GSDMS: Gasdermins; IKK: IκB kinase; Iκβ: Inhibitor of nuclear factor kappa beta; IL-6/18: Interleukin 6/18; IL-1β: Interleukin 1 β; IRE1: Inositol-requiring enzyme type 1; JNK: Jun N-terminal kinase; mtROS: Mitochondrial reactive oxygen species; NFkβ: Nuclear factor kappa beta; NLRP3: NOD-like receptor protein 3; NOXA: Phorbol-12-myristate-13-acetate-induced protein 1; NPs- Nanoparticles; p53: Tumor suppressor protein p53; PERK: Protein kinase RNA like endoplasmic reticulum kinase; Pro-Casp 1: Pro- Caspase 1; Pro-IL-18: Pro- Interleukin 18; Pro-IL-1β: Pro- Interleukin 1 β; PUMA- p53 upregulated modulator of apoptosis; ROS: Reactive Oxygen Species; TNFR: Tumor necrosis factor receptor; TNFα: Tumor necrosis factor alpha; TRAF2: TNF receptor associated factor 2.

(Cu), gold (Au), iron (Fe), lead (Pb), silver (Ag), and zinc (Zn), exhibit unique optoelectrical properties due to localized surface plasmon resonance[31,32]. Specifically, alkali and noble metals like Cu, Ag, and Au, when utilized in nanoparticle construction, show significant absorption in the visible region of the solar spectrum[33]. The synthesis of metal nanoparticles with specified facets, sizes, and forms necessitates controlled conditions, and their advanced optical properties make them versatile across various research domains[5,34]. These nanoparticles, distinguished by their small dimensions and surface properties, including pore size, surface charge, *etc.*, find applications in biomedical science, such as cancer treatment, disease diagnostics, radiation enhancement, drug delivery, and gene transport[35].

Metal oxide based nanoparticles: Metal oxide nanoparticles result from modifying the properties of metal-based nanoparticles. These nano-scale metal oxides find diverse applications in fluorescence, optical sensors, catalysts, biomedicine, gas sensors, and fuel cell anode materials[22,36-38]. Various synthesis methods, including inert gas condensation, co-precipitation, and lithography, have been used, but traditional methods often lack control over morphological structure, affecting essential nanomaterial properties[39,40]

Ceramic nanoparticles: Ceramic nanoparticles, resistant to environmental stresses, form with a solid core through heat or a combination of heat and pressure, incorporating metallic or non-metallic elements[41,42]. Typically composed of inorganic compounds like silica or alumina, they may also include metals and metal oxides, yielding diverse nano molecules with varying shapes, sizes, and porosities. Engineered to evade the reticuloendothelial system, ceramic NPs undergo size and surface composition modifications[43]. Widely used in medical applications, ceramics such as calcium phosphates, alumina, silica iron oxides, carbonates, and titanium dioxide have been found[44].

Ceramics also play an important role in various applications in photocatalysis, dye photodegradation, imaging, and catalysis[45]. Researchers aim to develop advanced ceramics with minimal cytotoxicity and enhanced biocompatibility, addressing challenges through innovative strategies that integrate ceramic nanoparticles with biocompatible materials, considering characteristics like shape, size, and physicochemical attributes[46].

Lipid-based nanoparticles: Lipid-based nanoparticles (LBNPs), typically 10-100 nm in diameter, consist of a lipid core surrounded by lipophilic molecules, finding applications in oncology and biomedicine[47]. Liposomes, a key type of LBNP, use a phospholipid bilayer for enhanced drug solubility and stability, accommodating both hydrophobic and hydrophilic molecules. Incorporating cholesterol improves stability, decreases fluidity, and enhances permeability for hydrophobic drugs in liposomal formulations[48]. Solid lipid nanoparticles, sized between 50-1000 nm, and composed of physiological lipids in a solid state, offer a compelling alternative for drug delivery, featuring a matrix of mono-, di-, or triglycerides, fatty acids, and complex glyceride mixtures, with stability ensured by surfactants or polymers[49].

Semiconductor nanoparticles: Semiconductor nanoparticles, possessing hybrid characteristics of metals and nonmetals, have garnered attention for their versatility in diverse applications[50,51]. Their crucial broad bandgap, adjustable by researchers, makes them valuable in photocatalysis, photo optics, and electronic devices[52]. Additionally, their nano-scale dimensions provide benefits such as increased surface area-to-volume ratio, enhanced quantum confinement effects, and improved catalytic activity, contributing to exceptional performance in various applications[53].

Quantum dots

Quantum dots (QDs), semiconductor nanoparticles with size- and composition-dependent optoelectronic properties (1.5 to 10.0 nm), play a significant role in the electronic and biomedical industries[8]. Their success is attributed to superior features like photostability, size-dependent optical properties, high extinction coefficient, brightness, and a large Stokes shift, overcoming limitations of organic dyes. QDs, due to their ultrasmall size, are well-suited for imaging and biosensing applications. They facilitate the development of multimodal/multifunctional probes with increased surface area for optical trackability *in vitro* and in vivo, designed to detect pH, metal ions, DNA, and enzyme activity, and deliver various therapeutics[8].

Carbon-based nanoparticles

Carbon-based nanoparticles encompass five main materials: carbon nanotubes, graphene, fullerenes, carbon nanofiber, and carbon black, each with unique structural configurations and diverse applications in nanotechnology.

Graphene: Graphene, a two-dimensional carbon allotrope, is a single layer of carbon atoms arranged in a hexagonal lattice with exceptional properties, such as elasticity, mechanical strength, and unparalleled thermal and electrical conductivity. Synthesized in the laboratory, it forms a 1nm-wide honeycomb lattice, exhibiting semiconductor properties without an effective mass and zero band gap. Graphene demonstrates an ambipolar electric field effect, with a breaking strength of 42 Nm^{-1} and a Young's modulus of approximately 1.0, making it the strongest material ever tested. These attributes position graphene as a promising material for electrical and photonic devices, sensing platforms, and clean energy applications[5].

Fullerene: Fullerenes, a molecular form of carbon allotrope, consists of Cn clusters (n > 20) arranged on a spherical surface with carbon atoms at pentagon and hexagon vertices[54]. The extensively studied C60 fullerene, composed of 60 carbon atoms, is highly symmetric and spherical, with a 0.7 nm diameter and sp2 hybridized carbon atoms. Exhibiting exceptional symmetry and stability, fullerenes have 20 tripled axes, 12 fivefold axes, and 30 twofold axes[54]. These unique properties position fullerenes as promising nanoparticles widely utilized in biomedical sciences, acting as inhibitors for human immunodeficiency virus, contrast agents for magnetic resonance imaging, and sensitizers for photodynamic therapy[5,55].

Carbon nanotubes: CNTs, unique in carbon-based nanomaterials, possess versatile characteristics like length, diameter, chirality, and layer number, showcasing exceptional properties and widespread applications. Composed of graphite, CNTs, typically with at least two layers and an outer diameter ranging from 3 nm to 30 nm, are divided into two categories: single-walled nanotubes (SWCNTs) and multi-walled nanotubes (MWCNTs). SWCNTs, with a diameter of around 1 nm, exhibit high electrical conductivity, mechanical strength, and thermal conductivity due to their nearly one-dimensional structure, indicated by a length-to-diameter ratio of approximately 1000[56]. MWCNTs, robust cylindrical structures with a minimum diameter of 100 nm, demonstrate resilience and diverse structures rooted in graphene sheets, with an interlayer distance resembling that in graphite, about 3.3 Å. The initial proposal for gram-scale synthesis of double-walled carbon nanotubes in 2003 involved chemical vapor deposition, selectively reducing oxide solid solutions in methane and hydrogen[10,56-58]. Applications of CNTs include bicables, AFM tips, hydrogen storage, electrochemical electrodes, nanocomposites, field emission displays, and diverse electrical devices[59].

Composite nanoparticles

Composite nanoparticles are produced *via* the integration of two or more different components. The components bear different properties at the nanoscale level. This integration of diverse components eliminates the limitation of individual components which enables researchers to produce nanomaterials with specific properties and uses. These NPs exhibit unique physical and chemical properties and each component has strong mutual coupling effects on the other. The chemical properties of composite nanoparticles depend on their composition and structure. The mutual coupling effect between the components of composite NPs can lead to changes in the chemical properties of composite NPs[12]. Composite NPs are used in a variety of applications including electronics, optoelectronics, and biomedical sciences[60].

Composite nanoparticles can be classified into three main categories based on their structural features:

Simple hybrid NPs: These types of composite NPs formed by combining two or more components without a specific structural hierarchy. They exhibit unique properties due to the combination of different materials[61].

Core or shell structured composite NPs: These NPs are made up of two different regions: an inner core region and an outer shell. These two regions of NPa are composed of two or more different materials. The core and shell structure influences the properties of the nanoparticles, such as electromagnetic wave attenuation capacity, *etc*[62].

Multifunctional quantum NPs: These NPs have multiple functionalities, such as magnetooptical, and electrochemical properties. The specific structure of Multifunctional Quantum Composite NP is used in applications like biosensing, bioassays, catalysis, and separations[12].

EXPOSURE ROUTES OF NANOPARTICLES

A myriad number of nanoparticles are manufactured from diverse materials to serve a multitude of purposes, it is crucial to ensure the unswerving safety of these particles within the human body. To understand the degree and mechanism of nanoparticle-induced toxicity, it is essential to understand their route of exposure, toxicological profile, and fate in the human body. The route of exposure also acts as a crucial factor in deciding the potential toxicity of NPs. The potential routes of NP exposure are as follows:

Oral exposure

Oral Exposure of NPs occurs following intake of food, drinks, or additives and supplements containing NPs, swallowing of inhaled NPs, or oral administration of nanomedicines or nano-formulations. These particles are then passed through the following organs esophagus, stomach, small intestine, and large intestine, and are readily absorbed in the stomach epithelial cells[13,14,63].

However, the absorption rate of NPs depends on multiple factors such as shape and size, concentration, pH of the medium, *etc.* The size and charge of the NPs also influence the absorption rate; positively charged NPs were captured through negatively charged mucus, whereas, negatively charged nano-molecules easily entered the mucus layer. Particle size also plays a crucial role because larger NPs required more for ingestion as well as digestion[64,65]. It has been observed that NPs lower than 100 nm diameter, are directly taken up by endocytosis through regular epithelial cells of the small intestine[66,67]. Absorption can also occur through epithelial cells of Peyer's patches in the gut-associated lymphoid tissue. Some other research studies proposed that oral intake of NPs could be absorbed in the gastrointestinal tract, from where the particles can transmigrate to the liver and spleen *via* lymph nodes.

Inhalation

Nanoparticles have been observed to exert their effect on human health, primarily *via* dermal contact or inhalation. The NPs inhaled during production or usage, get deposited all over the respiratory tract and the smaller particles penetrate the lungs where they accumulate in the alveolar regions. The larger NPs with diameters ranging from 5-30 μm usually reside in the nasopharyngeal region and the smaller particles, with diameters ranging from 1-5 μm tend to deposit in the tracheobronchial region. The smallest NPs (0.1–1 μm) deposited over the alveolar region[68,69]. The particles smaller than 10mm are primarily absorbed inside the lung and may undergo translocation to various parts of the body including the kidney. Insoluble particles accumulated in the lung have the potential to trigger diverse local toxicological reactions. The smaller NPs easily translocated compared to the bigger ones, and after reaching the lung they can remain there for years and can make their way into the circulatory or lymphatic system and subsequently disseminate into other organs like the liver, spleen, and kidneys[15].

The elimination procedure of NPs is very complex and lengthy and depends on its physicochemical properties. The larger particles which are deposited at the extra-thoracic and intrathoracic bifurcation, have been trapped in the mucus layer and transported through the mucociliary escalator into the pharyngeal region. These mucus-laden NPs are then swallowed and enter into the gastrointestinal tract for further processing. The smaller particles in bronchioles and alveoli undergo mucus-associated transport and are then phagocytosed by alveolar macrophage. However, if these strategies are unable to reduce the toxicity, the lung defense system becomes stronger and eventually causes lung tissue damage[11,26,70].

Dermal exposure

Skin, the largest organ and primary protective barrier of the human body acts as the easiest route of NP entrance. The skin is divided into three layers: epidermis, dermis, and hypodermis While the epidermis effectively prevents the entry of micrometer-sized particles, but less effective as a barrier for particles in the nanoscale range. Dermal exposure to nanoparticles is unavoidable with the use of various cosmetics and medications. Several experimental investigations examined the feasibility of nanoparticle penetration through the skin barrier and reported that NPs are unable to traverse the skin whereas, contrasting findings from other studies, specifically those focused on metal NPs such as iron NPs, reported that they can successfully penetrate through hair follicles and ultimately reached to the basal and spinous layers [71,72] The epidermal entry of NPs is influenced by a variety of factors such as exposure medium, medium pH, temperature, *etc*[13,14,63].

The existing evidence suggests that NPs with a diameter of about 4 nm can permeate intact skin whereas, when the size grows up to 45 nm, NPs can only permeate *via* impaired or injured skin[73]. Beneath the dermal layer rich with blood vessels, macrophages, lymph vessels, dendritic cells, and nerve endings. Consequently, particles absorbed beneath distinct layers of the skin undergo swift transport within diverse circulatory systems[1].

NPS MEDIATED HEPATOTOXICITY

Silica nanoparticles

A series of investigations revealed that the administration of silica nanoparticles with smaller diameters (30 nm) exhibited more liver injury or lethality compared to larger ones (1000 nm)[2,74,75]. Suggesting an inverse correlation between the silica nanoparticle size and hepatotoxicity. Also in combinatorial toxicity assessment, SP30 (30 nm), the smallest NPs was found to synergize the other known chemical liver toxins (carbon tetrachloride, paraquat, cisplatin) in causing hepatic damage[75]. In another study, increased biodistribution with reduced urinary excretion was observed for lower aspect ratio of mesoporous silicon nanoparticles[76]. In an *in vitro* study when four amorphous SiNPs with different surface areas were applied on HepG2 cells, a clear perturbation in cholesterol biosynthesis was observed. Increased cholesterol biosynthesis was found to be directly proportional to the increased surface area, which might have an impact on steroidogenesis and bile formation[19]. In a metabolomic study, the same group demonstrated amorphous SiNPs mediated depletion of glutathione, NADPH oxidase mediated reactive oxygen species (ROS) production, and alterations in antioxidant profile indicating perturbation of glutathione metabolism and glutathione pool in hepatocytes[77].

In a dose and time-dependent manner, mesoporous SiNPs (MSN) caused cytotoxicity in L-02 cells. In NLRP3 knockout mice and caspase-1 knockout mice model, MSN-promoted inflammation and hepatotoxicity were found to be abolished compared to the normal mice, suggesting mSiNPs mediated ROS overproduction followed by activated NOD-like receptor protein 3 (NLRP3) inflammasome, resulting into pyroptosis through caspase-1 activation[78]. Rat exposed to silica NPs compared to control exhibited altered liver biochemical parameters such as elevated levels of low-density lipoproteins (LDL), alkaline phosphatase (ALP), aspartate aminotransferase (AST), and alanina aminotransferasa (ALT) along with procalcitonin, iron, phosphorus, and potassium concentration. Histological modifications include Hydropic degeneration, Karyopyknosis, Sinusoidal dilatation, Hyperplasia of Kupffer cells, and infiltration of inflammatory cells with lowered liver index. Also negatively affects the expression of phase I and phase II drug metabolizing and drug transporter genes (*slc2a1, cyp4a12, ephx2, nat2*)[79].

Kupffer cells are well-known resident macrophages of the liver, contributing to the maintenance of liver normal physiological activity and homeostasis. Excessive accumulation of ROS and simultaneous release of bioactive mediators (H_2O_2, NO, and TNFα) indicates SiO_2NPs mediated activation and hyperplasia of KCs. BRL cells exhibited reduced viability, and structural alterations along with elevated levels of marker enzymes [lactate dehydrogenase (LDH), AST] when co-cultured (contactless) with SiNPs activated KCs, clearly suggesting that KCs activated by SiO_2NPs can cause liver injury *via* the release of H_2O_2, NO, and TNFα. In addition to that, infiltration of inflammatory cells and subsequent increase of TNFα, monocyte, lymphocytes, and neutrophils in the liver can be correlated with SiNPs activated KCs mediated inflammation in the liver[80].

Analysis of ^{1}H nuclear magnetic resonance (^{1}H NMR) results, unveiled lipid metabolism disorder in rats receiving intratracheal instillation of SiNPs causing hepatotoxicity in a dose-dependent manner. Biochemical analysis showed a significant increase in ALT, AST, triglyceride (TG), and LDL-C levels but a decrease in HDL-C levels in the treated group. Ten metabolic pathways were affected due to treatment, including the metabolism of amino acids (glutamate, cysteine, aspartate), purines, and glucose-alanine cycle that resulted in the production of 11 different metabolites compared to control[81].

Autophagy-mediated liver toxicity involves autophagic lysosomal reformation (ALR) an event where anomalous autophagy fails to terminate, which results in a persistent accumulation of enlarged autolysosomes. Mouse hepatocytes on exposure to SiO_2NPs prevent conversion of PI(4)P to PI(4,5)P2 on enlarged autolysosomal membrane due to loss of PIP5K1B, also clathrin fails to be recruited, leading to suppression of ALR and resulted into enlarged autolysosomes[82]. The molecular mechanism behind SiNp-induced autophagosome synthesis, accumulation, and autophagic dysfunction was worked out on L-02 cells. When treated with different concentrations of SiNPs, readily get internalized and induce ROS production, which in turn causes ER stress and UPR. Upregulated expressions of ATF4 and DDIT3 indicate involvement of EIF2AK3 and ATF6 pathway but not ERN1-XBP1 pathway. ATF4 and DDIT3 then transcriptionally upregulate expressions of LC3B and ATG12 (autophagic genes) that result in autophagosome formation[83]. In HepG2 cells accumulation of amorphous SiNPs in mitochondria leads to excessive ROS generation that in turn triggers autophagy and autophagic cell death in hepatocytes *via* the phosphatidylinositol 3-kinase (PI3K)/serine/threonine kinase/mammalian target of rapamycin (mTOR) pathway[84].

Overexpression of p53, bax, and caspase-3 in contrast to bcl-2 downregulation along with ROS generation in HepG2 cells insulted with SiNPs suggests activation of cell cycle check point genes and apoptotic pathway in accordance to cytotoxicity due to oxidative stress. Restoration of cell viability with an altered apoptotic marker profile was observed in the same cell when co-treated with vitamin C, a ROS scavenger[85]. Amorphous SiNPs exposure to human cells (HL-7702) and rat cells (BRL-3A) showed elevated expression of p53, Bax, cleaved caspase-3, and negative expression of Bcl-2 and caspase-3 levels, with increased ROS generation and decreased GSH level indicating oxidative stress-mediated cytotoxicity that leads to apoptotic activation *via* p53/casp-3/Bax/Bcl-2 pathway. Human liver cells exhibited more sensitivity than rat liver cells[86].

Compared to normal mice, SiNPs exhibited more severe effects in the liver of metabolic syndrome mice though improved insulin resistance. It has been established that SiNP exposure can accelerate liver damage in metabolic syndrome mice following deposition to mitochondria which results in mitochondrial injury and overproduction of ROS. That aggravated liver fibrosis (higher collagen deposition), hepatic ballooning, DNA damage (genotoxicity), and infiltration of inflammatory cells[87]. A recent study reveals SiNPs induced hepatotoxicity *via* perturbating mitochondrial quality control (MQC) process, promoting excessive mitochondrial fission (DRP1, FIS1, and MFN2 were up-regulated under SiNPs exposure, but MFN1 was down-regulated), mitophagy disorder (PINK/Parkin signaling, up-regulated PINK1 and *p*-Parkin, as well as an enhanced conversion of LC3B-I to LC3B-II) and downregulating mitochondrial biogenesis (inhibited mitochondrial biogenesis *via* PGC1α-NRF1-TFAM signaling, decline PGC1α, NRF1 and TFAM), leading to mitochondrial dysfunction followed by hepatocyte damage and liver biotoxicity[88]. From the above findings, it can be speculated that mitochondrial injury & instability in hepatocytes due to SiNP exposure resulted in liver oxidative stress.

Recent *in vitro* as well as *in vivo* investigation results indicate silicon NP insult can trigger LDH, ALT, and AST in serum concentration owing to hepatic damage. Compromised antioxidant enzyme profile [catalase (CAT), SOD, and GPx] with elevated levels of oxidative stress markers [NO, malondialdehyde (MDA), PCO, and H_2O_2] and MDA levels are engaged in hepatic ROS production[89]. Altered hepatic metabolism is observed in both free fatty acid - treated L-O2 cells and ApoE$^{-/-}$ mice model receiving SiNps treatment. Increased fatty acid biosynthesis, lipid deposition, liver total cholesterol/TG index along with decreased β-oxidation and lipid efflux resulting into perturbated lipid metabolism can be corroborated with the induction of oxidative stress-related liver injuries, may help the acceleration of liver diseases like metabolic associated fatty liver disease[90]. More over-upregulated expressions of pro-apoptotic genes (Bax, p53, Caspase-9/3) and downregulated anti-apoptotic genes Bcl-2 along with histopathological alterations of the liver such as sinusoidal dilatation, Kupffer cell hyperplasia, infiltration of inflammatory cells strongly indicates SiNPs induced hepatic toxicity *via* ROS-activated caspase signaling pathway, leading to induction of apoptosis in the liver[89]. Through integrative proteomic and metabolomic analyses, Zhu *et al*[91] identified key proteins (RPL3, HSP90AA1, SOD, PGK1, GOT1, PNP) indicative of abnormal protein synthesis, oxidative stress, and metabolic dysfunction in SiNP-induced hepatotoxicity. Metabolomic data revealed disruptions in vital metabolites [glucose, alanine, GSH, CTP, adenosine triphosphate (ATP)]. Bioinformatic analysis highlighted disturbances in glucose and amino acid metabolism, suggesting potential exacerbation of oxidative stress and liver injury. Key proteins associated with SiNP-induced hepatotoxicity include SOD, TKT, PGM1, GOT1, PNP, and NME2[91]. This study underscores the power of integrative omics analyses for nanoparticle toxicity assessments. Follow Table 1 for a comprehensive account.

Metal oxides nanoparticles

Consult Tables 2-10 for a comprehensive account of different metal oxide-induced hepatotoxicity.

Nickel oxides nanoparticles: The findings of several stress assays, liver function tests, and histopathology analyses make it abundantly evident that rats given NiO-NPs experience nitrative stress and oxidative stress-related liver damage[92, 93]. Chang *et al*[16] demonstrated that the liver cells of rats injected with NiO underwent ER stress and that this brought about the induction of apoptosis *via* many routes, including the PERK/eIF-2α, IRE-1α/XBP-1S, and caspase-12/-9/-3 pathways. A different investigation using a comparable experimental design found that the nuclear factor kappa B (NF-κB) signaling pathway is associated with hepatotoxicity[94].

In the HepG2 cells model, NiONPs caused cytotoxicity through ROS production and Bax/Bcl-2 pathway-mediated apoptotic induction. Also treated cells exhibited micronuclei formation, chromatin condensation, and DNA damage suggesting NiONPs mediated genotoxicity[95]. NiO was additionally found to induce hypoxic stress in the same human liver cells in a concentration-dependent manner, as evidenced by the activation of hallmark candidate genes, hypoxia-inducible transcription factor-1α (HIF-1α), and miR-210 microRNA and decreased levels of ribosome biogenesis. Nitric oxide (NO) levels that were too high caused Ca++ influx, which in turn led to mitochondrial instability and oxidative stress, further encouraging lysosomal degradation in connection with autophagic processes. Subsequently led to the development of apoptosis *via* the p53 and MAPKAPK-2 signaling pathways[96]. Rat liver and HepG2 cells under Nano-NiO exposure resulted in hepatic fibrosis. Upregulation of transforming growth factor 1 beta (TGF-β1), Smad2, Smad3, alpha-smooth muscle actin (α-SMA), matrix metalloproteinase 9 (MMP9), tissue inhibitors of metalloproteinase1 but simultaneously downregulation of E-cadherin and Smad7 in both models can be corroborated with hepatic fibrosis *via* activation of TGF-β1/Smad pathway, epithelial-mesenchymal transition (EMT), reformation and deposition of extracellular matrix[97]. A recent study reported NiNps-mediated hepatic injury following hepatic inflammatory response, ER stress, abnormal lipid metabolism that leads to hepatocyte apoptosis[98]. NiNPs exposure (15-45 mg/kg) in rats induced dose-dependent liver dysfunction, histological injuries, and oxidative stress. Elevated NF-kβ, nitrative stress markers, and inflammatory and apoptotic mediators were observed. The study highlights Ni NPs-induced hepatotoxicity, crucial for health risk assessment[99].

Tungsten trioxide nanoparticles: WO3 nanorods of varying lengths have been shown to cause hepatotoxicity in mice when given intraperitoneally. This effect is evident in the form of hepatocytic lesions, which include cellular edema, nuclear pyknosis in most hepatocytes, cytoplasmic vacuolation, and hydropic degeneration in hepatocytes surrounding the central vein. Additionally, liver function is impaired, as evidenced by elevated levels of serum ALT and AST, which are caused by oxidative stress (increased intracellular ROS, significant reduction in GSH and SOD activity), as well as an inflammatory response [increased NF-κB, tumor necrosis factor alpha (TNF-α), IFN-γ, and interleukin (IL)-4]. Shorter nanorods showed greater toxicity than longer nanorods in terms of severity. Adversity of WO3 nanorod was decreased by melatonin administration[17].

Table 1 Effects and molecular mechanisms underlying SiO_2NPs induced hepatonanotoxicity

NPs	Size	Tested model	Dose & route of administration	Effects & Mechanism	Ref.
SiO_2NPs	15 nm (TEM)	HepG2 cell	1-200 ug/mL for 72hrs.	Bcl-2, GSH, Cell viability (decreased); p53, Bax, caspase-3, ROS production, LPO (increased)	[85]
				Oxidative stress & Apoptosis	
SiO_2NPs	15 nm (TEM)	Kupffer cells from Sprague Dawley rats; Sprague Dawley rats	50, 100, 200, 400, and 800 μg/mL for 24 h. 50 mg/kg single (i.v.)	ROS, AST, LDH, TNFα, H_2O_2, NO (increased); Kupffer cells (activation); Infiltration of inflammatory cells	[80]
				Activated Kupffer cells-mediated inflammation in liver toxicity	
SiO_2NPs	30, 50, 70, 300, 1000 nm (TEM)	BALB/c male mice	10-40 mg/kg (i.v.)	ALT, AST (increased)	[75]
				Acute liver injury	
Amorphous SiO_2 NPs	62.26nm (DLS)	HepG2	25, 50, 75, 100 μg/mL, 24 h	ROS levels; Autophagy and autophagic cell death *via* PI3K/Akt/mTOR pathway	[84]
				Oxidative stress	
Amorphous SiO_2 NPs	aSiNP-189 (20nm), aSiNP-116 (50nm), aSiNP-26 (110nm), aSiNP-8 (250nm) (EM)	HepG2	10–200 μg/mL, 24 h	Cholesterol biosynthesis (increased); May affect steroidogenesis & bile formation	[19]
Amorphous SiO_2 NPs	19.8 ± 2.7 nm (TEM)	HL-7702 cells; BRL-3A cells	31.4–500 μg/mL, 72 h	p53, Bax, cleaved caspase-3 (increased); GSH levels, caspase-3, Bcl-2 (decrease); Activation of p53/casp-3/Bax/Bcl-2 pathway; Human cells are more sensitive than rat cell	[86]
				Oxidative stress & apoptosis	
SiO_2NPs	30 nm (TEM)	Mouse hepatocytes	500 μg/mL, 24 h	ALT, AST (increased); ALR (blockage); Enlarged autolysosomes	[82]
				Inflammation	
Amorphous SiO_2 NPs	202.3 (DLS)	HepG2; ICR mice	50 mg/kg b.w. for 24 h (oral)	GSH, NADPH oxidase depletion; ROS (increased); Altered GSH metabolism	[77]
				Oxidative stress	
SiO_2NPs	10 nm (BET)	Albino Wistar rats	2 mg/kg daily 20, 35 or 50 injections (i.p.)	ALP, AST, ALT, LDH, procalcitonin, iron, phosphorus, potassium (increased); Phase I and II drug metabolizing and transporting enzymes (downregulation); Hydropic degeneration, karyopicnosis, Sinusoidal dialation, Kupffer cell hyperplasia, lowered liver index, infiltration of inflammatory cells	[79]
				Oxidative stress & Inflammation	
SiO_2NPs	15.4 ± 1.8 nm (TEM)	Kunming mice (normal & metabolic syndrome model)	10 mg/kg b.w. daily 30 d (oral)	Liver fibrosis (collagen deposition); Hepatic ballooning; DNA damage (genotoxicity) ROS production, mitochondrial damage, infiltration of inflammatory cells	[87]
				Mitochondrial instability & inflammation	
Mesoporous SiO_2 NPs	109.2 (DLS)	L02 cells; BALB/c mice	5–120 μg/mL, 24 and 48 h; 50 mg/kg 3 times a week for 3 wk (i.v.)	ALT, AST, ROS (increased); NLRP3 inflammasome activation; Pyroptosis *via* caspase-1 activation	[78]
				Oxidative stress and inflammation	
SiO_2NPs	58 nm (TEM)	L-02 cells	6.25, 12.5, 25, 50, and 100 μg/mL) for 12 h and 24 h	ROS production; ER stress; Activation of EIF2AK3 and ATF6 pathway; Induction of autosome formation	[83]
				Oxidative stress	
SiO_2NPs	58.04 ± 7.41 (TEM)	L02 cells	12.5, 25, 50, 100 μg/mL, 24 h	Affect mitochondrial quality control (MQC) process, Mitochondrial fission (increased); Induced mitophagy *via* activated	[88]

				PINK/Parkin signaling pathway; Decreased mitochondrial biogenesis *via* PGC1α-NRF1-TFAM signaling pathway; Mitochondrial dysfuntion **Mitochondrial dysfunction & oxidative stress**	
SiO_2NPs	58.11 ± 7.30 nm (TEM)	Sprague dawley rats	1.8, 5.4, 16.2 mg/kg b.w. (i.t.)	ALT, AST, TG, LDL-C (increased) HDL-C (decreased); Impact on Purine, amino acids metabolism, glucose-alanine cycle **Metabolic disorder**	[81]
SiO_2NPs	15nm (XRD)	Wistar rat	25 and 100 mg/kg b.w. for 28 consecutive days (i.p.)	AST, ALT, LDH, NO, MDA, PCO, H_2O_2, Bax, p53, Caspase-9/3 (increased) CAT, SOD, GPx, Bcl2 (decreased) **Oxidative stress & apoptosis**	[89]
SiO_2NPs	59.98nm (TEM)	Free Fatty Acid treated – L-02 cells; ApoE-/- mice	1.5, 3, 6 mg/kg b.w once per week for 12 times (i.t.)	LDH, AST, ALT, MDA (increased); GSH/GSSG (decreased); Fatty acid synthesis (increased); β-oxidation(decreased); Disturbed amino acid & lipid metabolism; Lipid accumulation leads to ER stress; Downregulated Nrf2 signaling **Oxidative stress, altered lipid metabolism**	[90]

Akt: Protein kinase B; ALP: Alkaline phosphatase; ALT: Alanine aminotransferase; AST: Aspartate aminotransferase; ATF6: Activating transcription factor 6; Bax: Bcl-2 associated X protein; Bcl2: B-cell lymphoma 2; CAT: catalase; DNA: Deoxy ribonucleic acid; EIF2AK3: Eukaryotic translation initiation factor 2-alpha kinase 3; ER: Endoplasmic reticulum; GPx: Glutathione peroxidase; GSH: Glutathione; GSSG: Glutathione disulfide.H_2O_2-hydrogen peroxide; HDL-C: High-density lipoprotein; LDH: Lactate dehydrogenase; LDL-C: Low-density lipoprotein; LPO: Lipid peroxidation; MDA: Malondialdehyde; mTOR: Mammalian target of rapamycin; NADPH: Reduced nicotinamide dinucleotide phosphate; NLRP3: NOD-like receptor protein 3; GSH: Glutathione; NO: Nitric oxide; NRF1/Nrf2: Nuclear factor erythroid 2-related factor1/2; p53-tumor suppressor protein p53; PGC1α: Peroxisome proliferator-activated receptor gamma coactivator 1 alpha; PI3K: Phosphatidylinositol 3-kinase; PINK: PTEN induced kinase, ROS: Reactive oxygen species, SOD: Superoxide dismutase; TFAM: Mitochondrial transcription factor A; TG: Triglyceride; TNFα: Tumor necrosis factor alpha.

Copper oxide nanoparticles: Transmission electron microscope investigation has confirmed the accumulation and distribution of CuONPs in rat liver tissue after oral administration. This would indicate that CuONPs can be easily absorbed through the intestinal wall and transported to the liver *via* blood. Serum levels of bilirubin that are high, heightened catalase and SOD activity, and altered glutathione metabolism enzyme profiles [glutathione reductase, GPx, and glutathione S-transferases (GST)], all strongly suggest that NPs exacerbated oxidative stress-related liver damage[100]. The primary marker of hepatic injury is an increase in vital enzymes such as serum ALT, and serum AST in the liver. CuONP-treated Wister rats have been shown to have histopathological changes, such as pyknotic, pleomorphic nuclei, binucleated hepatocytes with an increased population of apoptotic cells, with elevated levels of AST, ALT, and decreased levels of albumin in serum[18]. Mice receiving both chemically and biologically synthesized CuO-NPs (CNPs and BNPs), but mostly BNPs, showed distinct histopathological, biochemical, and apoptotic changes. Various types of histopathological alterations in hepatic tissues against their normal functioning range from hydropic degeneration and vacuolization to cell necrosis, loss of plasma membrane, more eosinophilic cytoplasm, karyorrhexis and complete loss of nucleus in few cells, activated Kupffer cells, lymphocytic infiltration around necrotized cells and congestion in sinusoids. Biochemical examination showed elevated levels of serum ALT and AST. Increased expression pattern of P^{53}, Casp-3 immunoreactivity suggested induction of apoptosis due to CuO toxicity in liver cells[101]. A comparable study has reported additional architectural abnormalities, such as ER swelling with lower count, increased intracellular space, fat accumulation, and cellular shrinkage related to the distribution of Nano-CuO in the liver. These discrepancies have been shown to affect hepatocyte growth, metabolism, and viability in both *in vitro* and *in vivo* investigations. JNK, PERK, C/EBP homologous protein (CHOP), ATF4, eIF2α, IRE1, Calpain, GRP78, ATF6, Bax, Caspase-3, and Caspase-12 have all been shown to have upregulated expressions in treatment group while Bcl-2 expression level gets diminished, is consistent with ROS-mediated oxidative stress-induced activation of the ER-stress pathway, that triggered apoptosis in liver tissue cells[102]. The liver of adult rats treated with CNPs (chemically synthesized CuO NPs) showed dose-dependent genotoxicity (DNA tailing), an enhanced oxidative stress response (lipid peroxidation), and histopathological changes (dilation and congestion of sinusoids) in contrast to GNPs (green synthesized CuO NPs)[103]. Mild to severe deleterious alterations in hepatic tissues including disorganized hepatic rays, dilated sinusoids with congestion, hepatocytic necrosis, glycogen breakdown, hemosiderosis, steatosis, hyperplasia of the bile duct and fibrous tissue proliferation, anti-inflammatory cell infiltration with caspase 3 immunoreactivity were also observed against the administration of nano-Cuo in dose-dependent manner[104].

Zinc oxide nanoparticles: In a study, Pasupuleti *et al*[20] reported that when SD rats were orally given nano-sized and micro-sized ZnO (5-2000 mg/kg), compared to micro-sized zinc oxide, nano-size zinc oxide exhibited an inverse dose-

Table 2 Effects and molecular mechanisms underlying NiONPs & NiNPs induced hepatonanotoxicity

NPs	Size	Tested model	Dose & route of administration	Effects & mechanism	Ref.
NiO NPs	44 nm (TEM)	HepG2 cells	2-100 μg/mL for 24 h	Cell viability (reduced); ROS (increased); Micronuclei induction, chromatin condensation and DNA damage; bax and caspase-3 (upregulated); bcl-2 (downregulated) **Oxidative stress, apoptosis**	[95]
NiO NPs	20 nm (TEM)	Wistar rat	0.015, 0.06 or 0.24 mg/kg b.w. twice a week for 6 wk (i.t.)	NO, TNOS, iNOS, ·OH, LPO, HO1 (increased); CAT, GSHPx, T-SOD and TAOC, MT1 (decreased) **Oxidative & nitrative stress**	[93]
NiO NPs	20 nm (SEM)	Wistar rat	0.015, 0.06, and 0.24 mg/kg b.w. twice a week for 6 wk (i.t.)	GRP78, CHOP (increased); Activation of PERK/eIF-2α, IRE-1α/XBP-1S, and caspase-12/-9/-3 pathways **ER stress, apoptosis**	[16]
NiO NPs	20 nm (SEM)	Wistar rat	0.015, 0.06, and 0.24 mg/kg b.w. twice a week for 6 wk (i.t.)	ALT, AST, ALP, GGT, IL-1β and IL-6, TNF-α, NIK, IKK-α, NF-κB (increased); IL-4, IL-10, IκB(α) (decreased); Activation of NF-kB signalling pathway **Inflammation**	[94]
NiO NPs	13.16 ± 2.98 nm (TEM)	Wistar rat	125, 250 and 500 mg/kg single dose (oral)	ALP, LDH, ALT, AST, LPO (upregulation); GSH, SOD (downregulation) **Oxidative stress**	[92]
NiO NPs	21.6 ± 3.6 nm (TEM)	HepG2	5, 10, 25, 50 and 100 μg/mL, 24 h	HIF-1α, miR210, p53, Caspase-3, 8 and 9, NO, MMP (increased); Phagosome formation by lysosomal pathway **Hypoxia & oxidative stress, apoptosis**	[96]
NiO NPs	44 nm (TEM)	Wistar rat; HepG2	0.015, 0.06, and 0.24 mg/kg twice a week for 9 wk (i.t.); 25-200 μg/mL	TGF-β1, Smad2, Smad3, α-SMA, MMP9, TIMP1, EMT (upregulation); E-cadherin, Smad7 (downregulation); activation of TGF-β1/Smad pathway **Hepatic fibrosis, ECM deposition**	[97]
NiNPs	55.8 ± 14.0 nm (TEM)	C57/BL6 mice	10, 20 and 40 mg/kg/d for 7 and 28 d	ALT, AST, Ire1α, Perk and Atf6, TG increased; Lipid metabolism dysfunction; Inflammation **ER stress, apoptosis**	[98]

OH: Hydroxyl radical; ALP: Alkaline phosphatase; ALT: Alanine aminotransferase; AST: Aspartate aminotransferase; Atf6: Activating transcription factor 6; CAT: Catalase; CHOP: C/EBP Homologous Protein; ECM: Extra cellular matrix; eIF2α: Eukaryotic initiation factor 2 α; EMT: Epithelial mesenchymal transition; GGT: Gamma-glutamyl transpeptidase; GRP78: Glucose regulated protein 78; GSH: Glutathione; GSHPx: Glutathione peroxidase; HIF-1α: Hypoxia inducible factor 1; HO1: Heme oxygenase 1; IKK-α: IκB kinase alpha; IL-1β: Interleukin 1 β; IL-6: Interleukin 6; iNOS: Inducible nitric oxide synthase; IRE-1α: Inositol-requiring enzyme type 1α; IκB(α): Inhibitor kappa B alpha; LDH: Lactate dehydrogenase; LPO: Lipid peroxidation; miR210: miRNA210; MMP9: Matrix metallopeptidase 9; MMP: Mitochondrial membrane potential; MT1: Metallothionein 1; NF-κB: Nuclear factor kappa beta; NIK: NF-κB-inducible kinase; NO: Nitric oxide; p53-tumor protein p53; PERK: Protein kinase RNA like ER kinase; Smad2: Suppressor of mothers against decapentaplegic2; SOD: Superoxide dismutase; TAOC: Total antioxidative capacity; TG: Triglyceride; TGF-β1: Transforming growth factor 1 beta; TIMP1: TIMP metallopeptidase inhibitor 1; TNF-α: Tumor necrosis factor α; TNOS: Total nitric oxide synthase; TSOD: Total superoxide dismutase; XBP-1S: X box binding protein-1S; α-SMA: Alpha smooth muscle actin.

dependent increase in AST and ALT, that means nano-sized ZnO have shown higher toxicity at lower doses. Suggesting liver tissue assault and degeneration. Contrary to this result, Yang *et al*[105] demonstrated dose-dependent nanotoxicity of ZnO in mice models. A significant decrease in antioxidant (GSH) level causes an imbalance between oxidants and antioxidants, resulting in oxidative stress in the liver. Elevated expressions of transcription factor (xbp-1), ER chaperons (grp78, grp94, pdi-3), and phosphorylation of PERK and eIF2α in association to ER swelling and damage in hepatocytes strongly indicate ER stress. Upregulated expressions of proapoptotic genes (bax, chop), initiator caspase (Casp-9,12), effector caspase (casp-3), and subsequent diminished expression of bcl2, phosphorylation, and activation of JNK and CHOP/GADD153 strongly suggested ER stress-mediated opening of apoptotic pathways in liver tissue treated with nano-ZnO. Exposure to ZnONPs produces histological and histochemical modifications in liver tissues that may affect

Table 3 Effects and molecular mechanisms underlying WO_3NPs induced hepatonanotoxicity

NPs	Size	Tested model	Dose & route of administration	Effects & mechanism	Ref.
WO_3 NPs	60-70 nm, length WO_3nanorods shorter (125−200 nm) and longer (0.8−2 μm)	BALB/c mice	2.5/5/10/20 mg/kg/d of shorter WO3 nanorods; 2.5/5/10/20 mg/kg/d longer WO3 nanorods for 14 d (i.p.)	ALT, AST; NF-κB, TNF-α, IFN-γ, IL-4 (increased); GSH, SOD (decreased) **Oxidative stress, inflammation**	[17]

ALT: Alanine aminotransferase; AST: Aspartate aminotransferase; GSH: Glutathione; IFN-γ: Interferon gamma; IL-4: Interleukin 4; NF-κB: Nuclear factor kappa B; SOD: Superoxide dismutase; TNF-α: Tumor necrosis factor α.

Table 4 Effects and molecular mechanisms underlying CuONPs induced hepatonanotoxicity

NPs	Size	Tested model	Dose & route of administration	Effects & mechanism	Ref.
CuO-NPs	33 nm (XRD)	Wister rats	300 mg/kg b.w. per day for 7 d (i.g.)	ALT, AST (increased)	[18]
CuO- NPs	40 nm (TEM)	Mature rats (Rattus norvegicus var. albinos)	0.5, 5, and 50 mg/kg b.w./d for 14 d (oral)	CAT, GPx, GR (increased) GST (decreased)	[100]
CuO-NPs	BNPs 4.14-12.82 nm CNPs 4.06-26.82 nm (XRD)	Mature mice	500 mg/kg b.w. single dose (oral)	ALT, AST, P^{53}, Caspase - 3 (increased); Hepatic necrosis	[101]
Nano-CuO	20-40 μm (TEM)	BRL-3A cells; Wister rat	5, 10, 20 μg/mL; 10 μg/g b.w. for 60 d (i.n.)	ALT, AST, T-BIL, D-BIL, I-BIL (increased) ALP (decreased); SOD (decreased); MDA, iNOS, GSH-PX (increased); MCP-1, IL-1, IL-1β, TNF-α, IL-6 (increased); JNK, PERK, CHOP, ATF4, eIF2α, IRE1, Calpain, GRP78, ATF6, Bax, Caspase-3, Caspase-12 (upregulated) **Oxidative stress induced ER stresspathway activation**	[102]
CuO-NPs	GNPs & CNPs	Sprague dawley rat	50 & 100 mg/kg b.w. twice a week starting before mating (oral)	CAT, GSH, GPx (decreased)	[103]
CuO-NPs	< 50 nm (TEM)	Wistar rat	5 mg, 10 mg, 25 mg/kg b.w. per day for 9 d (i.p.)	Mild to severe Liver tissue damage including necrosis of hepatocyte, anti-inflammatory cell infiltration	[104]

ALP: Alkaline phosphatase; ALT: Alanine aminotransferase; AST: Aspartate aminotransferase; ATF4/6: Activating transcription factor4/6; Bax: Bcl-2 associated X protein; CAT: Catalase; CHOP: C/EBP Homologous Protein; D-BIL: Direct bilirubin; eIF2α: Eukaryotic initiation factor 2 α; BNP: Biologically synthesized nanoparticle; CNP: Chemically synthesized nanoparticle; GNP: Green nanoparticle; ER: Endoplasmic reticulum; GPx: Glutathione peroxidase; GR: Glutathione reductase; grp78: Glucose regulated protein 78; GSH: Glutathione; GSH-PX: Glutathione peroxidase; GST: Glutathione-S-transferase; I-BIL: Indirect bilirubin; IL-1: Interleukin 1; IL-1β: Interleukin 1 β, IL-6: Interleukin 6; iNOS: Inducible nitric oxide synthase; IRE-1: Inositol-requiring enzyme type 1; JNK: Jun N-terminal kinase; MCP-1: Monocyte chemoattractant protein 1; MDA: Malondialdehyde; P^{53}: Tumor protein p53; PERK: Protein kinase RNA like ER kinase; SOD: Superoxide dismutase; T-BIL: Total bilirubin; TNF-α: Tumor necrosis factor α.

normal functioning. Degenerative liver cells exhibited nuclear changes (nuclear membrane irregularity, binucleation, nuclear vesiculation, anisokaryosis, and karyolysis), cytoplasmic changes (cytoplasmic vacuolation with parietal cytoplasmic swelling), and glycogen depletion followed by necrosis under ZnO insult. Inflammatory signs were sinusoidal dilation following Kupffer cell activation and enlargement, infiltration of inflammatory cells at lobular and portal triad[106]. ZnO-NPs-induced inflammatory liver injury *via* the production of inflammatory mediators (NO, TNF-, IL-6, C reactive protein, immunoglobulin G) has been documented[107]. Human liver cell HepG2 in response to short exposure to ZnO exhibited oxidative stress-mediated cytotoxic effects leading to LDH leakage, DNA damage, reduction in MMP, and increment in the ratio of proapoptotic/antiapoptotic proteins that lead to activation of mitochondrial apoptotic pathway. In addition to that ZnO was found to induce the phosphorylation of JNK, P38, and $P53^{ser15}$ without any significant changes in their expression level[108]. Above mentioned hepatic histopathological and immunohistochemical alterations along with oxidative stress are found to be promoted *via* modulation of JNK/p38MAPK and the STAT-3 signaling pathways[109]. A separate investigation in HepG2 cells revealed that ZnONPs override the toxic effects of ZnO (zinc oxide), exhibiting more hepatocyte inactivation, oxidative stress, mitochondrial damage, elevated

Table 5 Effects and molecular mechanisms underlying ZnONPs induced hepatonanotoxicity

NPs	Size	Tested model	Dose & route of administration	Effects & mechanism	Ref.
ZnO NPs	Micro size; Nano size 63 nm (SEM)	Sprague Dawley rat	5, 50, 300, 100, 2000 mg/kg b.w for 14 d (oral)	AST, ALT (increased)	[20]
ZnO NPs	35 nm (TEM)	Wistar albino rats	2 mg/kg b.w. for 21; Days (i.p.)	Histopathological alterations; Kupffer cell activation	[106]
				Inflammation	
ZnO NPs	50 nm (TEM)	Wistar albino rats	600 mg/kg/b.w and 1 g/kg/b.w for 5 d	ALT, NO, TNF-α, IL-6, CRP, IgG (increased)	[107]
				Inflammation	
ZnO NPs	80 nm (TEM)	C57BL/6 mice	200 mg/kg/d (low dose) and 400 mg/kg/d (high dose) for 90 d (oral)	ALT, AST (increased); grp78, grp94, pdi-3, xbp-1(increased ER stress related proteins); Increased phosphorylation of PERK & eIF2α; caspase-3, 9, 12 (apoptosis); phosphorylation of JNK, and CHOP/GADD153; upregulation of Chop, Bax	[105]
				ERstress mediated activation of apoptotic pathway	
ZnO NPs	30 nm (TEM)	HepG2 cell	14–20 μg/mL for 12 h	AST, ALT, Bax (increased) Bcl2 (decreased) LDH leakage; JNK, P^{38} activation	[108]
				Apoptosis	
ZnO NPs	Less than 15 nm (TEM)	Sprague dawley albino rats	100, 200, 300 mg/kg b.w. per day for 14 d (oral)	ALT, AST, ALP (increased); Bax, caspase-3 (increased); Bcl2 (decreased); Modulation of JNK/p38MAPK & STAT-3 signalling pathways	[109]
				Apoptosis	
ZnO NPs	20-50 nm (TEM)	HepG2 cells; sprague dawley rat	20 μg/mL for 24 h; 25 mg/kg b.w. for 7 d (i.p.)	Cell inactivation; Intracellular calcium overload; Mitochondrial damage	[110]
				Oxidative stress	

ALP: Alkaline phosphatase, ALT: Alanine aminotransferase, AST: Aspartate aminotransferase, Bax: Bcl-2 associated X protein, Bcl2: B-cell lymphoma 2, CHOP: C/EBP Homologous Protein, CRP: C reactive protein, IgG: Immunoglobulin G, eIF2α: Eukaryotic initiation factor 2 α, GADD153: Growth arrest and DNA damage 153, Grp 78/94: Glucose regulated protein 78/94, IgG: Immunoglobulin G, IL-6: interleukin 6, JNK: Jun N-terminal kinase, LDH: Lactate dehydrogenase, MAPK: Mitogen activated protein kinase, NO: Nitric oxide, p38: Protein kinase, pdi-3: Protein disulfide isomerase -3, PERK: Protein kinase RNA like ER kinase, STAT-3: Signal transducer and activator of transcription 3, TNF-α: Tumor necrosis factor α, IL-6: Interleukin 6; xbp-1: X box binding protein-1.

intracellular calcium load along with weaker antioxidant level, and severe histopathological distortions. The expression pattern of differentially expressed genes and their transcripts are more for ZnONPs[110]. A recent study confirms the cytotoxic and genotoxic potentiality of ZnONPs in HepG2 cells in 2D and 3D culture after 24 h of exposure[111]. In dogs overused ZnONPs enhanced zinc accumulation in the liver with elevated serum liver indexes along with ROS generation and altered mitochondrial function. Strikingly ZnONPs attenuated apoptosis *via* the cytochrome c pathway instead, it induced autophagy through activating the mTOR/ATG5 pathway. Also involved in the disruption of the intestinal microbiome and 81 liver metabolites[112]. ZnO NPs induce crosstalk between protective autophagy and pyroptosis in hepatocytes. TFEB-mediated regulation influences ZnO NP-induced pyroptosis, with TFEB knockout exacerbating and overexpression alleviating it. TRAF-6 is identified in TFEB-mediated global regulation[113]. TFEB-regulated autophagy and lysosome prevent ZnO NPs-induced hepatocyte pyroptosis, providing insights for risk assessment and therapeutic strategies[113]. ZnO NPs also widely used in various applications, induce oxidative stress, leading to NLRP3-ASC-Caspase-1 complex assembly and pyroptosis in rat liver and HepG2 cells[114]. Inhibiting oxidative stress protects against ZnONPs-induced pyroptosis in hepatocytes, revealing a novel mechanism and potential clinical treatment strategies[114].

Titanium dioxide nanoparticles: Several major effects and molecular mechanisms underlying hepatotoxicity due to TiO_2 NP exposure have been reported in both *in vitro* and *in vivo* studies. Titanium dioxide exists in different commercially available forms. The natural one is an agglomerated, rod-shaped rutile form and the other is a glomerated metastable form, the anatase. Chen *et al*[115], in a study proved that both forms can significantly activate inflammatory signaling pathways like mitogen-activated protein kinase (MAPK) and NF-κB in HepG2 cells with reduced cell viability and ultrastructural alterations, though rutile form has more cytotoxic effect. In 80 CD-1 (ICR) mice, intragastric administration of TiO_2NPs resulted in increased expressions of Toll-like receptors (TLR2 &TLR4) and inflammation-related genes (IKK1, IKK2, NF-kB, NF-kBP52, NF-kBP65, TNF-α, NIK) with decreased expressions of IkB and Il-2 indicating TLRs/NIK/IkB kinase/NF-kB/TNF-α signaling pathway mediated inflammation in liver. At higher doses significant changes in liver coefficient, biochemical parameters (ALT, AST, ALP, LDH, pseudocholinesterase, leucine acid peptide) along with

Table 6 Effects and molecular mechanisms underlying TiO_2NPs induced hepatonanotoxicity

NPs	Size	Tested model	Dose & route of administration	Effects & mechanism	Ref.
TiO_2NPs (Anatase)	7 nm (XRD)	80 CD-1 (ICR) mice	5, 10, 50 mg/kg b.w. every other day for 60 d (i.g.)	SOD, CAT, GSH-Px, MT, HSP70, GST (downregulation); CYP1A (upregulation)	[117]
				Oxidative stress, apoptosis	
TiO_2NPs (Anatase)	5 nm (XRD)	CD-1 (ICR) mice	5, 10, 50, 100, 150 mg/kg b.w. daily for 14 d (abdominal injection)	Accumulated in liver DNA; Inserted in DNA base pairs; Binds to DNA nucleotides; Alter DNA secondary structure; Liver DNA cleavage at higher dose	[119]
				Genotoxicity	
TiO_2NPs	< 25 nm anatase; < 100 nm rutile (SEM)	HepG2 cell	1, 10, 100 and 250 mg/mL incubated for 4, 24, 48 h	p21, mdm2, p53, gadd45α (increased expression); DNA strand break; DNA damage; ROS production	[120]
				Genotoxicity	
TiO_2NPs (Anatase)	5 nm (XRD)	80 CD-1 (ICR) mice	5, 10, 50 mg/kg b.w. for 60 d (i.g.)	TLR2, TLR4, IKK1, IKK2, NF-kB, NF-kBP52, NF-kBP65, TNF-α, NIK (upregulation); IkB, IL-2 (downregulation); ALT, AST, ALP, LDH, PCh, LAP (upregulation)	[116]
				Inflammation, apoptosis	
TiO_2NPs (Anatase & rutile)	Anatase –561.63 ± 26.26 nm; Rutile – 206.22 ± 2.18 nm (TEM)	HepG2 cell	5-320 μg/mL for 24 h	ERK1/2, p38 (increased phosphorylation); TNFα (upregulated); A20 (downregulated); Activation of MAPK & NF-kB pathway	[115]
				Inflammation	
TiO_2NPs; Rutile anatase; P25 (anatase: rutile = 75:25)	Rutile – 50 nm; Anatase – 50 nm; P25 – 21 nm (TEM)	Primary hepatocytes of Sprague Dawley rats	50 μg/mL, 72 h	ROS (upregulated); Urea, albumin, MnSOD, MMP, Mfn 1, Opa 1 (downregulated)	[122]
				Perturbation of mitochondrial dynamics, oxidative stress	
TiO_2NPs; Rutile	12-18 nm (TEM)	BRL 3A cells; sprague dawley rats	0.1-100 μg/mL for 6 h; 0.5-50 mg/kg BW intraperitoneal injection 24 h	Rapid G0/G1 to S transition, G2/M arrest; ALT, AST, ALP, LDH (upregulated)	[123]
				Hepatocytes with oxidative stress show more cytotoxicity	
TiO_2NPs; Anatase	10 (TEM)	B6C3F1 mice	50 mg/kg b.w. daily for 3 d (i.p.)	DNA strand break nucleotide oxidization; MT1H, MT1E (upregulation); Differential gene expression(increased)	[121]
				Oxidative stress, Genotoxicity, metabolic imbalance	
TiO_2NPs; Anatase	19 (XRD)	Wistar rat	100 mg/kg daily for 60 d (oral)	ALT, AST, ALP, LPO (increased); GSH, SOD, GPx, CAT (decreased); vacuolization, Sinusoidal dilation, inflammatory cells infiltration	[124]
				Oxidative stress	
TiO_2NPs; Anatase	10 nm (TEM)	Albino rats	100 mg/kg daily	ALT, AST, ALP, Bax, LPO (increased); GPx, SOD, GSH, Bcl-2, (decreased); hepatic apoptosis; Sinusoidal dilation, infiltration inflammatory cells, steatosis, hepatocellular necrosis	[125]
			60 d (oral)	**Oxidative stress**	
TiO_2NPs; anatase: Rutile (80: 20)	20 nm (TEM)	Wistar rat	300 mg/kg daily for 2 wk (oral)	ALT, AST, ALP, LDH, TNFα, NF-Kβ, TOS, LPO (upregulated); SOD, CAT, GPx, TAC (downregulated)	[118]
				Inflammation, Oxidative stress	
TiO_2NPs; Anatase	29 ± 9 nm (SEM)	Sprague dawley rats	2, 10, 50 mg/kg b.w. daily	LPO, GPx, SOD, GSSG, IL-1α, IL-4 and	[126,127]

			for 90 d (oral)	TNFα (increased); GSH (decreased); Mitochondrial swelling increased gut microbiota altered glycerophospholipid, Phosphatidylcholines metabolism; Hepatotoxicity indirectly through gut liver axis **Oxidative stress, inflammation**

A20: Alpha-induced protein-3; ALP: Alkaline phosphatase; ALT: Alanine aminotransferase; AST: Aspartate aminotransferase; Bax: Bcl-2 associated X protein; Bcl2: B-cell lymphoma 2; CAT: Catalase; CYP1A: Cytochrome p450 1A; DNA: Deoxy ribonucleic acid; ERK1/2: Extracellular signal-regulated protein kinases 1 and 2; gadd45α: Growth arrest and DNA damage 45 alpha; GPx/GSH-Px: Glutathione peroxidase; GSH: Glutathione; GSSG: Glutathione disulfide; GST: Glutathione S transferase; HSP70: Heat shock protein 70; IkB: Inhibitor kappa B; IKK1,2: IκB kinase; IL-1α: Interleukin 1 alpha; IL-2,4: Interleukin-2,4; LAP: Leucine acid peptide; LDH: Lactate dehydrogenase; LPO: Lipid peroxidation; MAPK: Mitogen activated protein kinase; mdm2: Murine double minute 2; Mfn 1: Mitofusin 1; MMP: Mitochondrial membrane potential; MnSOD: Manganese superoxide dismutase; MT: Metallothionein; MTIE: Metallothionein 1E; MTIH: Metallothionein 1H; NF-kB: Nuclear factor kappa beta; NIK: NF-κB-inducible kinase; Opa 1: Optic atrophy 1; p21: Cyclin-dependent kinase inhibitor 1; p38: Puncture38; p53: Tumor suppressor protein p53; PCh: Pseudocholinesterase; ROS: Reactive oxygen species; SOD: Superoxide dismutase; TLR2/4: Toll like receptor 2/4; TNF-α: Tumor necrosis factor α; TOS: Total oxidant status.

Table 7 Effects and molecular mechanisms underlying MgONPs induced hepatonanotoxicity

NPs	Size	Tested model	Dose & route of administration	Effects & mechanism	Ref.
MgO	-	3D Human Liver organoids male Sprauge Dawley rat	100 µg/mL incubated for 48 h. 40 mg/kg daily for 4 wk (oral)	ATP synthesis (decreased); ROS & Super oxide production (increased); ALT, AST (increased) **Oxidative stress**	[21]

ALT: Alanine aminotransferase; AST: Aspartate aminotransferase; ATP: Adenosine triphosphate; ROS: Reactive oxygen species.

Table 8 Effects and molecular mechanisms underlying Al_2O_3NPs induced hepatonanotoxicity

NPs	Size	Tested model	Dose & route of administration	Effects & mechanism	Ref.
Al_2O_3	< 50 nm	Developing chicken embryo, HepG2 cell culture model	10, 20, 40 µg/egg *via* injection from 8th to 12th day of incubation on an alternate day basis, 05, 10, 20 µg/mL for 12 h	ROS & Super oxide production (increased); ALP, ALT, AST activity (increased); HO-1, NQO-1 level (increased); Cell viability (decreased); SOD, CAT, GPx, TBARS, TNF-α, Caspase-3 activity (decreased) **Oxidative stress and cytotoxicity**	[128]

ALP: Alkaline phosphatase; ALT: Alanine aminotransferase; AST: Aspartate aminotransferase; HO-1: Heme oxygenase-1; NQO-1: NAD(P)H quinone oxidoreductase 1; SOD: Superoxide dismutase; CAT: Catalase; GPx: Glutathione peroxidase; TBARS: Thiobarbituric acid reactive substances; TNF-α: Tumor necrosis factor α; ROS: Reactive oxygen species.

Table 9 Effects and molecular mechanisms underlying Cr_2O_3NPs induced hepatonanotoxicity

NPs	Size	Tested model	Dose & route of administration	Effects & mechanism	Ref.
Cr_2O_3-NPs	22.50 + 1.76 nm (TEM)	Wistar rats	50 mg/100 g bwt (LD), 200 mg/100 g bwt (HD); single dose for 1, 7, 14 d (oral)	ALT, AST, ALP, γGT, total bilirubin (increased)	[23]

ALP: Alanine phosphatase, ALT: Alanine aminotransferase, AST: Aspartate aminotransferase, HD: High dose, LD: Low dose, γGT: Gamma glutamyltransferas.

mitochondrial swelling, apoptotic body formation, chromatin condensation, inflammatory cell infiltration suggests liver tissue injury caused by inflammation that in turn trigger activation of apoptosis[116]. The same group showed that TiO_2 NPs insult leads to ROS accumulation, over-expression of cytochrome p450 1A, and suppressed expression of stress-related genes (SOD, CAT, GSH-Px, MT, HSP70, GST), and NPs detoxifying/metabolizing genes[117]. Other investigation result shows that TiO_2NP ingestion at higher doses for longer periods leads to Kupffer cells hypertrophy, hydropic degeneration and vacuolization in hepatocytes, necrosis around the central vein followed by edema, infiltration of inflammatory cells along reduced antioxidant enzymes. Elevated levels of liver enzymes, higher lipid peroxidation, and upregulated expressions of inflammatory mediators (TNFα and NF-Kβ) suggest hepatic damage due to oxidative stress

Table 10 Effects and molecular mechanisms underlying iron oxide NPs induced hepatonanotoxicity

NPs	Size	Tested model	Dose & route of administration	Effects & mechanism	Ref.
Na-oleate coated Fe_3O_4	8 ± 3 nm (TEM)	Wistar rat	0.0364, 0.364, & 3.64 mg/kg b.w. for 1 d, 1, 2, 4 wks (i.v.)	Temporary change in mitochondrial respiration; GPx, GST (increased); Lipidosis, mild necrosis; Enlarged sinusoid space **Oxidative stress**	[133]
Polyethylene glycol – 8000 coated Fe_3O_4	8.82 ± 0.70 nm (TEM)	Wistar rat	10 mg/kg b.w. single dose, once in a week, twice in a week for 30 d (i.v.)	ALT, AST, ALP (slightly increased); AST, LPO, SOD, GPx, Neutrophil count (increased); No significant tissue damage	[135]
Fe_3O_4	20 nm (TEM)	Wistar rat	40 mg/kg b.w. for 14 d (i.t.)	Congestion of sinusoid; Hepatocytic ballooning; Mononuclear cell infiltration; Tissue damage **Inflammation**	[132]
Fe_3O_4	41.3 ± 5.9 nm for USPIO, 112.6 ± 38.4 nm for SPIO (DLS)	L-02 cells	2.5, 5, 10, and 20 μg/mL) for 12 h	Cell survivility (decreased); Elevated expression of Genes related to acute phase inflammation, ER stress. HSP70, IL-6, PERK, ATF4, ER Ca^{++} (increased); USPIO show higher toxicity than SPIO **ER stress, inflammation**	[136]
Fe_3O_4	10 nm (TEM)	Hepatocytes of Lewis rat in sandwich culture model	100, 200, 400 μg/mL, single dose & cumulative dose; 24 h to 7 d	Cell survivility (decreased); ROS (increased); Albumin & urea synthsis (decreased) **Oxidative stress**	[134]
Fe_3O_4	29.6 ± 12.2 nm (TEM)	Albino wistar rat	30, 300, 1000 mg/kg b.w. for 28 d (nano & bulk) (oral)	GSH, CAT (decreased); SOD, GR, GST, LPO (increased); GPx (unchanged); Congested central vein in higher dose **Oxidative stress**	[130]
Fe_2O_3	30 nm (TEM)	Wistar rat	100, 200 mg/kg single dose (oral)	ALT (increased) iron deposition in hepatocyte & Kupffer cells Inflammation	[131]
Fe_2O_3	30 nm (TEM)	L-02 cells; BALB/C mice	2.5, 7.5, and 12.5 lg/mL) for 1, 3, 6 h; 20 mg/kg body weight for 24 h. (i.v.)	Cox2 (overexpression); COX-2 interaction with IP3R-GRP75-VDAC1 complex; Ca++ transfer increased; Bax, Cleaved Casp-3 (increased); Bcl2 (decreased) **Apoptosis**	[137]

ALP: Alanine phosphatase; ALT: Alanine aminotransferase; AST: Aspartate aminotransferase; Atf4: Activating transcription factor 4; Bax: Bcl-2 associated X protein; Bcl2: B-cell lymphoma 2; Ca++: Calcium ion; CAT: Catalase; COX-2: Cyclooxygenase-2; ER: Endoplasmic reticulum; GPx: Glutathione peroxidase; GR: Glutathione reductase; GRP75: Glucose regulated protein 75; GSH: Glutathione; GST: Glutathione S-transferase; HD: High dose; HSP-70: Heat shock protein 70; IL-6: Interleukin-6; IP3R: Inositol 1,4,5 triphosphate receptor; LD: Low dose; LPO: Lipid peroxidation; PERK: Protein kinase RNA like ER kinase; ROS: Reactive oxygen species; SOD: Super oxide dismutase; SPIO: Superparamagnetic iron oxide; USPIO: Ultra-small superparamagnetic iron oxide; VDAC1: Voltage-dependent anion channel 1; γGT: Gamma glutamyl transferase.

and inflammation[118].

Different spectral analyses and gel electrophoresis results of *in vivo* experiments unveil that liver DNA is a prime target of TiO_2NPs. In liver DNA, anatase form get accumulates either by inserting itself between base pairs or directly binding to 3 oxygen or nitrogen atoms [Ti-O(N)=1.87A] and 2 phosphorous atoms (Ti-P=2.38A) of nucleotide, affecting the configuration of DNA secondary structure. DNA laddering in gel slab at a higher dose of 150 mg/kg can be corroborated with liver DNA cleavage by NPs[119]. *In vitro* study with HepG2 cells also exhibited oxidative stress-induced DNA damage for both rutile and anatase forms. Elevated expression level of p53 and subsequent upregulated expression pattern of downstream DNA damage responsive genes (p21, mdm^2, gadd45α) confirms the TiO_2NPs mediated genotoxicity in hepatocytes[120]. Gene expression analysis and genotoxicity assessment demonstrated similar results, that TiO_2NPs promote oxidization of nucleotides which results in DNA strand break (DNA damage). Also disturbs the metabolic homeostasis of the liver through oxidative and stress-related impairment of glucose, lipid, and xenobiotic metabolism [121].

When primary hepatocytes were given exposure to rutile, anatase, and P25 (mixture of rutile & anatase) NPs, all three significantly exhibited hepatotoxicity. The Mitochondrial morphology and dynamics get compromised due to the downregulation of the fusion process, which leads to mitochondrial fragmentation in hepatocytes. Over production of ROS and subsequent loss of MnSOD enzyme activity and reduced MMP leads to oxidative stress that hampers the normal functionality of liver cells including biosynthesis of urea and albumin[122]. In a remarkable *in vitro* as well as *in vivo* experimentation Sha *et al*[123] click or tap here to enter text. Have proven that liver cells already in oxidative stress condition exhibit more susceptibility towards nano-TiO_2 mediated cytotoxicity. In contrast to G0/G1 phase arrest under only NM exposure, BRL-3A cells with prior oxidative stress conditions exhibited very fast G0/G1 phase to S transition, G2/M arrest with elevated cell death ratios. Increased expression levels of liver marker enzymes (ALT, AST, ALP, LDH) under the same experimental regime in an *in vivo* study indicated liver damage with prominent histopathological perturbation. Micro-TiO_2 didn't show such effects both in cells and rat liver. Again, in different studies orally administered thymol and tiron were seen to ameliorate TiO_2NPs mediated lipid peroxidation (LPO), oxidative stress, non-enzymatic and enzymatic alterations of antioxidant levels, augmentation of proapoptotic and downregulation of antiapoptotic genes along with biochemical and histopathological changes in liver tissue. Supporting hepatic injury by TiO_2NPs is mediated by oxidative stress and apoptosis[124,125].

In a dose-dependent manner TiO_2NPs treated rats show an increment in diversity and abundance of gut microbiota (*Firmicutes, Bacteroidetes, Tenericutes, Proteobacteria, etc*.) that has been found to produce a significant quantity of lipopolysaccharides and increased number of *Lactobacillus reuteri* but not *Romboutsia* in feces. On the contrary, it produces mitochondrial swelling, and an imbalance in oxidation/antioxidation status with the generation of altered metabolites (Glutamate, glutamine, and glutathione) in connection to energy-related metabolic disorders. Therefore, it can be predicted from the results that the indirect pathway of the gut-liver axis may play an important role, in connecting gut microbiota and liver metabolism. Subsequent investigation confirms that the gut microbiota under oxidative stress led to lipid metabolism disorders (glycerophospholipid and phosphatidylcholines) and caused liver toxicity *via* the gut-liver axis[126,127].

Mg-nano nanoparticles: In a recent experiment, researchers have tried to verify the hepatotoxic potentiality of Mg-nano in combination with valproate (anticonvulsant drug) and PTZ (pentylenetetrazole- used to induce convulsion mouse model) using 3D liver organoid and rat model. In the *in vitro* model the prepared suspension carrying Mg-nano decreased the production of ATP and increased ROS generation and super oxide production while *in vivo* result showed a significant increase of ALT, AST in serum but without any change in albumin or globulin concentration, suggesting Mg-nano as well as Valporate both can induce hepatotoxicity[21].

Aluminium oxide nanoparticles: Aluminum oxide nanoparticles (Al_2O_3-NPs) pose hepatotoxic effects on chicken embryos and cell cultures, inducing histological abnormalities, elevating tissue damage markers, causing oxidative stress, and impacting antioxidant enzymes[128]. Additionally, Al_2O_3-NPs affect red blood cells, liver metabolism, and stress response gene expression. The study reveals dose-dependent ROS generation, cytotoxic responses, and potentiating effects on TNF-α-induced apoptosis. Inhibition of p38 MAPK and JNK pathways modulates Al_2O_3-NPs-induced apoptosis in HepG2 cells, highlighting novel mechanisms and potential prevention strategies[128].

Chromium oxide nanoparticles: The investigated liver function biomarkers (ALT, AST, ALP, γgamma glutamyl transferase, total bilirubin levels) get elevated in a dose and exposure time-dependent fashion in rats after orally consuming Cr_2O_3-NPs. Routine histological examination clearly showed moderate to severe architectural damage including liver cell degeneration, Kupffer cell hyperplasia, parenchymal distortions, dilated central vein, and hemorrhage for both low and high doses, indicating the role of chromium oxide-NPs in liver toxicity[23].

Iron oxides nanoparticles: The bioavailability of nano iron oxide was found to be greater compared to bulk in different organs, including the liver[24,129]. Similarly, nano magnetite (Fe_3O_4) showed higher bioaccumulation, oxidative stress, and liver tissue damage than its bulk counterpart in another experiment also[130]. Orally administered nano maghemite (Fe_2O_3) was found deposited in hepatocytes and kupffer cells, resulting in very little perturbation of biochemical parameters with minimum effects on the liver[131]. Histopathological study revealed infiltration of mononuclear cells, ballooning, and hepatic damage with congestion in sinusoids but surprisingly with a decreased level of ALT during the investigation of concurrent effects of aerobic exercise and IONPs in liver enzymes of the treated subject[132]. In the rat model administration of coated Fe_3O_4 caused mild liver tissue injury with an altered antioxidant enzyme profile, suggesting oxidative stress-related response[133]. Similarly, increased ROS production and decreased cell viability with hampered albumin and urea synthesis in a dose-dependent manner was evident from another study with primary hepatocytes[134]. On dose interval treatment with PEG-8000 coated ultra-small superparamagnetic iron oxide nanoparticles, have shown temporary alterations in the liver biomarkers and hematological parameters, with lipid peroxidation[135]. In a separate experiment, USPIO was found to exhibit more toxic effects on liver tissue than SPIO. In USPIO treated L-02 cells, upregulated expressions of IL-1B, IL-6, IL-18, TNFSF12, TNFRSF12, SAA1, SAA2, JAK1, STAT5B, and CXCL14 genes with increased secretion of Il-6 and altered ER structure due to ER stress supports the occurrence of ER stress-mediated acute-phase inflammatory response that leads to cytotoxicity. Application of ER stress blocker or ATF4 siRNA attenuated the USPIOs effects supporting the involvement of PERK/ATF4 pathway[136]. MAMs [Mitochondria-associated endoplasmic reticulum (ER) membranes], a dynamic microdomain made up of proteins that maintain crosstalk between ER and mitochondria, play a crucial role in Ca^{++} ion and metabolite transfer between two organelles and cellular homeostasis. Both *in vitro* and *in vivo* results suggest SPIO-Nps (iron oxide) accumulation in hepatocytes triggers the overexpression followed by interaction of COX-2 with IP3R-GRP75-VDAC1 complex (inositol 1,4,5 triphosphate receptor, glucose-regulated protein 75, voltage-dependent anion channel 1), the fraction of MAMs that

facilitates Ca^{++} transfer. Thereby resulted in profuse Ca^{++} transfer from ER to mitochondria, producing Ca^{++} overload in mitochondria that sparks apoptosis in hepatocytes[137].

Orally administered nano-iron oxide, commonly used in food, disrupts the small intestinal barrier, leading to hepatic lipid metabolism disorders through the gut–liver axis. This disruption causes hepatic damage and iron deposition, impacting lipid homeostasis with decreased phosphatidylcholine and phosphatidylethanolamine and increased triglyceride levels. The study highlights the subchronic toxicity of nano-iron oxide and emphasizes the pivotal role of the gut-liver axis in its hepatotoxicity[138]. Fe_2O_3 nanoparticles (E172 food additive) exhibit no evident toxicity in body weight, histopathology, or oxidative stress in animal experiments. However, a sensitiveLC–MS/MS-based lipidomic study reveals significant alterations in hepatic glycerophospholipid metabolism, including decreased triacylglycerol and increased phosphatidylcholine. This study enhances understanding of the subacute effects of Fe_2O_3 NPs beyond conventional toxicology assessments[139].

Graphene oxide nanoparticles

Because of its special physico-chemical characteristics, graphene oxides are easily produced and tailored to order. They have a wide range of uses in the fields of electronics, nanomedicine, textiles, water purification, nanocomposite, and catalysis[140-143]. Several investigations unveiled the subacute toxicity caused by GO in different organs including the liver[144,145]. Patlolla *et al*[146] showed that in an SD rat model, GO-induced liver inflammation was associated with lower levels of cholesterol, HDL, and LDL. A separate study with a similar model revealed oxidative stress in accordance with the enhanced ROS production, increased activity of AST/GPT, ALT/GOT, alkaline phosphatase, and lipid hydro peroxide with structural alterations in hepatocytes. Varied degrees of histopathological modifications (sinusoidal abnormality, inflammation around portal and central vein, hepatocytic vacuolation) with an elevated level of serum enzyme markers and alterations in MDA, CAT contents concerning oxidative stress indicate GO-induced hepatotoxicity in Wistar rat[147] GO induced mild early apoptosis and inhibited phase-I drug-metabolism enzymes (CYP3A4, CYP2C9) in upcyte® hepatocytes[148]. Notably, CYP3A4 impairment coincided with an acute-phase response activation. The study highlights the potential health consequences of drug detoxification[148]. Follow Table 11 for a comprehensive account.

Carbon nanotubes nanoparticles

Carbon nanotubes are of two types, single-walled (SWCNTs) with one layer and multi-walled (MWCNTs) with multiple layers. When acid-oxidized MWCNTs (O-MWCNTs) and Tween-80-dispersed MWCNTs (T-MWCNTs) were administered intravenously to mice bodies both types showed inflammatory responses and oxidative stress-mediated liver toxicity. Compared to O-MWCNTs (with carboxyl group), T-MWCNTs (without carboxyl group) exhibited greater effects suggesting hepatotoxicity might be dependent on modification of carboxyl group. Whole genome-wise expression array revealed, upregulated expression of genes related to TNF-α, NF-κB signaling pathway, NK cell-mediated cytotoxicity, biosynthesis of cholesterol, metabolism by cytochrome P450, GPCRs (G protein-coupled receptors) were recorded for both the treatments[149].

NMR-based metabonomic study unveiled disruption of important metabolic pathways in rat model receiving SWCNTs. Decreased alanine but increased lactate concentration in plasma indicates impairment of amino acid metabolism. Similarly, decreased level of lipoproteins, and lipids together with the rise in choline, and phosphocholine in serum and liver extract support the disruption of membrane fluidity due to lipid peroxidation. All these strongly support nanotubes-induced hepatic injury through the modulation of energy, amino acid, and lipid metabolism[150].

Several investigations have revealed that MWCNT resulted in increased ROS production (H_2O_2), and LPO with a compromised antioxidant defense system (SOD, GPx, GSH, GST), suggesting oxidative stress-mediated hepatotoxicity[4,151,152]. In a series of experiments, Patlolla *et al*[153] and Patlolla *et al*[154] had shown that in a dose-dependent manner both carboxylated functionalized carbon nanotubes (SWCNT and MWCNT) exposure to mice resulted in ROS-mediated oxidative stress in association to increased liver biochemical markers and tissue damage.

Again, MWCNT exposure was found to stimulate pro-inflammatory cytokines (IL-6, IL-1B, COX-1, TNF-α), that serve as an inflammatory mediator to elicit inflammatory responses in the liver[4,151,152]. In an *in vivo* toxicity study, administration of both P- MWCNT (PEGylated) and NP- MWCNT (non-PEGylated) exhibited induction of hepatic inflammation through TNF-α and NF-κB signaling pathway without any oxidative damage to the liver tissue, though NP- MWCNT shows slightly higher toxicity[155]. Orally administered aqueous extract of *Cinnamomum burmannii* was reported to protect the liver against MWCNT assault by downregulating pro-inflammatory cytokine production and ameliorating the antioxidant system. Suggesting nanotubes triggered liver toxicity is due to oxidative stress and inflammation[4].

Histopathological examinations revealed that MWCNT insult produces clear ultrastructural perturbations including cellular swelling, hydropic degeneration, sinusoidal leukocytosis, sinusoidal space enlargement, vacuolar degeneration, inflammatory cell infiltration associated with focal hepatic and focal perivascular hepatic necrosis, spot necrosis, mitochondrial destruction, congested central vein, macrophage injury even blood coagulation[4,155,156].

Cd-MT (accumulated cadmium-metallothionein) mice when treated with oxidized MWCNTs have shown some striking results. Different doses of MWCNT exposure, alone promoted the release of free Cd^{++} from Cd-MT, a portion freely available in circulation for elimination while the other portion adsorbed by MWCNT, stayed together in the tissue. Also, co-exposure alleviated hepatotoxicity compared to single exposure[157]. But co-administration of a higher dose of MWCNTs with PbAc in NAFLD (non-alcoholic fatty liver disease) mice resulted in severe liver damage compared to lower combined or single dose (lower or higher) of MWCNTs or PbAc. Remarkable reduction in body weight, liver function, and augmentation of nonalcoholic steatohepatitis (steatosis, lobular inflammation) phenotype was noticed. MWCNTs alone or in combination were found to induce collagen deposition and lipidosis, which leads to hepatic fibrosis. Primary hepatocytes isolated from co-exposed NAFLD mice exhibited a higher rate of apoptosis followed by

Table 11 Effects and molecular mechanisms underlying GONPs induced hepatonanotoxicity

NPs	Size	Tested model	Dose & route of administration	Effects & mechanism	Ref.
GO	100-500 nm (TEM)	Sprague dawley rats	2.5, 5, and 10 mg/kg/d for 7 d (i.v.)	Liver inflammation; Cholesterol, HDL, LDL (decreased)	[144]
GO	40 nm (TEM)	Sprague Dawley rats	10, 20 and 40 mg/Kg b.w. once for 5 d, (oral)	ROS, AST, ALT, LHP (increased)	[146]
GO	0.8-2 nm (TEM)	Wistar rats	0.4/2/10 mg/kg b.w.	AST, ALP, ALT, MDA (increased); CAT (decreased)	[147]

ALP: Alkaline phosphatase; ALT: Alanine aminotransferase; AST: Aspartate aminotransferase; CAT: Catalase; HDL: High density lipoprotein; LDL: Low density lipoprotein; LHP: Lipid hydro peroxide; MDA: Malondialdehyde; ROS: Reactive oxygen species.

oxidative stress and inflammation. A significant decrease in expression patterns of p-AMPKα and PPARγ at combined low doses but reverse expression pattern in the presence of AMP activated protein kinase (AMPK) activators suggests inhibition of AMPK/PPARγ pathway (adenosine 5'-monophosphate activated protein kinase/peroxisome proliferator-activated receptors γ) may be the reason behind hepatotoxicity[152]. Follow Table 12 for a comprehensive account.

Copper sulfide/cadmium sulfide nanoparticles

In a study using biomimetic synthesis and ion exchange strategy CuS/CdS nanocomposites were synthesized and tested for hepatotoxicity in liver cells and mice models. *In vitro,* study results unveiled that CuS/CdS nanocomposites cause oxidative stress-mediated apoptosis in liver cells which can be correlated with the perturbated intracellular antioxidant defense system in hepatocytes (SOD & GSH) and excessive accumulation of oxidative products (ROS, GSSG, MDA) that resulted into oxidative stress-mediated apoptosis in both hepatoma cells (BEL7402) and normal liver cells (L-02). Though the first one was more responsive than the latter one. Intravenous injection of nanocomposites to Balb/c mice has shown time-dependent accumulation of Cd^{2+} and Cu^{2+} in the liver, spleen, and kidney. Compared to Cu^{2+}, the liver and kidney retained a significant amount of Cd^{2+} which the physiological system was unable to remove[158]. Compared to CdS microparticles CdNPs exhibited more toxic effects in rat liver. Greater bioaccumulation of CdNPs leads to the overproduction of metallothionein and ligand formation that has increased its hydrophilicity, facilitating penetration through hepatocyte membrane and such interactions between membrane and NPs further facilitated ROS generation (H_2O_2, NO) and oxidative stress (lipid peroxidation), disrupting membrane integrity. Biochemical analysis showed increased ALT, AST, and ALP in serum. Ultrastructural study exhibited cytoplasmic degeneration, organellar proliferation (microsome, ER, peroxisome, mitochondria), and extensive parenchymal degeneration suggesting hepatotoxicity[159].

The hepatic bile salt export pump (BSEP) is crucial for secreting bile salts from hepatocytes to bile and the hepatic MRP2 transporter contributes to bile flow, detoxification, and chemoprotection maintaining a healthy liver. Lowered expression of BSEP mRNA and protein followed by diminished activity of BSEP was observed in the CuSNPs treated group while MRP2 function remain unaltered. Hepatocytes also showed spheroid injury with altered ROS and mitochondrial membrane potential[160]. In a separate experiment, different-sized (LNPs - 17.8 nm and SNPs -2.8 nm) copper sulfide nanoparticles ($Cu_{2-x}S$ NPs), biomineralized with Bovine Serum Albumin were administered in SD rats through tail vein to assess safety and liver toxicity. Both the particles were found to intervein important biochemical pathways including, lipid metabolism, cholesterol/bile acid metabolism, copper ion transport/metabolism, inflammatory and drug metabolism-cytochrome P450 pathway. SNPs are discharged through feces, 7 and 14 d after single administration causing manageable liver toxicity, so it could be a promising nano agent. On the contrary LNPs with more retention power in Kupffer cells, were found to be involved in prolonged and delayed liver toxicity[161]. Follow Table 13 for a comprehensive account.

Cobalt nanoparticle

The human fetal liver cell line L02 demonstrated dose- and time-dependent cytotoxicity following exposure to varying doses of Nano-Co for 12 or 24 h. It has been predicted that cobalt nanoparticles reach hepatocyte intracellular regions through both endocytosis-driven and endocytosis-free pathways. This led to the generation of ROS and mtROS (mitochondrial reactive oxygen species), which in turn caused oxidative stress damage. Availability of IL-1β and IL-18 in the extracellular space suggests mtROS-mediated activation of NLRP3 (NOD-like receptor protein 3) inflammosome response, resulting in the upregulation of caspase-1 p20, IL-1β, and IL-18. Thus Nano-Co induced modulation of ROS/NLRP3 pathway was found to be involved in hepatotoxicity[162]. Follow Table 14 for a comprehensive account.

Nanoclay particles

In mice, intra-veinous administration of nanoclay resulted in acute hepatotoxicity. Elevated level of ALT and AST in serum with routine histological study results indicates toxic effects for higher doses (10 or 20 mg/kg). When co-administered with chemical (carbon tetra chloride, paraquat) or drug (cisplatin) exhibited synergistic increment in liver biomarkers compared to their individual effects[163]. Follow Table 15 for a comprehensive account.

Table 12 Effects and molecular mechanisms underlying carbon nanotube induced hepatonanotoxicity

NPs	Size	Tested model	Dose & route of administration	Effects & mechanism	Ref.
MWCNTs	O-MWCNT; T-MWCNT; Length 356 ± 185 nm	Kunming mice	10 and 60 mg/kg b.w. (Iv) sacrificed at 15 & 60 d	GSH, SOD (decreased at 15 days); AST, T-Bil (increased); Spotty necrosis, Infiltration of inflammatory cells in portal region, mitochondrial swelling and lysis; Cyp2B19 (upregulated); Cyp2C50, Gsta2 (downregulated) **Oxidative stress, Inflammation**	[149]
PEGylated; MWCNT	P- MWCNT; NP-MWCNT; Length of less than 1 μm; Diameter of 10-20 nm	Kunming mice	10 and 60 mg/kg b.w. (Iv) sacrificed at 15 & 60 d	Blackish discoloration of the liver (MWCNTs accumulation); AST, Bag4, Gab1 genes (increased); Infiltration inflammatory cells, cellular necrosis, focal necrosis; Mitochondrial swelling/lysis; NP- MWCNT shows more toxicity than P-MWCNT **Inflammation**	[155]
Carboxylated functionalized SWCNT	lengths of 15–20 μm; Diameter of 15–30 nm	Swiss webster mice	0.25, 0.5 & 0.75 mg/kg b.w. per day for 5 d (Ip)	ROS, LHP, ALT, AST, ALP, (increased); Histological alterations **Oxidative stress**	[153]
Carboxylated functionalized; MWCNTs	lengths of 15–20 μm; Diameter of 15–30 nm	Swiss webster mice	0.25, 0.5 & 0.75 mg/kg b.w. per day for 5 d (Ip)	ROS, LHP, ALT, AST, ALP, (increased); Histological alterations **Oxidative stress**	[154]
MWCNTs	Length 5-50 μm; Diameter 20-30 nm (SEM)	Swiss albino mice	10 and 60 mg/kg b.w. (oral) sacrificed at 7, 14, 21, 28 d	SOD, CAT activity (decreased); Macrophage injury, cellular swelling, unspecific inflammation, spot necrosis, blood coagulation. The sinusoid and hepaticvenule diameter increased by the high dose **Oxidative stress**	[156]
SWCNTs	Length several μm; Diameter 0.8-1.2 nm (TEM)	Wistar rat	7.5 (low), 15 (medium), and 22.5 (high) mg/kg b. w. Intratracheal instillation once for 15 d	ALB, ALP, TP, TC (decreased at high conc.); Focal necrosis, inflammatory cell infiltration, Cellular swelling at centrilobular part, membrane fluidity destruction, impaired amino acid & lipid metabolism **Metabolic disruption, Hepatotoxicity**	[150]
Oxidised MWCNTs	Length 1-2 μm; Diameter 10-30 nm (TEM)	Kunming mice (Cd-MT accumulated mice)	500 μg/mouse for 4 h	ALT, AST, TBil, BUN (increased); Released Cd^{++} from Cd-MT; Adsorb a part of free Cd^{++} **Coexpossure ameliorated hepatotoxicity**	[157]
Carboxylated MWCNTs	Length 12 μm; Diameter 11.5 nm (TEM)	Wistar rat	0.25, 0.50, 0.75 and 1.0 mg/kg b.w. for 5 consecutive days (Ip)	ALT, AST, ALP, GGT (increased); LPO, H_2O_2, CAT, GPx, activity (increased); SOD, GST (decreased); IL-6, IL-1β, COX-1, iNOS, TNF-α (increased); micronucleated polychromatic erythrocytes (MNPCE) **Oxidative stress, Inflammation**	[151]
MWCNTs	Polycrystalline; Length 600-700 nm; Size 650 nm	Albino rat	1 g/kg b. w. (oral) 4 wk	LPO, H_2O_2, TT, CATactivity (increased); SOD, GSH, GPx, GST (decreased); IL-6, IL-1β, COX-1, TNF-α (increased); hydropic degeneration focal hepatic & perivascular hepatic necrosis associated with inflammatory cells, infiltration, sinusoidal leukocytosis, vacuolar degeneration, congestion of central vein **Oxidative stress, Inflammation**	[4]
Carboxylated MWCNTs	diameter: 5–15 nm, length: 0.5-2 μm (TEM)	C57BL/6J mice (NAFLD)	MWCNT; LD-10 mg/kg b.w. HD-30 mg/kg b.w. PbAc LD-150 mg/kg b.w. HD-300 mg/kg	Death at high dose on 5th day. ALT, AST, ALP (decreased); Nonalcoholic steatohepatitis lobular inflammation, hepatic	[152]

	b.w. MWCNT+ PbAc, LD-10 mg/kg +150 mg/kg HD-30 mg/kg +300 mg/kg (Intragastrically) daily for 80 d	fibrosis, steatosis, apoptotic induction in primary hepatocytes of NAFLD mice; SOD, GST, GSH (decreased); H_2O_2, GPx, MDA, LPO (increased); Lipid peroxidation; IL-6, IL-1β and TNF-α (inflammatory cytokines) inhibiting AMPK/PPARγ pathway **Oxidative stress, Inflammation**	

ALB: Albumin; ALP: Alkaline phosphatase; ALT: Alanine aminotransferase; AMPK: AMP activated protein kinase; AST: Aspartate aminotransferase; Bag4: BAG cochaperone 4; BUN: Blood urea nitrogen; CAT: Catalase; COX-1,2: Cyclooxygenase-1,2; Cyp2B19: Cytochrome P4502B19; Cyp2C50: Cytochrome P4502C50; Gab1: GRB2 associated binding protein 1; GGT: Gamma glutamyl transferase; GPx: Glutathione peroxidase; GSH: Glutathione; Gsta2: Glutathione S-transferase, alpha2; GST: Glutathione-S transferase; H_2O_2: Hydrogen peroxide; IL-1β: Interleukin-1beta; IL-6: Interleukin-6; iNOS: Inducible nitric oxide synthase; LHP: Lipid hydroperoxide; LPO: Lipid peroxidation; MDA: Malondialdehyde; NAFLD: Non-alcoholic fatty liver disease; O-MWCNT-acid: Oxidized multi-walled CNTs; PPARγ: Peroxisome proliferator-activated receptor-γ; ROS: Reactive oxygen species; SOD: Superoxide dismutase; TBil: Total bilirubin; TC: Total cholesterol; T-MWCNT: Tween-80-dispersed multi-walled CNTs; TNF-α: Tumor necrosis factor alpha; TP: Total protein; TT: Total thiol.

Table 13 Effects and molecular mechanisms underlying CuS/CdS-NPs induced hepatonanotoxicit

NPs	Size	Tested model	Dose & route of administration	Effects & mechanism	Ref.
CdS NPs	5-9 nm (TEM)	Wistar rat	10 mg/kg alternate days for 45 d	Hepatosomatic index (decreased); ALT, AST, ALP, LPO, H_2O_2, NO (increased); GSH (depletion); Cytoplasmic degeneration/coagulation, sinusoidal inflammation, parenchymal degeneratin, mitochondria, peroxisome, microsomes increased in number **Oxidative stress**	[159]
CuS/CdS	8.7 nm	hepatoma cells BEL7402 and L-02 normal liver cells; Balb/c mice	4 mg/kg, i,v injection	SOD, GSH (down regulation); ROS, GSSG, MDA (up regulation) **Oxidative stress**	[158]
$Cu_{2-x}S$	17.8 nm (LNPs); 2.8 nm (SNPs)	Sprague Dawley rats	5 mg/kg through tail vein single dose	ALT, AST, TBA, LDH (increased) ALB (decreased)	[161]

ALB: Albumin, ALP: Alkaline phosphatase, ALT: Alanine aminotransferase, AST: Aspartate aminotransferase, GSH: Glutathione, GSSG: Glutathione disulfid, H_2O_2: Hydrogen peroxide, LDH: Lactate dehydrogenase, LPO: Lipid peroxidation, MDA: Malondialdehyde, NO: Nitric oxide, ROS: Reactive oxygen species, SOD: Superoxide dismutase, TBA: Total bile acid.

Table 14 Effects and molecular mechanisms underlying cobalt NPs induced hepatonanotoxicity

NPs	Size	Tested model	Dose & route of administration	Effects & mechanism	Ref.
Nano-Co	10-40 nm	Normal human liver L02 cells	2.5, 5, 7.5, 10, 20, and 40 μg/mL) for 12 h or 24 h	Modulation of ROS/NLRP3 pathway	[162]

NLRP3: NOD-like receptor protein 3; ROS: Reactive oxygen species.

Nanocellulose modified with oxalate ester

Structural alteration of nanocellulose (CNS) may increase its application but such modification can lead to toxicity. Short-term exposure of Wistar rat to chemically modified CNS (NCD), mainly higher dose showed an elevated level of ALT, and AST in serum, with increased myeloperoxidase (MPO) but decreased CAT, and glutathione peroxidase (GPx) activities, indicating disruption in ROS balance. Further over-expressions of iNOS and Bax in treated groups compared to control suggests oxidative stress-mediated inflammation and induction of apoptosis in hepatocytes[29].

Polystyrene nanoparticles

Polystyrene nanoparticles (PS NP) owe their origin to the degradation of microplastics. In aged -PS NPs (aPS) the oxygen-containing functional groups get increased on its surface. In a recent investigation, comparative toxicity of PS NPs and aPS NPs was done to evaluate their effects on the liver after short-term exposure. Metabolomic, biochemical, and histopathological results reveal that both types of NPs can affect glucose and lipid metabolism through modulating

Table 15 Effects and molecular mechanisms underlying nanoclay, NCD, polystyrene, chytosan induced hepatonanotoxicity

NPs	Size	Tested model	Dose & route of administration	Effects & mechanism	Ref.
Nano-Clay	57.8 ± 12.3 nm & 648.3 ± 232.2 nm	BALB/C mice	1, 5, 10, 20 mg/kg b.w. (Iv) 24 h; Co-administered with Ccl4, paraquat, cisplatin	ALT, AST (increased)	[163]
NCD (modified nanocellulose with oxalate esters)	100 nm (SEM)	Wistar rat	50 & 100 mg/kg b.w. (oral) for 7 d	ALT, AST (increased); CAT, GPx activity (decreased); MPO activity (increased); iNOS, Bax (increased); dialated sinusoidal space, vacuolated hepatocytes, cellular infiltration **Oxidative stress**	[29]
Polystyrene	PS NPs 158.8 ± 1.3 nm; aPS NPs 117.0 ± 1.8 nm (SEM)	ICR mice	50 mg/kg/d (oral) for 7 d	Glucose, HDL-C, TG, TC (increased in blood); LDL-C (decreased in blood); Activation of PI3K/AKT/GLUT4 & SREBP-1/PPARγ/ATGL signaling pathways; TG decomposition; Lipid accumulation (increased); Nuclear pyknosis, blurred intercellular space, central hepatic vein congestion, hepatic ballooning; Compared to PS NPs, aPS NPs showed higher toxicity **Disruption of glycolipid metabolism**	[28]
Chitosan (CsNPs)	18 ± 1 nm (DLS)	BHAL cell	≥ 0.5% w/v for 4 h	Readily internalized; Disrupt membrane integrity; ALT leakage; CYP3A4 enzyme activity (increased); necrotic or autophagic cell death	[27]

ALT: Alanine aminotransferase, aPS: UV aging Polystyrene, AST: Aspartate aminotransferase, ATGL: Adipose triglyceride lipase, Bax: Bcl-2 associated X protein, CAT: Catalase, CYP3A4: Cytochrome P4503A4, GLUT4: Glucose transporter 4, GPx: Glutathione peroxidase, HDL-C: High-density lipoprotein, iNOS: Inducible nitric oxide synthase, LDL-C: Low-density lipoprotein, MPO: Myeloperoxidase, NLRP3: NOD-like receptor protein 3, p-AKT: Phosphoprotein kinase B, PI3K: Phosphatidylinositol 3-kinase, PPARγ: Peroxisome proliferator-activated receptor-γ, PS: Polystyrene, ROS: Reactive oxygen species, SREBP-1: Sterol regulatory element binding protein-1, TC: Total cholesterol, TG: Triglyceride.

PI3K/AKT/GLUT4 and SREBP-1/PPARγ/ATGL signaling pathways respectively. Increased glucose but decreased lipoprotein concentration in serum indicates NPs mediated glycolipid metabolism disruption that provokes the exposed mice to self-regulate various lipoprotein levels in serum. Pyknotic nucleus, congested central vein, unclear sinusoids. vacuolation, hepatocyte ballooning suggests polystyrene NPs mediated liver toxicity[28].

Chitosan nanoparticles

Chitosan molecules being considered biocompatible have been tested for liver toxicity. Compared to the chitosan molecule, CsNPs showed higher cellular uptake though having poor cell adhesiveness. Availability of more ALT in the extracellular space of BHAL cells after 4 h of exposure indicates loss of membrane integrity. In a concentration-dependent manner CYP3A4 activity was seen to increase suggesting activation of defence mechanism for clearance of CsNPs. Also, it caused significant damage to the nucleus and cytoplasm, indicating necrotic cell death of hepatocytes[27].

Hydroxyapatite nanoparticles

Hydroxyapatite NPs (HANP) showed antitumor activity in HepG2 cells within a range of 20-80nm particle size. Its cellular uptake and nuclear localization followed by efficacy was found to diminish with increasing particle size. Treated cells exhibited caspase-3, and caspase-9 activation with increased proapoptotic markers (Bax, Bid) and with a concomitant decrease in Bcl-2 and cytochrome c release from mitochondria to the cytoplasm, confirmed HAPN-mediated activation of mitochondrial-dependent apoptotic pathway[164]. A similar result was documented in another *in vitro* experiment, where incubation of buffalo rat liver (BRL) cells with 80 nm HANPs at 200 μg/mL, exhibited diminished cell viability, LDH leakage, induced apoptosis, and necrosis, and MAPK pathway-mediated cytotoxicity. *In vivo*, study results showed infiltration of inflammatory cells near the portal area, increased WBC count, ALT, AST, and TNF-α in serum of treated rats with increased levels of H_2O_2, MDA suggesting HANPs induced oxidative stress-related liver injury[165]. Follow Table 16 for a comprehensive account.

Quantum dots

Mice with both acute and chronic exposure to cadmium selenium (CdSe) QDs showed predominant liver accumulation. Enlarged central vein and disordered hepatic cords were observed for chronic exposure only. In contrast the *in vitro* study unveiled that, Hepa 1-6 cells (murine liver cells) became condensed and decreased in size while J774A.1 cell (macrophage -substitute for Kupffer cell) became condensed and round. Beta-mercaptoethanol (β-ME) pretreatment was found to attenuate the QDs-induced increase of MDA level, suggesting QDs-induced oxidative stress in the liver involves the production of free radicals with compromised ROS scavengers (GSH-Px) that have provoked cytotoxicity in hepatocytes and macrophages, potentiating impairment of cellular differentiation without causing any death[166]. Similarly, perturbated redox homeostasis in mice treated with Cd/Se/Te-based quantum dot 705 has been documented. Increased levels of copper, zinc, and selenium with trace elements and their corresponding transporters (ZIP8, ZIP14, and CTR-1),

Table 16 Effects and molecular mechanisms underlying hydroxyapatite nanoparticles induced hepatonanotoxicity

NPs	Size	Tested model	Dose & route of administration	Effects & mechanism	Ref.
Hydroxyapatite nanoparticles	50 nm (XRD)	HepG2 cells; L-02 cells	100 μg/mL for 24, 48 h	Caspase-3, 9 (activated); Bax, Bid (upregulated); Bcl-2 (downregulated); Cytosolic appearance of cytochrome c **Apoptosis**	[164]
Hydroxyapatite nanoparticles	80 nm (TEM)	BRL cells; Sprague–Dawley rat	25, 50, 100, 200, 400 and 800 μg/mL for 1 h; 50 mg/kg (Iv) single dose, sacrificed at 48 h	Decreased cell viability; Increased LDH leakage; Induced apoptosis & necrosis; MAPK signaling pathway activation; WBC count, ALT, AST, TNF-α, H_2O_2, MDA (increased); Infiltration of inflammatory cells near portal area **Oxidative stress, inflammation, apoptosis, necrosis**	[165]

ALT: Alkaline phosphatase; AST: Aspartate aminotransferase; Bax: Bcl-2 associated X protein; Bcl2: B-cell lymphoma 2; Bid: BH3 interacting-domain death agonist; H_2O_2: Hydrogen peroxide; LDH: Lactate dehydrogenase; MAPK: Mitogen activated protein kinase; MDA: Malondialdehyde; TNF-α: Tumor necrosis factor alpha.

over-expressed oxidative stress markers (heme oxygenase-1 expression, 8-oxo-7,8-dihydro-2¢-deoxyguanosine) along with reduced SOD, GPx activity, GSH/GSSG ratio indicates oxidative stress. Also upregulated pro-inflammatory mediators (Il-6, TNF-α) and liver markers (ALT, AST) signify liver damage due to oxidative stress-mediated inflammatory response[167]. CdSe/ZnS QDs were also reported to induce oxidative stress, inflammation, pyroptosis, and liver dysfunction. Application of Z-YVAD-FMK (caspase-1inhibitor), 2-APB (Ca^{2+} channel blocker), BAPTA-AM (intracellular Ca^{2+} chelator), NAC (a total ROS scavenger), Mito-TEMPO (a mtROS scavenger) and further silencing NLRP3 was reported to alleviate QDs mediated pyroptosis of hepatocytes, confirming the underlying mechanisms includes intracellular Ca^{2+} mobilization that triggered mtROS generation and subsequent activation of NLRP3 inflammosome leading to caspase-1mediated pyroptosis. A similar result was in agreement when NLRP3 knocked out mice exposed to QDs[168]. On the contrary except QDs accumulation in mitochondria, lysosome, and lipid droplets no significant signs of liver damage were observed when Kunming mice were subjected to Mn-doped ZnS QDs and polyethylene glycol-coated QDs exposure[169]. Similarly except slight increment of liver markers (ALT, AST, ALP) in serum, no such remarkable liver tissue damage was recorded in mice exposed to cadmium-free inidium-based QDs[25]. Again, cadmium telluride (CdTe) QDs administration was found to elevate oxidative stress in AML 12 (murine hepatoma cells alpha mouse liver 12) and mice model, concomitant increased expression pattern of the tumor-suppressor gene (p53), proapoptotic gene (Bax) and decreased level of antiapoptotic marker (Bcl-2) suggests activation of mitochondria-mediated apoptotic pathway in hepatocytes. NF-E2-related factor 2 (Nrf2) deficiency was found to attenuate CdTe-QDs provoked injury and apoptosis suggesting the underlying mechanism involves modulation of the Nrf2 signaling pathway[170]. A series of investigations have proved that mitochondria are the prominent target of CdTe-QDs in hepatocytes. In different cell lines and mice models, it was found that interaction between CdTe-QDs and mitochondrial membrane resulted in mitochondrial enlargement, membrane potential disruption, opening of permeability transition pore, impaired oxidative phosphorylation *via* diminishing activity of electron transport chain enzymes, ROS accumulation, redox damage, ATP depletion and increased PGC-1α. Together all these indicate oxidative mediated stress-mediated release of cytochrome c and Bax to promote intrinsic and extrinsic pathways of apoptosis in CdTe-QDs exposed hepatocytes[9,171-173]. When normal and carcinoma liver cells were incubated with CdTe/CdS QDs for 24 h, both the cells showed similar lysosomal accumulation of QDs followed by abnormal activation of lysosomal enzymes that triggered lysosome-dependent ROS production and autophagy. Inhibition of lysosomal enzymes were also found to prevent ROS production and activation of autophagic flux and thereby rescued hepatocytes from cytotoxic effects of QDs[3] A recent *in vivo* investigation unveils the sub-acute low dose of CdTe QDs uptake leads to both activation of NF-KB pathway through overproduction of ROS that also indirectly regulates NLRP3 inflammasome assembly to trigger inflammatory cascades *via* inflammatory cytokines (IL-1β, TNF-α, IL-6) and activation of Kupffer cells to cause liver tissue injury. In *in vitro* study pretreatment of KUP5 cells with NAC (*N*-acetylcysteine – ROS scavenger) and DHMEQ (Dehydroxymethylepoxyquinomicin- NF-KB translocation inhibitor) before QDs, reversed the activation of Kupffer cells following down-regulation of NF-κB, caspase-1, and NLRP3[174]. A recent study highlights the varied impact of CDs (Carbon Quantum Dots) on liver cells (KUP5 and AML12 cells *in vitro*) and the importance of the TFEB-lysosome pathway in regulating autophagy and apoptosis induced by CDs on liver cells for a comprehensive toxicological safety evaluation[175]. Follow Table 17 for a comprehensive account.

Gold nanoparticles

Gold is generally unreactive in its natural state but becomes reactive in its ionic form. It can also exist as gold salts, allowing the synthesis of nanomaterials with properties like easy synthesis, high particle reactivity, and strong optical characteristics[176,177]. In recent days, gold nanoparticles (AuNPs) have gained considerable attention in various fields, especially in biomedical sciences due to their unique physicochemical properties[178]. Nevertheless, there are many concerns regarding their potential hepatotoxic effects that have raised questions about their safety use in such applications. Numerous inflammatory and cytotoxic responses have been observed with smaller-sized AuNPs in comparison to

Table 17 Effects and molecular mechanisms underlying quantum dots induced hepatonanotoxicity

NPs	Size	Tested model	Dose & route of administration	Effects & mechanism	Ref.
Cd/Se/Te QD705	12.3 ± 5.2 nm (TEM)	ICR mice	100 µL of 40 and 160 pmol (IV) sacrificed at 12 and 16 wk	ALT, AST (increased); GPx, HO-1, 8-oxo-dG (increased); Cu/Zn/Se (increased); SOD activity (decreased); GSH/GSSG; Unbalanced antioxidation systems; Trace metals, trace metal transporters; TNFα, IL-6 (increased) **Oxidative stress and inflammation**	[167]
CdSe QD	4 nm (TEM)	Kunming mice Hepa 1–6 cells	200 nMCdCl2, 20 nM & 200 nM QDs (acute) for 48 h (IP); 20 nMCdCl2, 5 nM & 10 nM QDs for 6 wk (chronic) (IP); 20 nM CdCl2, 5 nM, 10 nM and 20 nM QDs for 24 & 48 h	ROS, MDA (increased); GSH-Px (decreased); Enlarged central vein, disordered hepatic cords; Reduced cell size, condensation; Round and condensed macrophage **Oxidative stress**	[166]
Mn-doped ZnS QDs	3.8 ± 0.1 nm (TEM)	Kunming mice	1 & 5 mg/kg (QDs); 5 mg/kg (QDs PEG) (IV) for 7 da sacrificed on 8th & 28th day	QDs accumulated in mitichondia, lysosome, lipid droplets; No hepatic damage	[169]
CdTe QDs	2.2 nm (TEM)	AML 12; ICR mice	27.66, 41.49, 53.94, 70.12, 91.16 & 118.50 µg/mL for 24 & 48 h. 4.125, 8.25 and 16.5 mg/kg body weight (IV) once a week for 4 wk	LPO, MDA, SOD, CAT, P53, Bcl-2, Nrf2, HO-1 (increased); Bax (decreased); ATP concentration (decreased); Nrf2 signaling pathway activation **Oxidative stress, apoptosis**	[170]
CdTe QDs	7.3 ± 1.2 nm (TEM)	HepG2 cell	10 µg/mL containing 1 µg/mL of cadmium for 24 h	MMP disruption, mitochondrial swelling, increased intracellular ca2+ levels, impaired cellular respiration & decreased ATP synthesis; PGC-1α (increased) **Mitochondrial toxicity & dysfunction**	[171]
CdTe QDs	15.25 ± 0.34 nm (TEM)	BALB/c mice	0.4, 2, 5, 6, 7, and 10 mg/kg b.w (Iv) for 24 h; 5 mg/kg bw (Iv) 2 h, 24 h, 3 d, and 1 wk	Enlarged mitochondria with increment in number; Affects ETC complex & ATP synthesis energy metabolism impairment **Mitochondrial dysfunction**	[172]
CdSe/Zn-QD	7.1 nm (TEM)	L02 cells; C57BL/6 mice; NLRP3 knockout mice	5, 10, 20, 40, 80 nM, 24 and 48 h; 10 nmol/kg (IV) results at 2 wk	Dose-dependent decrease in cell viability pyroptosis; Caspase-1 activity(increased); NLRP3 inflammasome activation; mt ROS production (increased); Cytoplasmic Ca2+ (increased) levels ALT, AST, MPO, TNFα, IL-1β (increased); γ-GT (decreased) **Oxidative stress and inflammation**	[168]
Cd free indium - based QDs	4 nm (TEM)	Lister Hooded rats	12.5 & 50 mg/kg b.w. (Iv) for 24 h. 1 wk, 4 wk	ALT, AST, ALP (slightly increased); No hepatic damage	[25]
CdTe/CdS QDs	12 nm (TEM)	HL-7702; HepG2 cells	1- 32 nM for 48 h	Lysosomal internalization; Abnormal activation of lysosomal enzymes; ROS generation (increased); Autophagy **Apoptosis independent nanotoxicity**	[3]
CdTe QDs	15.25 ± 0.34 nm (TEM)	BALB/c mice	0.4, 2, 5, 6, 7, and 10 mg/kg b.w (Iv) for 24 h. 5 mg/kg b.w. (Iv)2 h, 24 h, 3 d (d), and 1 wk (w)	AST, ALT, T-bil (increased); Albumin (decreased); liver accumulation	[173]
CdTe QDs	15.25 ± 0.34 nm (TEM)	BALB/c mice	0.4, 2, 5, 6, 7, and 10 mg/kg b.w (Iv) for 24 h. 5 mg/kg b.w. (Iv) 2 h, 24 h, 3 d (d), and 1 wk (w)	tGSH, ATP (depletion) GST, CAT (decreased) SOD activity (increased); Hmox I, Ncf-1, Ncf-2 (upregulated expression); PGC-1α (increased) **Oxidative stress, apoptosis**	[9]
CdTe QDs	2.2-3.0 nm (TEM)	ICR mice; KUP5 cells	2.5 & 10 µM/kg·b.w. (Iv) single dose once per wekk for 14 d; 5, 50 & 500 NM	IL-1β, TNF-α, IL-6 (increased); Assembly of NLRP3 inflammasome; ROS productin (increased); Activation of NF-KB pathway; Kupffer cell activation **Oxidative stress, Inflammation**	[174]

8-oxo-dG: 8-oxo-7,8-dihydro-2¢-deoxyguanosine; ALP: Alkaline phosphatase; ALT: Alanine aminotransferase, AST: Aspartate aminotransferase, ATP: Adenosine triphosphate; Bax: Bcl-2 associated X protein; Bcl-2: B-cell lymphoma 2; CAT: Catalase; Cu-copper; ETC: Electron transport chain; GSH-Px: Glutathione peroxidase; GSSG: Glutathione disulfide; GST: Glutathione S-transferase; HO-1/Hmox I: Heme oxygenase 1; IL-1β: Interleukin 1 β; IL-6: Interleukin-6; LPO: Lipid peroxidation; MDA: Malondialdehyde; MMP: Mitochondrial membrane potential; MPO: Myeloperoxidase; Ncf-1,2: Neutrophil cytosolic factor 1,2; NF-κB: Nuclear factor kappa beta; NLRP3: NOD-like receptor protein 3; Nrf2: Nuclear factor erythroid 2-related factor 2; P53: Tumor suppressor protein p53; PGC-1α: Peroxisome proliferator-activated receptor gamma coactivator 1-alpha; ROS: Reactive oxygen species; Se: Selenium; SOD: Superoxide dismutase; T-Bil: Total bilirubin; tGSH: Total glutathione; TNFα: Tumor necrosis factor alpha; γ-GT: Gamma glutamyl transferase; Zn: Zinc.

contact with larger-sized AuNPs with the same mass concentration because of their highly reactive role with biological constituents, and have stressed the harmful effects produced by a large number of nanoparticles[179]. AuNPs activate hepatic macrophages and consequently stimulate the occurrence of immune hepatitis and liver dysfunction[180,181]. Serum ALT and AST levels, indicative of liver damage, remained within the normal range in NC (Normal Chow) diet-fed mice 24 h or 7 d after AuNP administration, suggesting AuNPs' non-toxicity under normal diet conditions[182]. Conversely, MCD (methionine and choline-deficient) diet-fed mice exhibited elevated ALT and AST levels post-AuNP administration, indicating hepatotoxicity. The experiment revealed that MCD diets induced hepatic TG accumulation through the inhibition of mitochondrial beta-oxidation and blocking hepatic export of very low-density lipoprotein, but AuNP-induced hepatotoxicity was attributed to increased inflammatory response and apoptosis, not accumulated TG contents[182]. Intravenously injected AuNPs rapidly accumulate in Kupffer cells in the liver, stimulating these cells and leading to increased monocyte function, upregulated cytokine secretion, and subsequent liver damage through enhanced necrosis, apoptosis, and abnormal ROS production[183]. The toxicity of AuNPs is associated with their capacity to stimulate inflammatory responses and accelerate stress-induced apoptosis, with smaller nanoparticle sizes contributing to toxicity[184]. AuNPs induce hepatocellular injury through ROS generation, promoting oxidative stress[185]. This oxidative stress, characterized by lipid peroxidation, protein damage, and DNA modifications, is exacerbated by inflammatory responses and pro-inflammatory cytokines. The correlation between nanoparticles and oxidative stress suggests fatty acid peroxidation as a probable cause for AuNP-triggered DNA destruction[186]. Khan *et al*[187] measured oxidative stress markers in rats exposed to AuNPs, revealing increased MDA levels specifically in the liver, indicating AuNPs' liver-specific oxidative stress. The mutagenic and carcinogenic nature of MDA, a product of fatty acid peroxidation, suggests its potential to combine with DNA, leading to DNA damage and potentially activating programmed cell death pathways[187]. Research has shown that AuNPs can enter hepatocytes through various mechanisms, including endocytosis and direct penetration of the cell membrane[188,189]. Once internalized, these may accumulate in specific subcellular compartments, such as the ER or mitochondria which leads to inducing organelle-specific toxicity. The disruption of cellular organelles can trigger a cascade of events leading to hepatocellular damage [190,191]. Cell migration, crucial for mammalian cell survival and differentiation and regulated by external signals, was significantly reduced by 70% in HeLa cells treated with MUAM-AuNPs, as demonstrated in a gap-filling assay by Lee *et al*[192]; this reduction was attributed to the loss of long F-actins aligned with the migration axis, impacting migration-related signaling pathways, disrupting extracellular matrix organization, and ultimately impeding cell migration[192-194]. Additionally, AuNPs induced differential gene expression in treated samples, involving both upregulated and downregulated genes associated with cellular metabolism, protein catabolism, cell cycle, and G1/S transition; notably, downregulation of genes related to the G1 phase and nucleic acid metabolism suggested inhibition of DNA synthesis. In a separate experiment, 1.4-nm triphenyl monosulfonate (TPPMS)-coated AuNPs caused necrotic cell death through elevated oxidative stress and loss of mitochondrial potential, while Tiopronin-coated AuNPs induced necrosis *via* increased ROS production and apoptosis due to mitochondrial dysfunction; citrate AuNPs also exhibited dose-dependent ROS production leading to apoptosis[195,196]. Moreover, Au clusters significantly increased ROS production by inhibiting TrxR1 activity, inducing apoptosis, and disrupting mitochondrial membrane polarization[197]. Finally, irradiation in the presence of AuNPs led to an interaction with the cell membrane protein disulfide isomerase, disrupting thiol balance, causing cellular redox imbalance, and ultimately inducing oxidative stress[196].

Silver nanoparticles

Silver nanoparticles (AgNP)-intoxication significantly disturbs normal liver function, elevates hepatic lipid peroxidation, increases liver DNA damage, and induces biochemical and histological alterations in rats[198]. The toxicity of AgNPs mainly originates from the degraded forms of AgNPs, the "particle-specific effect" or the triggered oxidation stress[199]. After cellular intake, these (AgNPs) would enter the acidic endo/Lysosomes (pH4.5–6.5) and undertake chemical transformation from particulate silver to elemental silver, Ag+, Ag-O- and Ag-S- species[200]. The Ag+ released from AgNPs dissolution is thought to bind intracellular sulfhydryl group (−SH)-containing molecules and leads to cytotoxicity, which is known as the "Trojan-horse" mechanism[199]. AgNPs also help in intracellular ROS production and cause cellular damage, *e.g.* genotoxicity, mitochondrial dysfunction, and cell membrane damage[201]. Ag ions have been reported to cause disturbance and destruction of mitochondrial function through interaction with thiol groups of inner mitochondrial membrane proteins and AgNPs decrease the activity of mitochondrial respiratory chain complexes and reduce antioxidant factors like glutathione, thioredoxin, superoxide dismutase, and N-acetylcysteine in liver cells[202, 203]. Xu *et al*[201] investigated two normal hepatic cell lines (NCTC1469 and L-02) and two hepatoma cell lines (Hepa1–6 and HepG2) to assess the cytotoxicity of AgNPs. They have shown AgNPs could certainly lead to intra-cellular oxidation stress and cytotoxicity through acting GST molecules and thus suppressing its enzyme activity, although GST expressions were not significantly affected. The research also highlighted the binding of High Molecular Weight proteins to Ag+ became saturated and more Low molecular weight molecules (*e.g.* metallothionein) were continually synthesized by cells

to neutralize AgNPs and Ag+ for detoxification. It indicates that the dissolution of internalized AgNPs resulted in the formation of Ag-protein complexes. As a consequence, the damage of protein molecules by AgNPs and Ag+ would destroy the intra-cellular homeostasis of the liver. Assar *et al*[204] pointed out that after 15 and 30 d of exposure to the maximum dose of AgNPs in rats, a drop in liver weight was observed to a striking rise in lipid peroxidation, leading to structural changes to lipid vacuoles. This finding also showed that a state of oxidative injury was provoked by silver nanoparticles in a dose-dependent way by the raised hepatic MDA (malondialdehyde) levels and the depletion of the antioxidant defensive mechanism by reducing the hepatic reduced glutathione (GSH) levels. The most severe hepatic damage was associated with increasing the AgNP-administered dose and expanding exposure time. Research findings from Matés[205], Srivastava *et al*[206], Ansar *et al*[207], and Piao *et al*[208] have detailed that continuous elevation of Ag+ concentration leads to continuous induction of hydroxyl radical, ultimately consumes more intracellular GSH, and disturbing the homeostasis of free radical scavenging. AgNPs raised MDA levels causing oxidative damage in rats[209]. Many studies support that the liver is the main target organ for AgNP action. The histological assessment of the liver indicated pathological changes that were dose and time-dependent and happened in the liver after 30 d of increasing concentrations of AgNP exposure. Sooklert *et al*[210] and Elje *et al*[111] showed that low levels of dissolved Ag were found in the Ag-NPs exposure shortly after exposure in the HepG2 human liver cells, and the amounts were lower than the measured EC50 for cytotoxicity of $AgNO_3$ and identified six genes from HepG2 Liver cells, with three showing significant up-regulation of FOS and JUN, and two demonstrating up-regulation of EGR1, CXCL8, HSPB1, and MT2A. Notably, high-dosage AgNP exposure increased fold changes in genes associated with cell proliferation (FOS, JUN, and EGR1)[210]. An increased intracellular level of ROS can also activate cell-death-regulating pathways, such as p53, AKT, and MAP kinase[185]. Microscopic images revealed nuclear membrane distortion, blebbed nuclei formation, and accumulation of autophagic vacuoles in AgNP-treated liver cells, along with increased mitochondria, cytoplasmic vacuoles containing silver nanoparticles, and swollen lipid droplets. In hepatocytes, CEBPA (CCAAT enhancer binding protein alpha) is highly expressed and plays a critical role in regulating many metabolic liver genes, while CEBPB (CCAAT enhancer binding protein beta) is up-regulated during liver regeneration and plays a crucial role in the development of liver or acute inflammatory response[211]. The proto-oncogenes FOS and JUN, which are known to play important roles in both cell survival and the signaling pathway involved in hepatotoxicity, were highly up-regulated in the presence of AgNPs. In addition to that, heat shock protein family members HSPB1, HSPA4L, and HSPH1 were also significantly up-regulated[212]. Xin *et al*[213], reported that AgNPs induced oxidative stress, and consequently increased expression of heat shock protein and heme oxygenase (HMOX1) in both liver and lung cells. Sooklert *et al*[210] identified 24 interesting candidate genes as possible targets of AgNP-induced hepatocellular toxicity. SOX15, a highly upregulated gene, acts as a transcription activator involved in embryonic development regulation and cell fate determination. TLL1, the most noticeable down-regulated gene, is necessary for various developmental events. AgNPs may exert cytotoxic effects through SOX15 upregulation or TLL1 downregulation in hepatic cells. Deregulated autophagy after AgNP treatment was also seen which may lead to increased cell death either independently or synergistically with apoptosis or necrosis[214]. Wen *et al*[215] and Recordati *et al*[216] observed increased hepatocellular necrosis and gall bladder hemorrhage in mice injected with AgNPs, particularly with 10nm AgNPs. AgNP administration induced exacerbated hepatic steatosis, heightened liver injury, and elevated risk of NAFLD development and progression[215,216]. The effects were attributed to hyperactivation of SREBP-1c-mediated de novo lipogenesis, pro-inflammatory cytokine activation, and increased oxidative stress and DNA methylation[216]. Kim *et al*[217] demonstrated that cAgNPs (citrate-coated and stabilized) caused significant changes in ALP and LDH levels, indicating liver tissue damage persisting up to 28 d after exposure and suggesting prolonged impairment of liver structure and functions following a single exposure. From Lee *et al*[218], it was reported that the deposited AgNPs in hepatocytes were found to be individual particles with a size smaller than 100 nm in diameter. AgNPs accumulated in hepatocytes' endosomes and lysosomes, with additional deposition in Kupffer cells (> 100 nm agglomerates)[218]. Kupffer cells played a role in inflammation observed with mild inflammatory cell infiltration in portal vein areas. Elevated ALT and AST levels indicated liver damage persisting up to one month after AgNP administration[218]. Maternal exposure to AgNPs *via* the intragastric route led to increased silver content in rat offspring livers, causing a significant reduction in body weight and dilated blood vessels. Liver damage, indicated by vacuolation and lipid peroxidation, was associated with elevated caspase-9 concentration, suggesting AgNPs induce apoptosis through the intrinsic pathway in offspring livers[219].

CONCLUSION

In summary, the extensive examination sheds light on the intricate landscape of hepatotoxicity induced by various nanoparticles (NPs), revealing distinct mechanisms and effects associated with different nanomaterials. Size-dependent hepatotoxicity is observed in SiNPs, with smaller particles causing more severe liver injury. The combined toxicity of SiNPs with other liver toxins highlights potential synergies in NP-induced liver damage. Oxidative stress, inflammation, apoptosis, and genotoxicity are induced by NiO-NPs, WO3 NPs, Nano-CuO, and other nanomaterials, illustrating the complexity of NP-mediated hepatotoxic effects (Figures 1-3).

Integrative omics analyses identify key proteins and disrupted metabolic pathways in SiNP-induced hepatotoxicity, underscoring the necessity for a multifaceted understanding of NP-induced liver damage. CNTs, including SWCNTs and MWCNTs varieties, contribute to hepatotoxicity through inflammatory responses and oxidative stress, with variations in toxicity observed among different types of CNTs.

Moreover, exposure to CuS/CdS-NPs, cobalt nanoparticles, nanoclay particles, nanocellulose, polystyrene nanoparticles, chitosan nanoparticles, hydroxyapatite nanoparticles, quantum dots, and gold nanoparticles elucidates

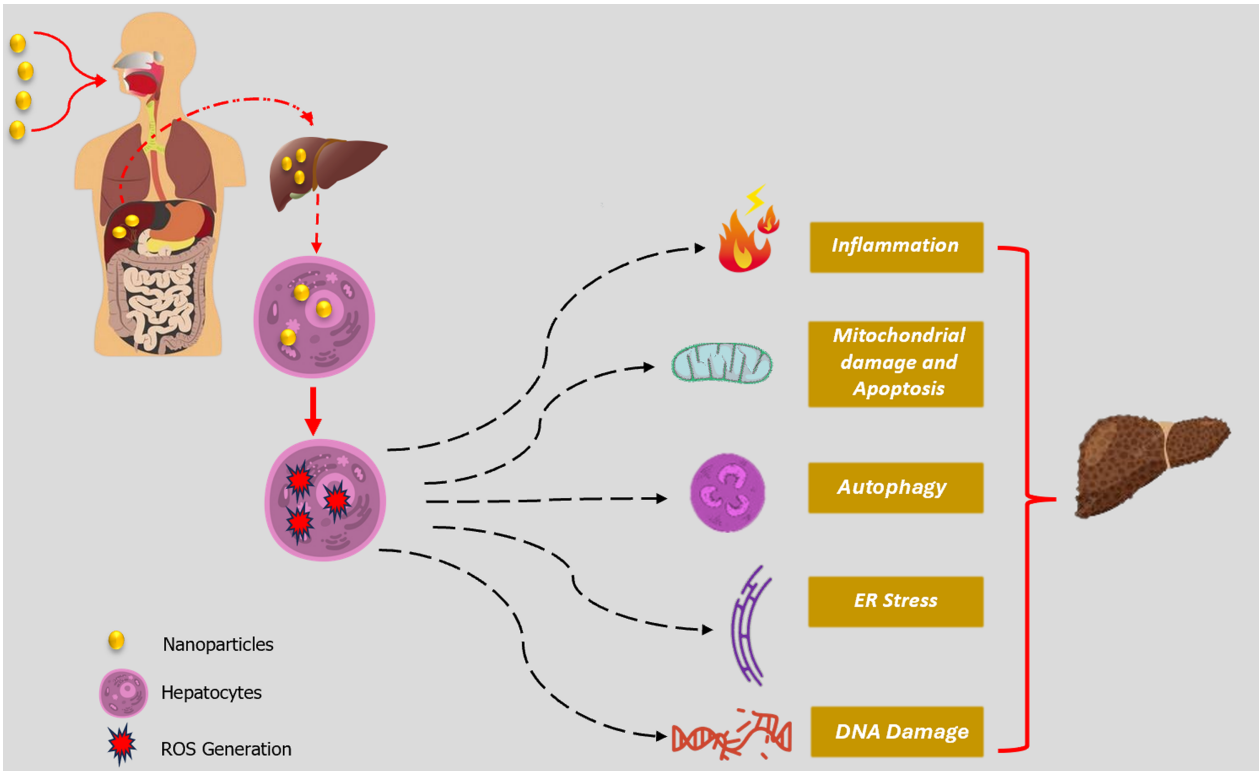

Figure 3 Different modalities of nanoparticles induced hepatotoxicity. ER: Endoplasmic reticulum; ROS: Reactive oxygen species.

diverse hepatotoxic effects, underscoring the importance of considering nanoparticle characteristics in toxicity assessments.

Despite these toxicities, it is noteworthy that nanoparticles play a pivotal role in diverse biomedical applications, showcasing their versatility and impact. In cancer therapy, catalytic strategies employing substances like hydrogen peroxide and glucose, alongside biocompatible nanomaterials, promise efficient treatment with minimal side effects[220]. Nanomaterials contribute significantly to the fight against coronavirus disease 2019, aiding in rapid diagnostics, vaccine development, and therapeutic interventions[221]. Transition metal-based nanoparticles, particularly those with anisotropic shapes, offer unique properties for biomedical applications, including drug delivery and imaging[222]. Precision nanoparticles (PNPs) emerge as discrete structures with precisely tailored heterogeneity, addressing challenges associated with uncontrolled nanoparticle variability[223]. PNPs significantly enhance the performance of nanoparticle-based vehicles in various biological processes, presenting a promising avenue for improved biomedical outcomes.

Therefore, the study concludes by emphasizing the urgent need for a comprehensive understanding of NP-induced hepatotoxicity to ensure the safe use of nanomaterials, suggesting further *in vivo* studies and exploration of potential protective strategies. Additionally, the proposal of herbal gold nanoparticles as a potential hepatoprotective agent opens avenues for future research and development in the field. Overall, the findings underscore the complexity and diversity of nanomaterial-induced hepatotoxicity, emphasizing the importance of continued research for safer nanomaterial applications in various contexts.

FOOTNOTES

Co-corresponding authors: Krishnendu Sinha and Parames C Sil.

Author contributions: Das SK, Sen K, Ghosh B, Ghosh N and Sinha K performed the research and wrote the manuscript; Sinha K and Sil P conceptualized and designed the study; Das SK drew the figures; all authors have read and approved the final manuscript. Sil PC initiated and conceptualized the review, bringing extensive experience and expertise in the field of hepatotoxicity and nanomaterials. Sil PC oversaw the overall design of the review, provided critical insights into the interpretation of scientific literature, and ensured the accuracy and relevance of the content presented. Additionally, Sil PC played a pivotal role in synthesizing complex scientific concepts and findings, contributing significantly to the intellectual content and scholarly rigor of the manuscript. Sinha K was selected as co-corresponding author based on his demonstrated scientific acumen, research leadership, and ability to effectively communicate and collaborate with co-authors. Sinha K actively participated in the review process, conducting thorough literature reviews, analyzing data, and synthesizing key findings. Moreover, Sinha K played a crucial role in manuscript preparation, including drafting sections, revising content based on feedback, and ensuring the coherence and clarity of the final manuscript.

Conflict-of-interest statement: All authors have no conflicts of interest to disclose.

Open-Access: This article is an open-access article that was selected by an in-house editor and fully peer-reviewed by external reviewers.

It is distributed in accordance with the Creative Commons Attribution NonCommercial (CC BY-NC 4.0) license, which permits others to distribute, remix, adapt, build upon this work non-commercially, and license their derivative works on different terms, provided the original work is properly cited and the use is non-commercial. See: https://creativecommons.org/Licenses/by-nc/4.0/

Country/Territory of origin: India

ORCID number: Krishnendu Sinha 0000-0001-9590-3875; Parames C Sil 0000-0003-0190-5904.

S-Editor: Liu JH
L-Editor: A
P-Editor: Cai YX

REFERENCES

1 **Oberdörster G**, Oberdörster E, Oberdörster J. Nanotoxicology: an emerging discipline evolving from studies of ultrafine particles. *Environ Health Perspect* 2005; **113**: 823-839 [PMID: 16002369 DOI: 10.1289/ehp.7339]
2 **Nishimori H**, Kondoh M, Isoda K, Tsunoda S, Tsutsumi Y, Yagi K. Silica nanoparticles as hepatotoxicants. *Eur J Pharm Biopharm* 2009; **72**: 496-501 [PMID: 19232391 DOI: 10.1016/j.ejpb.2009.02.005]
3 **Fan J**, Wang S, Zhang X, Chen W, Li Y, Yang P, Cao Z, Wang Y, Lu W, Ju D. Quantum Dots Elicit Hepatotoxicity through Lysosome-Dependent Autophagy Activation and Reactive Oxygen Species Production. *ACS Biomater Sci Eng* 2018; **4**: 1418-1427 [PMID: 33418671 DOI: 10.1021/acsbiomaterials.7b00824]
4 **HelmyAbdou KA**, Ahmed RR, Ibrahim MA, Abdel-Gawad DRI. The anti-inflammatory influence of Cinnamomum burmannii against multi-walled carbon nanotube-induced liver injury in rats. *Environ Sci Pollut Res Int* 2019; **26**: 36063-36072 [PMID: 31745806 DOI: 10.1007/s11356-019-06707-5]
5 **Alshammari BH**, Lashin MMA, Mahmood MA, Al-Mubaddel FS, Ilyas N, Rahman N, Sohail M, Khan A, Abdullaev SS, Khan R. Organic and inorganic nanomaterials: fabrication, properties and applications. *RSC Adv* 2023; **13**: 13735-13785 [PMID: 37152571 DOI: 10.1039/d3ra01421e]
6 **Pan K**, Zhong Q. Organic Nanoparticles in Foods: Fabrication, Characterization, and Utilization. *Annu Rev Food Sci Technol* 2016; **7**: 245-266 [PMID: 26735797 DOI: 10.1146/annurev-food-041715-033215]
7 **Jiao M**, Zhang P, Meng J, Li Y, Liu C, Luo X, Gao M. Recent advancements in biocompatible inorganic nanoparticles towards biomedical applications. *Biomater Sci* 2018; **6**: 726-745 [PMID: 29308496 DOI: 10.1039/c7bm01020f]
8 **Maxwell T**, Nogueira Campos MG, Smith S, Doomra M, Thwin Z, Santra S. Quantum Dots. In: Nanoparticles for Biomedical Applications. *Elsevier***2020**: 243-265 [DOI: 10.1016/B978-0-12-816662-8.00015-1]
9 **Nguyen KC**, Zhang Y, Todd J, Kittle K, Lalande M, Smith S, Parks D, Navarro M, Tayabali AF, Willmore WG. Hepatotoxicity of Cadmium Telluride Quantum Dots Induced by Mitochondrial Dysfunction. *Chem Res Toxicol* 2020; **33**: 2286-2297 [PMID: 32844644 DOI: 10.1021/acs.chemrestox.9b00526]
10 **Zhao Q**, Gan ZH, Zhuang QK. Electrochemical Sensors Based on Carbon Nanotubes. *Electroanalysis* 2002; **14**: 1609-1613 [DOI: 10.1002/elan.200290000]
11 **Muller J**, Huaux F, Moreau N, Misson P, Heilier JF, Delos M, Arras M, Fonseca A, Nagy JB, Lison D. Respiratory toxicity of multi-wall carbon nanotubes. *Toxicol Appl Pharmacol* 2005; **207**: 221-231 [PMID: 16129115 DOI: 10.1016/j.taap.2005.01.008]
12 **Luo GS**, Du L, Wang YJ, Wang K. Composite Nanoparticles. *Encyclopedia of Microfluidics and Nanofluidics* 2014; 1-9 [DOI: 10.1007/978-3-642-27758-0_243-3]
13 **Chen X**, Schluesener HJ. Nanosilver: a nanoproduct in medical application. *Toxicol Lett* 2008; **176**: 1-12 [PMID: 18022772 DOI: 10.1016/j.toxlet.2007.10.004]
14 **Arora S**, Rajwade JM, Paknikar KM. Nanotoxicology and in vitro studies: the need of the hour. *Toxicol Appl Pharmacol* 2012; **258**: 151-165 [PMID: 22178382 DOI: 10.1016/j.taap.2011.11.010]
15 **Ganguly P**, Breen A, Pillai SC. Toxicity of Nanomaterials: Exposure, Pathways, Assessment, and Recent Advances. *ACS Biomater Sci Eng* 2018; **4**: 2237-2275 [PMID: 33435097 DOI: 10.1021/acsbiomaterials.8b00068]
16 **Chang X**, Liu F, Tian M, Zhao H, Han A, Sun Y. Nickel oxide nanoparticles induce hepatocyte apoptosis *via* activating endoplasmic reticulum stress pathways in rats. *Environ Toxicol* 2017; **32**: 2492-2499 [PMID: 28945320 DOI: 10.1002/tox.22492]
17 **Mao L**, Zheng L, You H, Ullah MW, Cheng H, Guo Q, Zhu Z, Xi Z, Li R. A comparison of hepatotoxicity induced by different lengths of tungsten trioxide nanorods and the protective effects of melatonin in BALB/c mice. *Environ Sci Pollut Res Int* 2021; **28**: 40793-40807 [PMID: 33772475 DOI: 10.1007/s11356-021-13558-6]
18 **Khalid S**, Afzal N, Khan JA, Hussain Z, Qureshi AS, Anwar H, Jamil Y. Antioxidant resveratrol protects against copper oxide nanoparticle toxicity in vivo. *Naunyn Schmiedebergs Arch Pharmacol* 2018; **391**: 1053-1062 [PMID: 29936585 DOI: 10.1007/s00210-018-1526-0]
19 **Chatterjee N**, Yang J, Atluri R, Lee W, Hong J, Choi J. Amorphous silica nanoparticle-induced perturbation of cholesterol homeostasis as a function of surface area highlights safe-by-design implementation: an integrated multi-OMICS analysis. *RSC Adv* 2016; **6**: 68606-68614
20 **Pasupuleti S**, Alapati S, Ganapathy S, Anumolu G, Pully NR, Prakhya BM. Toxicity of zinc oxide nanoparticles through oral route. *Toxicol Ind Health* 2012; **28**: 675-686 [PMID: 22033421 DOI: 10.1177/0748233711420473]
21 **Mekky G**, Seeds M, Diab AEA, Shehata AM, Ahmed-Farid OA, Alzebdeh D, Bishop C, Atala A. The potential toxic effects of magnesium oxide nanoparticles and valproate on liver tissue. *J Biochem Mol Toxicol* 2021; **35**: e22676 [PMID: 33315275 DOI: 10.1002/jbt.22676]
22 **Kenawy SH**, Hassan ML. Synthesis and characterization high purity alumina nanorods by a novel and simple method using nanocellulose aerogel template. *Heliyon* 2019; **5**: e01816 [PMID: 31193879 DOI: 10.1016/j.heliyon.2019.e01816]
23 **Fatima R**, Ahmad R. Hepatotoxicity and chromosomal abnormalities evaluation due to single and repeated oral exposures of chromium oxide nanoparticles in Wistar rats. *Toxicol Ind Health* 2019; **35**: 548-557 [PMID: 31370753 DOI: 10.1177/0748233719863632]
24 **Yun JW**, Kim SH, You JR, Kim WH, Jang JJ, Min SK, Kim HC, Chung DH, Jeong J, Kang BC, Che JH. Comparative toxicity of silicon

dioxide, silver and iron oxide nanoparticles after repeated oral administration to rats. *J Appl Toxicol* 2015; **35**: 681-693 [PMID: 25752675 DOI: 10.1002/jat.3125]
25 **Yaghini E**, Turner H, Pilling A, Naasani I, MacRobert AJ. In vivo biodistribution and toxicology studies of cadmium-free indium-based quantum dot nanoparticles in a rat model. *Nanomedicine* 2018; **14**: 2644-2655 [PMID: 30048815 DOI: 10.1016/j.nano.2018.07.009]
26 **Buzea C**, Pacheco II, Robbie K. Nanomaterials and nanoparticles: sources and toxicity. *Biointerphases* 2007; **2**: MR17-MR71 [PMID: 20419892 DOI: 10.1116/1.2815690]
27 **Loh JW**, Yeoh G, Saunders M, Lim LY. Uptake and cytotoxicity of chitosan nanoparticles in human liver cells. *Toxicol Appl Pharmacol* 2010; **249**: 148-157 [PMID: 20831879 DOI: 10.1016/j.taap.2010.08.029]
28 **He S**, Wang J, Zhou L, Jia T, Mao Z, Zhang X, Zhang L, Yang M, Huang P. Short term exposure to polystyrene nanoplastics in mice evokes self-regulation of glycolipid metabolism. *Ecotoxicol Environ Saf* 2023; **256**: 114906 [PMID: 37062265 DOI: 10.1016/j.ecoenv.2023.114906]
29 **Otuechere CA**, Adewuyi A, Adebayo OL, Ebigwei IA. In vivo hepatotoxicity of chemically modified nanocellulose in rats. *Hum Exp Toxicol* 2020; **39**: 212-223 [PMID: 31607162 DOI: 10.1177/0960327119881672]
30 **Virlan MJ**, Miricescu D, Radulescu R, Sabliov CM, Totan A, Calenic B, Greabu M. Organic Nanomaterials and Their Applications in the Treatment of Oral Diseases. *Molecules* 2016; **21** [PMID: 26867191 DOI: 10.3390/molecules21020207]
31 **Patra A**, Balasubrahmaniyam M, Lahal R, Malar P, Osipowicz T, Manivannan A, Kasiviswanathan S. Localized Surface Plasmon Resonance in Au Nanoparticles Embedded dc Sputtered ZnO Thin Films. *J Nanosci Nanotechnol* 2015; **15**: 1805-1814 [PMID: 26353736 DOI: 10.1166/jnn.2015.9045]
32 **Salavati-Niasari M**, Davar F, Mir N. Synthesis and characterization of metallic copper nanoparticles *via* thermal decomposition. *Polyhedron* 2008; **27**: 3514-3518 [DOI: 10.1016/j.poly.2008.08.020]
33 **Khan I**, Saeed K, Khan I. Nanoparticles: Properties, applications and toxicities. *Arab J Chem* 2019; **12**: 908-931 [DOI: 10.1016/j.arabjc.2017.05.011]
34 **Anu Mary Ealia S**, Saravanakumar MP. A review on the classification, characterisation, synthesis of nanoparticles and their application. *IOP Conf Ser Mater Sci Eng* 2017; **263**: 032019 [DOI: 10.1088/1757-899X/263/3/032019]
35 **Islam T**, Rahaman MdM, Mia MdN, Ara I, Islam MdT, Alam Riaz T, Araújo ACJ, de Lima Silva JMF, de Lacerda BCGV, de Andrade EM, Khan MA, Coutinho HDM, Husain Z, Islam MT. Therapeutic Perspectives of Metal Nanoformulations. *DDC* 2023; **2**: 232-278 [DOI: 10.3390/ddc2020014]
36 **Maruthupandy M**, Zuo Y, Chen JS, Song JM, Niu HL, Mao CJ, Zhang SY, Shen YH. Synthesis of metal oxide nanoparticles (CuO and ZnO NPs) *via* biological template and their optical sensor applications. *Appl Surf Sci* 2017; **397**: 167-174 [DOI: 10.1016/j.apsusc.2016.11.118]
37 **Syal A**, Sud D. Development of highly selective novel fluorescence quenching probe based on Bi2S3-TiO2 nanoparticles for sensing the Fe(III). *Sens Actuators B Chem* 2018; **266**: 1-8 [DOI: 10.1016/j.snb.2018.03.104]
38 **Alhalili Z**. Metal Oxides Nanoparticles: General Structural Description, Chemical, Physical, and Biological Synthesis Methods, Role in Pesticides and Heavy Metal Removal through Wastewater Treatment. *Molecules* 2023; **28** [PMID: 37049850 DOI: 10.3390/molecules28073086]
39 **Rane AV**, Kanny K, Abitha VK, Thomas S. Methods for Synthesis of Nanoparticles and Fabrication of Nanocomposites. In: Synthesis of Inorganic Nanomaterials. *Elsevier***2018**: 121-139 [DOI: 10.1016/B978-0-08-101975-7.00005-1]
40 **Abdalla AM**, Hossain S, Azad AT, Petra PMI, Begum F, Eriksson SG, Azad AK. Nanomaterials for solid oxide fuel cells: A review. *Renew Sust Energ Rev* 2018; **82**: 353-368 [DOI: 10.1016/j.rser.2017.09.046]
41 **Shi J**, Yu X, Wang L, Liu Y, Gao J, Zhang J, Ma R, Liu R, Zhang Z. PEGylated fullerene/iron oxide nanocomposites for photodynamic therapy, targeted drug delivery and MR imaging. *Biomaterials* 2013; **34**: 9666-9677 [PMID: 24034498 DOI: 10.1016/j.biomaterials.2013.08.049]
42 **Wu X**, Wu M, Zhao JX. Recent development of silica nanoparticles as delivery vectors for cancer imaging and therapy. *Nanomedicine* 2014; **10**: 297-312 [PMID: 24028896 DOI: 10.1016/j.nano.2013.08.008]
43 **Whitters CJ**, Strang R, Brown D, Clarke RL, Curtis RV, Hatton PV, Ireland AJ, Lloyd CH, McCabe JF, Nicholson JW, Scrimgeour SN, Setcos JC, Sherriff M, van Noort R, Watts DC, Wood D. Dental materials: 1997 literature review. *J Dent* 1999; **27**: 401-435 [PMID: 10399409 DOI: 10.1016/S0300-5712(99)00007-X]
44 **Singh D**, Singh S, Sahu J, Srivastava S, Singh MR. Ceramic nanoparticles: Recompense, cellular uptake and toxicity concerns. *Artif Cells Nanomed Biotechnol* 2016; **44**: 401-409 [PMID: 25229834 DOI: 10.3109/21691401.2014.955106]
45 **Thomas SC**, Harshita, Mishra PK, Talegaonkar S. Ceramic Nanoparticles: Fabrication Methods and Applications in Drug Delivery. *Curr Pharm Des* 2015; **21**: 6165-6188 [PMID: 26503144 DOI: 10.2174/1381612821666151027153246]
46 **Mostofizadeh A**, Li Y, Song B, Huang Y. Synthesis, Properties, and Applications of Low-Dimensional Carbon-Related Nanomaterials. *J Nanomater* 2011; **2011**: 1-21 [DOI: 10.1155/2011/685081]
47 **Kraft JC**, Freeling JP, Wang Z, Ho RJ. Emerging research and clinical development trends of liposome and lipid nanoparticle drug delivery systems. *J Pharm Sci* 2014; **103**: 29-52 [PMID: 24338748 DOI: 10.1002/jps.23773]
48 **García-Pinel B**, Porras-Alcalá C, Ortega-Rodríguez A, Sarabia F, Prados J, Melguizo C, López-Romero JM. Lipid-Based Nanoparticles: Application and Recent Advances in Cancer Treatment. *Nanomaterials (Basel)* 2019; **9** [PMID: 31010180 DOI: 10.3390/nano9040638]
49 **Mydin RBSMN**, Moshawih S. Nanoparticles in Nanomedicine Application: Lipid-Based Nanoparticles and Their Safety Concerns. In: Nanotechnology: Applications in Energy, Drug and Food. Cham: Springer International Publishing, 2019: 227-232 [DOI: 10.1007/978-3-319-99602-8_10]
50 **Ali S**, Khan I, Khan SA, Sohail M, Ahmed R, Rehman A ur, Ansari MS, Morsy MA. Electrocatalytic performance of Ni@Pt core-shell nanoparticles supported on carbon nanotubes for methanol oxidation reaction. *Journal of Electroanalytical Chemistry* 2017; **795**: 17-25 [DOI: 10.1016/j.jelechem.2017.04.040]
51 **Khan I**, Abdalla A, Qurashi A. Synthesis of hierarchical WO3 and Bi2O3/WO3 nanocomposite for solar-driven water splitting applications. *Int J Hydrogen Energy* 2017; **42**: 3431-3439 [DOI: 10.1016/j.ijhydene.2016.11.105]
52 **Hisatomi T**, Kubota J, Domen K. Recent advances in semiconductors for photocatalytic and photoelectrochemical water splitting. *Chem Soc Rev* 2014; **43**: 7520-7535 [PMID: 24413305 DOI: 10.1039/c3cs60378d]
53 **Sun S**, Murray CB, Weller D, Folks L, Moser A. Monodisperse FePt nanoparticles and ferromagnetic FePt nanocrystal superlattices. *Science* 2000; **287**: 1989-1992 [PMID: 10720318 DOI: 10.1126/science.287.5460.1989]
54 **Kroto HW**, Heath JR, O'Brien SC, Curl RF, Smalley RE. C60: Buckminsterfullerene. *Nature* 1985; **318**: 162-163 [DOI: 10.1038/318162a0]
55 **Zaytseva O**, Neumann G. Carbon nanomaterials: production, impact on plant development, agricultural and environmental applications. *Chem*

Biol Technol Agric 2016; **3**: 17 [DOI: 10.1186/s40538-016-0070-8]

56 **Aqel A**, El-Nour KMMA, Ammar RAA, Al-Warthan A. Carbon nanotubes, science and technology part (I) structure, synthesis and characterisation. *Arab J Chem* 2012; **5**: 1-23 [DOI: 10.1016/j.arabjc.2010.08.022]

57 **Flahaut E**, Bacsa R, Peigney A, Laurent C. Gram-scale CCVD synthesis of double-walled carbon nanotubes. *Chem Commun (Camb)* 2003; 1442-1443 [PMID: 12841282 DOI: 10.1039/b301514a]

58 **Morsy M**, Helal M, El-Okr M, Ibrahim M. Preparation, purification and characterization of high purity multi-wall carbon nanotube. *Spectrochim Acta A Mol Biomol Spectrosc* 2014; **132**: 594-598 [PMID: 24892539 DOI: 10.1016/j.saa.2014.04.122]

59 **Kim YA**, Yang K-S, Muramatsu H, Hayashi T, Endo M, Terrones M, Dresselhaus MS. Double-walled carbon nanotubes: synthesis, structural characterization, and application. *Carbon Lett* 2014; **15**: 77-88 [DOI: 10.5714/CL.2014.15.2.077]

60 **Hanemann T**, Szabó DV. Polymer-Nanoparticle Composites: From Synthesis to Modern Applications. Materials 2010, Vol 3, Pages 3468-3517 2010; 3: 3468-3517 [DOI: 10.3390/ma3063468]

61 Al-Mutairi N, Hussien A, Khadim BJ. Nanocomposites Materials Definitions, Types and Some of Their Applications: A Review. *EJRDS* 2022; **3**

62 **Shameem MM**, Sasikanth SM, Annamalai R, Raman RG. A brief review on polymer nanocomposites and its applications. *Materials Today: Proceedings* 2021; **45**: 2536-2539 [DOI: 10.1016/j.matpr.2020.11.254]

63 **Oberdörster G**, Maynard A, Donaldson K, Castranova V, Fitzpatrick J, Ausman K, Carter J, Karn B, Kreyling W, Lai D, Olin S, Monteiro-Riviere N, Warheit D, Yang H; ILSI Research Foundation/Risk Science Institute Nanomaterial Toxicity Screening Working Group. Principles for characterizing the potential human health effects from exposure to nanomaterials: elements of a screening strategy. *Part Fibre Toxicol* 2005; **2**: 8 [PMID: 16209704 DOI: 10.1186/1743-8977-2-8]

64 **Hoet PH**, Brüske-Hohlfeld I, Salata OV. Nanoparticles - known and unknown health risks. *J Nanobiotechnology* 2004; **2**: 12 [PMID: 15588280 DOI: 10.1186/1477-3155-2-12]

65 **Szentkuti L**. Light microscopical observations on luminally administered dyes, dextrans, nanospheres and microspheres in the pre-epithelial mucus gel layer of the rat distal colon. *J Control Release* 1997; **46**: 233-242 [DOI: 10.1016/S0168-3659(96)01600-8]

66 **Powell JJ**, Faria N, Thomas-McKay E, Pele LC. Origin and fate of dietary nanoparticles and microparticles in the gastrointestinal tract. *J Autoimmun* 2010; **34**: J226-J233 [PMID: 20096538 DOI: 10.1016/j.jaut.2009.11.006]

67 **Axson JL**, Stark DI, Bondy AL, Capracotta SS, Maynard AD, Philbert MA, Bergin IL, Ault AP. Rapid Kinetics of Size and pH-Dependent Dissolution and Aggregation of Silver Nanoparticles in Simulated Gastric Fluid. *J Phys Chem C Nanomater Interfaces* 2015; **119**: 20632-20641 [PMID: 28373899 DOI: 10.1021/acs.jpcc.5b03634]

68 **Siegmann K**, Scherrer L, Siegmann HC. Physical and chemical properties of airborne nanoscale particles and how to measure the impact on human health. *THEOCHEM* 1998; **458**: 191-201 [DOI: 10.1016/S0166-1280(98)00361-3]

69 **De Matteis V**. Exposure to Inorganic Nanoparticles: Routes of Entry, Immune Response, Biodistribution and In Vitro/In Vivo Toxicity Evaluation. *Toxics* 2017; **5** [PMID: 29051461 DOI: 10.3390/toxics5040029]

70 **Kocbach A**, Li Y, Yttri KE, Cassee FR, Schwarze PE, Namork E. Physicochemical characterisation of combustion particles from vehicle exhaust and residential wood smoke. *Part Fibre Toxicol* 2006; **3**: 1 [PMID: 16390554 DOI: 10.1186/1743-8977-3-1]

71 **Watkinson AC**, Bunge AL, Hadgraft J, Lane ME. Nanoparticles do not penetrate human skin--a theoretical perspective. *Pharm Res* 2013; **30**: 1943-1946 [PMID: 23722409 DOI: 10.1007/s11095-013-1073-9]

72 **Donnelly RF**, Singh TRR, Morrow DIJ, Woolfson AD. Microneedle-mediated Transdermal and Intradermal Drug Delivery. 3 February 2012. John Wiley & Sons, Ltd [DOI: 10.1002/9781119959687]

73 **Larese Filon F**, Mauro M, Adami G, Bovenzi M, Crosera M. Nanoparticles skin absorption: New aspects for a safety profile evaluation. *Regul Toxicol Pharmacol* 2015; **72**: 310-322 [PMID: 25979643 DOI: 10.1016/j.yrtph.2015.05.005]

74 **Hasezaki T**, Isoda K, Kondoh M, Tsutsumi Y, Yagi K. Hepatotoxicity of silica nanoparticles with a diameter of 100 nm. *Pharmazie* 2011; **66**: 698-703 [PMID: 22026127]

75 **Isoda K**, Tetsuka E, Shimizu Y, Saitoh K, Ishida I, Tezuka M. Liver injury induced by thirty- and fifty-nanometer-diameter silica nanoparticles. *Biol Pharm Bull* 2013; **36**: 370-375 [PMID: 23268881 DOI: 10.1248/bpb.b12-00738]

76 **Li L**, Liu T, Fu C, Tan L, Meng X, Liu H. Biodistribution, excretion, and toxicity of mesoporous silica nanoparticles after oral administration depend on their shape. *Nanomedicine* 2015; **11**: 1915-1924 [PMID: 26238077 DOI: 10.1016/j.nano.2015.07.004]

77 **Chatterjee N**, Jeong J, Yoon D, Kim S, Choi J. Global metabolomics approach in in vitro and in vivo models reveals hepatic glutathione depletion induced by amorphous silica nanoparticles. *Chem Biol Interact* 2018; **293**: 100-106 [PMID: 30059657 DOI: 10.1016/j.cbi.2018.07.013]

78 **Zhang X**, Luan J, Chen W, Fan J, Nan Y, Wang Y, Liang Y, Meng G, Ju D. Mesoporous silica nanoparticles induced hepatotoxicity *via* NLRP3 inflammasome activation and caspase-1-dependent pyroptosis. *Nanoscale* 2018; **10**: 9141-9152 [PMID: 29722780 DOI: 10.1039/c8nr00554k]

79 **Almansour M**, Alarifi S, Jarrar B. In vivo investigation on the chronic hepatotoxicity induced by intraperitoneal administration of 10-nm silicon dioxide nanoparticles. *Int J Nanomedicine* 2018; **13**: 2685-2696 [PMID: 29765215 DOI: 10.2147/IJN.S162847]

80 **Chen Q**, Xue Y, Sun J. Kupffer cell-mediated hepatic injury induced by silica nanoparticles in vitro and in vivo. *Int J Nanomedicine* 2013; **8**: 1129-1140 [PMID: 23515466 DOI: 10.2147/IJN.S42242]

81 **Sun M**, Zhang J, Liang S, Du Z, Liu J, Sun Z, Duan J. Metabolomic characteristics of hepatotoxicity in rats induced by silica nanoparticles. *Ecotoxicol Environ Saf* 2021; **208**: 111496 [PMID: 33099137 DOI: 10.1016/j.ecoenv.2020.111496]

82 **Zhang JQ**, Zhou W, Zhu SS, Lin J, Wei PF, Li FF, Jin PP, Yao H, Zhang YJ, Hu Y, Liu YM, Chen M, Li ZQ, Liu XS, Bai L, Wen LP. Persistency of Enlarged Autolysosomes Underscores Nanoparticle-Induced Autophagy in Hepatocytes. *Small* 2017; **13** [PMID: 27925395 DOI: 10.1002/smll.201602876]

83 **Wang J**, Li Y, Duan J, Yang M, Yu Y, Feng L, Yang X, Zhou X, Zhao Z, Sun Z. Silica nanoparticles induce autophagosome accumulation *via* activation of the EIF2AK3 and ATF6 UPR pathways in hepatocytes. *Autophagy* 2018; **14**: 1185-1200 [PMID: 29940794 DOI: 10.1080/15548627.2018.1458174]

84 **Yu Y**, Duan J, Yu Y, Li Y, Liu X, Zhou X, Ho KF, Tian L, Sun Z. Silica nanoparticles induce autophagy and autophagic cell death in HepG2 cells triggered by reactive oxygen species. *J Hazard Mater* 2014; **270**: 176-186 [PMID: 24583672 DOI: 10.1016/j.jhazmat.2014.01.028]

85 **Ahmad J**, Ahamed M, Akhtar MJ, Alrokayan SA, Siddiqui MA, Musarrat J, Al-Khedhairy AA. Apoptosis induction by silica nanoparticles mediated through reactive oxygen species in human liver cell line HepG2. *Toxicol Appl Pharmacol* 2012; **259**: 160-168 [PMID: 22245848

DOI: 10.1016/j.taap.2011.12.020]
86 **Zuo D**, Duan Z, Jia Y, Chu T, He Q, Yuan J, Dai W, Li Z, Xing L, Wu Y. Amphipathic silica nanoparticles induce cytotoxicity through oxidative stress mediated and p53 dependent apoptosis pathway in human liver cell line HL-7702 and rat liver cell line BRL-3A. *Colloids Surf B Biointerfaces* 2016; **145**: 232-240 [PMID: 27187187 DOI: 10.1016/j.colsurfb.2016.05.006]
87 **Li J**, He X, Yang Y, Li M, Xu C, Yu R. Risk assessment of silica nanoparticles on liver injury in metabolic syndrome mice induced by fructose. *Sci Total Environ* 2018; **628-629**: 366-374 [PMID: 29448021 DOI: 10.1016/j.scitotenv.2018.02.047]
88 **Qi Y**, Ma R, Li X, Lv S, Liu X, Abulikemu A, Zhao X, Li Y, Guo C, Sun Z. Disturbed mitochondrial quality control involved in hepatocytotoxicity induced by silica nanoparticles. *Nanoscale* 2020; **12**: 13034-13045 [PMID: 32538421 DOI: 10.1039/d0nr01893g]
89 **Aouey B**, Boukholda K, Gargouri B, Bhatia HS, Attaai A, Kebieche M, Bouchard M, Fetoui H. Silica Nanoparticles Induce Hepatotoxicity by Triggering Oxidative Damage, Apoptosis, and Bax-Bcl2 Signaling Pathway. *Biol Trace Elem Res* 2022; **200**: 1688-1698 [PMID: 34110565 DOI: 10.1007/s12011-021-02774-3]
90 **Abulikemu A**, Zhao X, Xu H, Li Y, Ma R, Yao Q, Wang J, Sun Z, Guo C. Silica nanoparticles aggravated the metabolic associated fatty liver disease through disturbed amino acid and lipid metabolisms-mediated oxidative stress. *Redox Biol* 2023; **59**: 102569 [PMID: 36512914 DOI: 10.1016/j.redox.2022.102569]
91 **Zhu Y**, Zhang Y, Li Y, Guo C, Fan Z, Yang M, Zhou X, Sun Z, Wang J. Integrative proteomics and metabolomics approach to elucidate metabolic dysfunction induced by silica nanoparticles in hepatocytes. *J Hazard Mater* 2022; **434**: 128820 [PMID: 35427968 DOI: 10.1016/j.jhazmat.2022.128820]
92 **Dumala N**, Mangalampalli B, Kalyan Kamal SS, Grover P. Biochemical alterations induced by nickel oxide nanoparticles in female Wistar albino rats after acute oral exposure. *Biomarkers* 2018; **23**: 33-43 [PMID: 28748734 DOI: 10.1080/1354750X.2017.1360943]
93 **Yu S**, Liu F, Wang C, Zhang J, Zhu A, Zou L, Han A, Li J, Chang X, Sun Y. Role of oxidative stress in liver toxicity induced by nickel oxide nanoparticles in rats. *Mol Med Rep* 2018; **17**: 3133-3139 [PMID: 29257258 DOI: 10.3892/mmr.2017.8226]
94 **Liu F**, Chang X, Tian M, Zhu A, Zou L, Han A, Su L, Li S, Sun Y. Nano NiO induced liver toxicity *via* activating the NF-κB signaling pathway in rats. *Toxicol Res (Camb)* 2017; **6**: 242-250 [PMID: 30090495 DOI: 10.1039/c6tx00444j]
95 **Ahamed M**, Ali D, Alhadlaq HA, Akhtar MJ. Nickel oxide nanoparticles exert cytotoxicity *via* oxidative stress and induce apoptotic response in human liver cells (HepG2). *Chemosphere* 2013; **93**: 2514-2522 [PMID: 24139157 DOI: 10.1016/j.chemosphere.2013.09.047]
96 **Saquib Q**, Xia P, Siddiqui MA, Zhang J, Xie Y, Faisal M, Ansari SM, Alwathnani HA, Alatar AA, Al-Khedhairy AA, Zhang X. High-throughput transcriptomics: An insight on the pathways affected in HepG2 cells exposed to nickel oxide nanoparticles. *Chemosphere* 2020; **244**: 125488 [PMID: 31812053 DOI: 10.1016/j.chemosphere.2019.125488]
97 **Zhang Q**, Chang X, Wang H, Liu Y, Wang X, Wu M, Zhan H, Li S, Sun Y. TGF-β1 mediated Smad signaling pathway and EMT in hepatic fibrosis induced by Nano NiO in vivo and in vitro. *Environ Toxicol* 2020; **35**: 419-429 [PMID: 31737983 DOI: 10.1002/tox.22878]
98 **Zhou S**, Li H, Wang H, Wang R, Song W, Li D, Wei C, Guo Y, He X, Deng Y. Nickel Nanoparticles Induced Hepatotoxicity in Mice *via* Lipid-Metabolism-Dysfunction-Regulated Inflammatory Injury. *Molecules* 2023; **28** [PMID: 37570729 DOI: 10.3390/molecules28155757]
99 **Iqbal S**, Jabeen F, Peng C, Shah MA, Ijaz MU, Rasul A, Ali S, Rauf A, Batiha GE, Kłodzińska E. Nickel nanoparticles induce hepatotoxicity *via* oxidative and nitrative stress-mediated apoptosis and inflammation. *Toxicol Ind Health* 2021; **37**: 619-634 [PMID: 34569379 DOI: 10.1177/07482337211034711]
100 **Canli EG**, Ila HB, Canli M. Response of the antioxidant enzymes of rats following oral administration of metal-oxide nanoparticles (Al(2)O(3), CuO, TiO(2)). *Environ Sci Pollut Res Int* 2019; **26**: 938-945 [PMID: 30421368 DOI: 10.1007/s11356-018-3592-8]
101 **El Bialy BE**, Hamouda RA, Abd Eldaim MA, El Ballal SS, Heikal HS, Khalifa HK, Hozzein WN. Comparative Toxicological Effects of Biologically and Chemically Synthesized Copper Oxide Nanoparticles on Mice. *Int J Nanomedicine* 2020; **15**: 3827-3842 [PMID: 32581533 DOI: 10.2147/IJN.S241922]
102 **Liu H**, Lai W, Liu X, Yang H, Fang Y, Tian L, Li K, Nie H, Zhang W, Shi Y, Bian L, Ding S, Yan J, Lin B, Xi Z. Exposure to copper oxide nanoparticles triggers oxidative stress and endoplasmic reticulum (ER)-stress induced toxicology and apoptosis in male rat liver and BRL-3A cell. *J Hazard Mater* 2021; **401**: 123349 [PMID: 32659578 DOI: 10.1016/j.jhazmat.2020.123349]
103 **Naz S**, Nasir B, Ali H, Zia M. Comparative toxicity of green and chemically synthesized CuO NPs during pregnancy and lactation in rats and offspring: Part I -hepatotoxicity. *Chemosphere* 2021; **266**: 128945 [PMID: 33213883 DOI: 10.1016/j.chemosphere.2020.128945]
104 **Ghonimi WAM**, Alferah MAZ, Dahran N, El-Shetry ES. Hepatic and renal toxicity following the injection of copper oxide nanoparticles (CuO NPs) in mature male Westar rats: histochemical and caspase 3 immunohistochemical reactivities. *Environ Sci Pollut Res Int* 2022; **29**: 81923-81937 [PMID: 35739448 DOI: 10.1007/s11356-022-21521-2]
105 **Yang X**, Shao H, Liu W, Gu W, Shu X, Mo Y, Chen X, Zhang Q, Jiang M. Endoplasmic reticulum stress and oxidative stress are involved in ZnO nanoparticle-induced hepatotoxicity. *Toxicol Lett* 2015; **234**: 40-49 [PMID: 25680694 DOI: 10.1016/j.toxlet.2015.02.004]
106 **Almansour MI**, Alferah MA, Shraideh ZA, Jarrar BM. Zinc oxide nanoparticles hepatotoxicity: Histological and histochemical study. *Environ Toxicol Pharmacol* 2017; **51**: 124-130 [PMID: 28236584 DOI: 10.1016/j.etap.2017.02.015]
107 **Al-Rasheed NM**, Al-Rasheed NM, Abdel Baky NA, Faddah LM, Fatani AJ, Hasan IH, Mohamad RA. Prophylactic role of α-lipoic acid and vitamin E against zinc oxide nanoparticles induced metabolic and immune disorders in rat's liver. *Eur Rev Med Pharmacol Sci* 2014; **18**: 1813-1828 [PMID: 24992626]
108 **Sharma V**, Anderson D, Dhawan A. Zinc oxide nanoparticles induce oxidative DNA damage and ROS-triggered mitochondria mediated apoptosis in human liver cells (HepG2). *Apoptosis* 2012; **17**: 852-870 [PMID: 22395444 DOI: 10.1007/s10495-012-0705-6]
109 **Aboulhoda BE**, Abdeltawab DA, Rashed LA, Abd Alla MF, Yassa HD. Hepatotoxic Effect of Oral Zinc Oxide Nanoparticles and the Ameliorating Role of Selenium in Rats: A histological, immunohistochemical and molecular study. *Tissue Cell* 2020; **67**: 101441 [PMID: 32949962 DOI: 10.1016/j.tice.2020.101441]
110 **Pei X**, Jiang H, Xu G, Li C, Li D, Tang S. Lethality of Zinc Oxide Nanoparticles Surpasses Conventional Zinc Oxide *via* Oxidative Stress, Mitochondrial Damage and Calcium Overload: A Comparative Hepatotoxicity Study. *Int J Mol Sci* 2022; **23** [PMID: 35743165 DOI: 10.3390/ijms23126724]
111 **Elje E**, Mariussen E, Moriones OH, Bastús NG, Puntes V, Kohl Y, Dusinska M, Rundén-Pran E. Hepato(Geno)Toxicity Assessment of Nanoparticles in a HepG2 Liver Spheroid Model. *Nanomaterials (Basel)* 2020; **10** [PMID: 32197356 DOI: 10.3390/nano10030545]
112 **Yi J**, Li Y, Mai Q, Lin Y, Weng X, Ai Z, Li M, Shang P, Iqbal M, Mehmood K, Chang YF, Tang Z, Zhang H. Hepatotoxicity and the role of the gut-liver axis in dogs after oral administration of zinc oxide nanoparticles. *Metallomics* 2022; **14** [PMID: 36057841 DOI: 10.1093/mtomcs/mfac066]
113 **Pei X**, Liu D, Li J, Li L, Ding X, Zhang W, Li Z, Xu G, Li C, Li D. TFEB coordinates autophagy and pyroptosis as hepatotoxicity responses to

ZnO nanoparticles. *Sci Total Environ* 2023; **865**: 161242 [PMID: 36587696 DOI: 10.1016/j.scitotenv.2022.161242]
114 **Pei X**, Jiang H, Li C, Li D, Tang S. Oxidative stress-related canonical pyroptosis pathway, as a target of liver toxicity triggered by zinc oxide nanoparticles. *J Hazard Mater* 2023; **442**: 130039 [PMID: 36166902 DOI: 10.1016/j.jhazmat.2022.130039]
115 **Chen J**, Zhang J, Cao J, Xia Z, Gan J. Inflammatory MAPK and NF-κB signaling pathways differentiated hepatitis potential of two agglomerated titanium dioxide particles. *J Hazard Mater* 2016; **304**: 370-378 [PMID: 26590873 DOI: 10.1016/j.jhazmat.2015.11.002]
116 **Cui Y**, Liu H, Zhou M, Duan Y, Li N, Gong X, Hu R, Hong M, Hong F. Signaling pathway of inflammatory responses in the mouse liver caused by TiO2 nanoparticles. *J Biomed Mater Res A* 2011; **96**: 221-229 [PMID: 21105171 DOI: 10.1002/jbm.a.32976]
117 **Cui Y**, Gong X, Duan Y, Li N, Hu R, Liu H, Hong M, Zhou M, Wang L, Wang H, Hong F. Hepatocyte apoptosis and its molecular mechanisms in mice caused by titanium dioxide nanoparticles. *J Hazard Mater* 2010; **183**: 874-880 [PMID: 20724067 DOI: 10.1016/j.jhazmat.2010.07.109]
118 **Moradi A**, Ziamajidi N, Ghafourikhosroshahi A, Abbasalipourkabir R. Effects of vitamin A and vitamin E on attenuation of titanium dioxide nanoparticles-induced toxicity in the liver of male Wistar rats. *Mol Biol Rep* 2019; **46**: 2919-2932 [PMID: 30887259 DOI: 10.1007/s11033-019-04752-4]
119 **Li N**, Ma L, Wang J, Zheng L, Liu J, Duan Y, Liu H, Zhao X, Wang S, Wang H, Hong F, Xie Y. Interaction Between Nano-Anatase TiO(2) and Liver DNA from Mice In Vivo. *Nanoscale Res Lett* 2009; **5**: 108-115 [PMID: 20652136 DOI: 10.1007/s11671-009-9451-2]
120 **Petković J**, Zegura B, Stevanović M, Drnovšek N, Uskoković D, Novak S, Filipič M. DNA damage and alterations in expression of DNA damage responsive genes induced by TiO2 nanoparticles in human hepatoma HepG2 cells. *Nanotoxicology* 2011; **5**: 341-353 [PMID: 21067279 DOI: 10.3109/17435390.2010.507316]
121 **Li Y**, Yan J, Ding W, Chen Y, Pack LM, Chen T. Genotoxicity and gene expression analyses of liver and lung tissues of mice treated with titanium dioxide nanoparticles. *Mutagenesis* 2017; **32**: 33-46 [PMID: 28011748 DOI: 10.1093/mutage/gew065]
122 **Natarajan V**, Wilson CL, Hayward SL, Kidambi S. Titanium Dioxide Nanoparticles Trigger Loss of Function and Perturbation of Mitochondrial Dynamics in Primary Hepatocytes. *PLoS One* 2015; **10**: e0134541 [PMID: 26247363 DOI: 10.1371/journal.pone.0134541]
123 **Sha B**, Gao W, Wang S, Gou X, Li W, Liang X, Qu Z, Xu F, Lu TJ. Oxidative stress increased hepatotoxicity induced by nano-titanium dioxide in BRL-3A cells and Sprague-Dawley rats. *J Appl Toxicol* 2014; **34**: 345-356 [PMID: 23873220 DOI: 10.1002/jat.2900]
124 **Jafari A**, Rasmi Y, Hajaghazadeh M, Karimipour M. Hepatoprotective effect of thymol against subchronic toxicity of titanium dioxide nanoparticles: Biochemical and histological evidences. *Environ Toxicol Pharmacol* 2018; **58**: 29-36 [PMID: 29289817 DOI: 10.1016/j.etap.2017.12.010]
125 **Morgan A**, Ibrahim MA, Galal MK, Ogaly HA, Abd-Elsalam RM. Innovative perception on using Tiron to modulate the hepatotoxicity induced by titanium dioxide nanoparticles in male rats. *Biomed Pharmacother* 2018; **103**: 553-561 [PMID: 29677542 DOI: 10.1016/j.biopha.2018.04.064]
126 **Chen Z**, Zhou D, Han S, Zhou S, Jia G. Hepatotoxicity and the role of the gut-liver axis in rats after oral administration of titanium dioxide nanoparticles. *Part Fibre Toxicol* 2019; **16**: 48 [PMID: 31881974 DOI: 10.1186/s12989-019-0332-2]
127 **Chen Z**, Han S, Zheng P, Zhang J, Zhou S, Jia G. Landscape of lipidomic metabolites in gut-liver axis of Sprague-Dawley rats after oral exposure to titanium dioxide nanoparticles. *Part Fibre Toxicol* 2022; **19**: 53 [PMID: 35922847 DOI: 10.1186/s12989-022-00484-9]
128 **Maadurshni GB**, Tharani GK, Udayakumar I, Nagarajan M, Manivannan J. Al(2)O(3) nanoparticles trigger the embryonic hepatotoxic response and potentiate TNF-α-induced apoptosis-modulatory effect of p38 MAPK and JNK inhibitors. *Environ Sci Pollut Res Int* 2022; **29**: 54250-54263 [PMID: 35301628 DOI: 10.1007/s11356-022-19243-6]
129 **Singh SP**, Rahman MF, Murty US, Mahboob M, Grover P. Comparative study of genotoxicity and tissue distribution of nano and micron sized iron oxide in rats after acute oral treatment. *Toxicol Appl Pharmacol* 2013; **266**: 56-66 [PMID: 23142030 DOI: 10.1016/j.taap.2012.10.016]
130 **Reddy UA**, Prabhakar PV, Mahboob M. Comparative study of nano and bulk Fe(3)O(4) induced oxidative stress in Wistar rats. *Biomarkers* 2018; **23**: 425-434 [PMID: 29458263 DOI: 10.1080/1354750X.2018.1443508]
131 **Askri D**, Ouni S, Galai S, Chovelon B, Arnaud J, Sturm N, Lehmann SG, Sakly M, Amara S, Sève M. Nanoparticles in foods? A multiscale physiopathological investigation of iron oxide nanoparticle effects on rats after an acute oral exposure: Trace element biodistribution and cognitive capacities. *Food Chem Toxicol* 2019; **127**: 173-181 [PMID: 30878530 DOI: 10.1016/j.fct.2019.03.006]
132 **Vasili A**, Sharifi G, Faramarzi M, Noori A, Yazdanshenas S. The effect of aerobic exercise on hepatotoxicity induced by intratracheal instillation of iron oxide nanoparticles in Wistar rats. *Gen Physiol Biophys* 2016; **35**: 35-43 [PMID: 26492071 DOI: 10.4149/gpb_2015031]
133 **Volkovova K**, Handy RD, Staruchova M, Tulinska J, Kebis A, Pribojova J, Ulicna O, Kucharská J, Dusinska M. Health effects of selected nanoparticles in vivo: liver function and hepatotoxicity following intravenous injection of titanium dioxide and Na-oleate-coated iron oxide nanoparticles in rodents. *Nanotoxicology* 2015; **9** Suppl 1: 95-105 [PMID: 23763576 DOI: 10.3109/17435390.2013.815285]
134 **Gokduman K**, Bestepe F, Li L, Yarmush ML, Usta OB. Dose-, treatment- and time-dependent toxicity of superparamagnetic iron oxide nanoparticles on primary rat hepatocytes. *Nanomedicine (Lond)* 2018; **13**: 1267-1284 [PMID: 29949471 DOI: 10.2217/nnm-2017-0387]
135 **Rajan B**, Sathish S, Balakumar S, Devaki T. Synthesis and dose interval dependent hepatotoxicity evaluation of intravenously administered polyethylene glycol-8000 coated ultra-small superparamagnetic iron oxide nanoparticle on Wistar rats. *Environ Toxicol Pharmacol* 2015; **39**: 727-735 [PMID: 25721486 DOI: 10.1016/j.etap.2015.01.018]
136 **He C**, Jiang S, Yao H, Zhang L, Yang C, Zhan D, Lin G, Zeng Y, Xia Y, Lin Z, Liu G, Lin Y. Endoplasmic reticulum stress mediates inflammatory response triggered by ultra-small superparamagnetic iron oxide nanoparticles in hepatocytes. *Nanotoxicology* 2018; **12**: 1198-1214 [PMID: 30422028 DOI: 10.1080/17435390.2018.1530388]
137 **Che L**, Yao H, Yang CL, Guo NJ, Huang J, Wu ZL, Zhang LY, Chen YY, Liu G, Lin ZN, Lin YC. Cyclooxygenase-2 modulates ER-mitochondria crosstalk to mediate superparamagnetic iron oxide nanoparticles induced hepatotoxicity: an in vitro and in vivo study. *Nanotoxicology* 2020; **14**: 162-180 [PMID: 31703536 DOI: 10.1080/17435390.2019.1683245]
138 **Li J**, Wang L, Li S, Liang X, Zhang Y, Wang Y, Liu Y. Sustained oral intake of nano-iron oxide perturbs the gut-liver axis. *NanoImpact* 2023; **30**: 100464 [PMID: 37068656 DOI: 10.1016/j.impact.2023.100464]
139 **Ren D**, Shao H, Liu Y, Wang X, Li Y. Hepatic effect of subacute Fe(2) O(3) nanoparticles exposure in Sprague-Dawley rats by LC-MS/MS based lipidomics. *Biomed Chromatogr* 2023; **37**: e5582 [PMID: 36634911 DOI: 10.1002/bmc.5582]
140 **Das T**, Sharma BK, Katiyar AK, Ahn J-H. Graphene-based flexible and wearable electronics. *J Semicond* 2018; **39**: 011007 [DOI: 10.1088/1674-4926/39/1/011007]
141 Lonkar S, Abdala AA. Applications of Graphene in Catalysis. *J Biofertil Biopestic* 2014; **5** [DOI: 10.4172/2157-7544.1000132]
142 **Shen H**, Zhang L, Liu M, Zhang Z. Biomedical applications of graphene. *Theranostics* 2012; **2**: 283-294 [PMID: 22448195 DOI: 10.7150/thno.3642]

143 **Mohan VB**, Lau K, Hui D, Bhattacharyya D. Graphene-based materials and their composites: A review on production, applications and product limitations. *Compos B Eng* 2018; **142**: 200-220 [DOI: 10.1016/j.compositesb.2018.01.013]

144 **Li Y**, Wang Y, Tu L, Chen D, Luo Z, Liu D, Miao Z, Feng G, Qing L, Wang S. Sub-Acute Toxicity Study of Graphene Oxide in the Sprague-Dawley Rat. *Int J Environ Res Public Health* 2016; **13** [PMID: 27869683 DOI: 10.3390/ijerph13111149]

145 **Wang K**, Ruan J, Song H, Zhang J, Wo Y, Guo S, Cui D. Biocompatibility of Graphene Oxide. *Nanoscale Res Lett* 2011; **6**: 8 [PMID: 27502632 DOI: 10.1007/s11671-010-9751-6]

146 **Patlolla AK**, Rondalph J, Tchounwou PB. Biochemical and Histopathological Evaluation of Graphene Oxide in Sprague-Dawley Rats. *Austin J Environ Toxicol* 2017; **3** [PMID: 29503980]

147 **Nirmal NK**, Awasthi KK, John PJ. Hepatotoxicity of graphene oxide in Wistar rats. *Environ Sci Pollut Res Int* 2021; **28**: 46367-46376 [PMID: 32632678 DOI: 10.1007/s11356-020-09953-0]

148 **Romaldini A**, Spanò R, Catalano F, Villa F, Poggi A, Sabella S. Sub-Lethal Concentrations of Graphene Oxide Trigger Acute-Phase Response and Impairment of Phase-I Xenobiotic Metabolism in Upcyte(®) Hepatocytes. *Front Bioeng Biotechnol* 2022; **10**: 867728 [PMID: 35662849 DOI: 10.3389/fbioe.2022.867728]

149 **Ji Z**, Zhang D, Li L, Shen X, Deng X, Dong L, Wu M, Liu Y. The hepatotoxicity of multi-walled carbon nanotubes in mice. *Nanotechnology* 2009; **20**: 445101 [PMID: 19801780 DOI: 10.1088/0957-4484/20/44/445101]

150 **Lin B**, Zhang H, Lin Z, Fang Y, Tian L, Yang H, Yan J, Liu H, Zhang W, Xi Z. Studies of single-walled carbon nanotubes-induced hepatotoxicity by NMR-based metabonomics of rat blood plasma and liver extracts. *Nanoscale Res Lett* 2013; **8**: 236 [PMID: 23680025 DOI: 10.1186/1556-276X-8-236]

151 **Adedara IA**, Anao OO, Forcados GE, Awogbindin IO, Agbowo A, Ola-Davies OE, Patlolla AK, Tchounwou PB, Farombi EO. Low doses of multi-walled carbon nanotubes elicit hepatotoxicity in rats with markers of oxidative stress and induction of pro-inflammatory cytokines. *Biochem Biophys Res Commun* 2018; **503**: 3167-3173 [PMID: 30149914 DOI: 10.1016/j.bbrc.2018.08.112]

152 **Liu E**, Wang X, Li X, Tian P, Xu H, Li Z, Wang L. Co-exposure to multi-walled carbon nanotube and lead ions aggravates hepatotoxicity of nonalcoholic fatty liver *via* inhibiting AMPK/PPARγ pathway. *Aging (Albany NY)* 2020; **12**: 14189-14204 [PMID: 32680977 DOI: 10.18632/aging.103430]

153 **Patlolla A**, McGinnis B, Tchounwou P. Biochemical and histopathological evaluation of functionalized single-walled carbon nanotubes in Swiss-Webster mice. *J Appl Toxicol* 2011; **31**: 75-83 [PMID: 20737426 DOI: 10.1002/jat.1579]

154 **Patlolla AK**, Berry A, Tchounwou PB. Study of hepatotoxicity and oxidative stress in male Swiss-Webster mice exposed to functionalized multi-walled carbon nanotubes. *Mol Cell Biochem* 2011; **358**: 189-199 [PMID: 21725842 DOI: 10.1007/s11010-011-0934-y]

155 **Zhang D**, Deng X, Ji Z, Shen X, Dong L, Wu M, Gu T, Liu Y. Long-term hepatotoxicity of polyethylene-glycol functionalized multi-walled carbon nanotubes in mice. *Nanotechnology* 2010; **21**: 175101 [PMID: 20357413 DOI: 10.1088/0957-4484/21/17/175101]

156 **Awasthi KK**, John PJ, Awasthi A, Awasthi K. Multi walled carbon nano tubes induced hepatotoxicity in Swiss albino mice. *Micron* 2013; **44**: 359-364 [PMID: 23000350 DOI: 10.1016/j.micron.2012.08.008]

157 **Wei Q**, Juanjuan B, Longlong T, Zhan L, Peng L, Wangsuo W. The effect of multiwalled carbon nanotubes on hepatotoxicity of Cd2+ in accumulated cadmium-metallothione in mice. *Biomed Res Int* 2014; **2014**: 463161 [PMID: 25276789 DOI: 10.1155/2014/463161]

158 **Wang HJ**, Yang GG, Wu SS, Meng ZF, Zhang JM, Cao Y, Zhang YP. Toxicity of CuS/CdS semiconductor nanocomposites to liver cells and mice liver. *Sci Total Environ* 2021; **784**: 147221 [PMID: 34088078 DOI: 10.1016/j.scitotenv.2021.147221]

159 **Rana K**, Verma Y, Rana SVS. Possible Mechanisms of Liver Injury Induced by Cadmium Sulfide Nanoparticles in Rat. *Biol Trace Elem Res* 2021; **199**: 216-226 [PMID: 32342341 DOI: 10.1007/s12011-020-02128-5]

160 **Jiang T**, Guo H, Xia YN, Liu Y, Chen D, Pang G, Feng Y, Yu H, Wu Y, Zhang S, Wang Y, Wen H, Zhang LW. Hepatotoxicity of copper sulfide nanoparticles towards hepatocyte spheroids using a novel multi-concave agarose chip method. *Nanomedicine (Lond)* 2021; **16**: 1487-1504 [PMID: 34184559 DOI: 10.2217/nnm-2021-0011]

161 **Xia YN**, Zu H, Guo H, Jiang T, Yang S, Yu H, Zhang S, Ding H, Li X, Wang Y, Zhang LW. Preclinical safety and hepatotoxicity evaluation of biomineralized copper sulfide nanoagents. *J Nanobiotechnology* 2022; **20**: 185 [PMID: 35414075 DOI: 10.1186/s12951-022-01399-5]

162 **Feng S**, Zhang Z, Mo Y, Tong R, Zhong Z, Chen Z, He D, Wan R, Gao M, Zhang Q, Huang Y. Activation of NLRP3 inflammasome in hepatocytes after exposure to cobalt nanoparticles: The role of oxidative stress. *Toxicol In Vitro* 2020; **69**: 104967 [PMID: 32805375 DOI: 10.1016/j.tiv.2020.104967]

163 **Isoda K**, Nagata R, Hasegawa T, Taira Y, Taira I, Shimizu Y, Isama K, Nishimura T, Ishida I. Hepatotoxicity and Drug/Chemical Interaction Toxicity of Nanoclay Particles in Mice. *Nanoscale Res Lett* 2017; **12**: 199 [PMID: 28314361 DOI: 10.1186/s11671-017-1956-5]

164 **Yuan Y**, Liu C, Qian J, Wang J, Zhang Y. Size-mediated cytotoxicity and apoptosis of hydroxyapatite nanoparticles in human hepatoma HepG2 cells. *Biomaterials* 2010; **31**: 730-740 [PMID: 19836072 DOI: 10.1016/j.biomaterials.2009.09.088]

165 **Chen Q**, Xue Y, Sun J. Hepatotoxicity and liver injury induced by hydroxyapatite nanoparticles. *J Appl Toxicol* 2014; **34**: 1256-1264 [PMID: 25225040 DOI: 10.1002/jat.3073]

166 **Liu W**, Zhang S, Wang L, Qu C, Zhang C, Hong L, Yuan L, Huang Z, Wang Z, Liu S, Jiang G. CdSe quantum dot (QD)-induced morphological and functional impairments to liver in mice. *PLoS One* 2011; **6**: e24406 [PMID: 21980346 DOI: 10.1371/journal.pone.0024406]

167 **Lin CH**, Yang MH, Chang LW, Yang CS, Chang H, Chang WH, Tsai MH, Wang CJ, Lin P. Cd/Se/Te-based quantum dot 705 modulated redox homeostasis with hepatotoxicity in mice. *Nanotoxicology* 2011; **5**: 650-663 [PMID: 21142715 DOI: 10.3109/17435390.2010.539712]

168 **Lu Y**, Xu S, Chen H, He M, Deng Y, Cao Z, Pi H, Chen C, Li M, Ma Q, Gao P, Ji Y, Zhang L, Yu Z, Zhou Z. CdSe/ZnS quantum dots induce hepatocyte pyroptosis and liver inflammation *via* NLRP3 inflammasome activation. *Biomaterials* 2016; **90**: 27-39 [PMID: 26986854 DOI: 10.1016/j.biomaterials.2016.03.003]

169 **Yang Y**, Lv SY, Yu B, Xu S, Shen J, Zhao T, Zhang H. Hepatotoxicity assessment of Mn-doped ZnS quantum dots after repeated administration in mice. *Int J Nanomedicine* 2015; **10**: 5787-5796 [PMID: 26396512 DOI: 10.2147/IJN.S88789]

170 **Zhang T**, Hu Y, Tang M, Kong L, Ying J, Wu T, Xue Y, Pu Y. Liver Toxicity of Cadmium Telluride Quantum Dots (CdTe QDs) Due to Oxidative Stress in Vitro and in Vivo. *Int J Mol Sci* 2015; **16**: 23279-23299 [PMID: 26404244 DOI: 10.3390/ijms161023279]

171 **Nguyen KC**, Rippstein P, Tayabali AF, Willmore WG. Mitochondrial Toxicity of Cadmium Telluride Quantum Dot Nanoparticles in Mammalian Hepatocytes. *Toxicol Sci* 2015; **146**: 31-42 [PMID: 25809595 DOI: 10.1093/toxsci/kfv068]

172 **Nguyen KC**, Tayabali AF, Willmore WG. Hepatotoxicity of Cadmium Telluride Quantum Dot Nanoparticles: Mitochondrial Generated Reactive Oxygen Species as a Mechanism. *Free Radic Biol Med* 2016; **100**: S43 [DOI: 10.1016/j.freeradbiomed.2016.10.112]

173 **Nguyen KC**, Zhang Y, Todd J, Kittle K, Patry D, Caldwell D, Lalande M, Smith S, Parks D, Navarro M, Massarsky A, Moon TW, Willmore

WG, Tayabali AF. Biodistribution and Systemic Effects in Mice Following Intravenous Administration of Cadmium Telluride Quantum Dot Nanoparticles. *Chem Res Toxicol* 2019; **32**: 1491-1503 [PMID: 31251591 DOI: 10.1021/acs.chemrestox.8b00397]

174 **Pang Y**, Wu D, Ma Y, Cao Y, Liu Q, Tang M, Pu Y, Zhang T. Reactive oxygen species trigger NF-κB-mediated NLRP3 inflammasome activation involvement in low-dose CdTe QDs exposure-induced hepatotoxicity. *Redox Biol* 2021; **47**: 102157 [PMID: 34614473 DOI: 10.1016/j.redox.2021.102157]

175 **Pang Y**, Yao Y, Yang M, Wu D, Ma Y, Zhang Y, Zhang T. TFEB-lysosome pathway activation is associated with different cell death responses to carbon quantum dots in Kupffer cells and hepatocytes. *Part Fibre Toxicol* 2022; **19**: 31 [PMID: 35477523 DOI: 10.1186/s12989-022-00474-x]

176 **Yang L**, Kuang H, Zhang W, Aguilar ZP, Wei H, Xu H. Comparisons of the biodistribution and toxicological examinations after repeated intravenous administration of silver and gold nanoparticles in mice. *Sci Rep* 2017; **7**: 3303 [PMID: 28607366 DOI: 10.1038/s41598-017-03015-1]

177 **Jia YP**, Ma BY, Wei XW, Qian ZY. The in vitro and in vivo toxicity of gold nanoparticles. Chinese Chemical Letters 2017; 28: 691-702 [DOI: 10.1016/J.CCLET.2017.01.021]

178 **Giljohann DA**, Seferos DS, Daniel WL, Massich MD, Patel PC, Mirkin CA. Gold nanoparticles for biology and medicine. *Angew Chem Int Ed Engl* 2010; **49**: 3280-3294 [PMID: 20401880 DOI: 10.1002/anie.200904359]

179 **Abdelhalim MA**, Jarrar BM. Histological alterations in the liver of rats induced by different gold nanoparticle sizes, doses and exposure duration. *J Nanobiotechnology* 2012; **10**: 5 [PMID: 22276919 DOI: 10.1186/1477-3155-10-5]

180 **Bartneck M**, Ritz T, Keul HA, Wambach M, Bornemann J, Gbureck U, Ehling J, Lammers T, Heymann F, Gassler N, Lüdde T, Trautwein C, Groll J, Tacke F. Peptide-functionalized gold nanorods increase liver injury in hepatitis. *ACS Nano* 2012; **6**: 8767-8777 [PMID: 22994679 DOI: 10.1021/nn302502u]

181 **Waris A**, Sharif S, Naz S, Manzoor F, Jamil F, Hussain M, Choi YJ, Park YK. Hepatotoxicity induced by metallic nanoparticles at the cellular level: A review. *EER* 2023; **28**: 220625 [DOI: 10.4491/eer.2022.625]

182 **Hwang JH**, Kim SJ, Kim YH, Noh JR, Gang GT, Chung BH, Song NW, Lee CH. Susceptibility to gold nanoparticle-induced hepatotoxicity is enhanced in a mouse model of nonalcoholic steatohepatitis. *Toxicology* 2012; **294**: 27-35 [PMID: 22330258 DOI: 10.1016/j.tox.2012.01.013]

183 **Wahab R**, Dwivedi S, Khan F, Mishra YK, Hwang IH, Shin HS, Musarrat J, Al-Khedhairy AA. Statistical analysis of gold nanoparticle-induced oxidative stress and apoptosis in myoblast (C2C12) cells. *Colloids Surf B Biointerfaces* 2014; **123**: 664-672 [PMID: 25456994 DOI: 10.1016/j.colsurfb.2014.10.012]

184 **Chen YS**, Hung YC, Hong MY, Onischuk AA, Chiou JC, Sorokina I V. , Tolstikova T, Steve Huang G. Control of in vivo transport and toxicity of nanoparticles by tea melanin. *J Nanomater* 2012; 2012 [DOI: 10.1155/2012/746960]

185 **Li Y**, Guo M, Lin Z, Zhao M, Xiao M, Wang C, Xu T, Chen T, Zhu B. Polyethylenimine-functionalized silver nanoparticle-based co-delivery of paclitaxel to induce HepG2 cell apoptosis. *Int J Nanomedicine* 2016; **11**: 6693-6702 [PMID: 27994465 DOI: 10.2147/IJN.S122666]

186 **Xiong D**, Fang T, Yu L, Sima X, Zhu W. Effects of nano-scale TiO2, ZnO and their bulk counterparts on zebrafish: acute toxicity, oxidative stress and oxidative damage. *Sci Total Environ* 2011; **409**: 1444-1452 [PMID: 21296382 DOI: 10.1016/j.scitotenv.2011.01.015]

187 **Khan HA**, Abdelhalim MA, Al-Ayed MS, Alhomida AS. Effect of gold nanoparticles on glutathione and malondialdehyde levels in liver, lung and heart of rats. *Saudi J Biol Sci* 2012; **19**: 461-464 [PMID: 23961207 DOI: 10.1016/j.sjbs.2012.06.005]

188 **Zhang XD**, Wu D, Shen X, Liu PX, Yang N, Zhao B, Zhang H, Sun YM, Zhang LA, Fan FY. Size-dependent in vivo toxicity of PEG-coated gold nanoparticles. *Int J Nanomedicine* 2011; **6**: 2071-2081 [PMID: 21976982 DOI: 10.2147/IJN.S21657]

189 **Huo S**, Jin S, Ma X, Xue X, Yang K, Kumar A, Wang PC, Zhang J, Hu Z, Liang XJ. Ultrasmall gold nanoparticles as carriers for nucleus-based gene therapy due to size-dependent nuclear entry. *ACS Nano* 2014; **8**: 5852-5862 [PMID: 24824865 DOI: 10.1021/nn5008572]

190 **Shukla R**, Bansal V, Chaudhary M, Basu A, Bhonde RR, Sastry M. Biocompatibility of gold nanoparticles and their endocytotic fate inside the cellular compartment: a microscopic overview. *Langmuir* 2005; **21**: 10644-10654 [PMID: 16262332 DOI: 10.1021/la0513712]

191 **Li H**, Wen T, Wang T, Ji Y, Shen Y, Chen J, Xu H, Wu X. In Vivo Metabolic Response upon Exposure to Gold Nanorod Core/Silver Shell Nanostructures: Modulation of Inflammation and Upregulation of Dopamine. *Int J Mol Sci* 2020; **21** [PMID: 31936206 DOI: 10.3390/ijms21020384]

192 **Lee E**, Jeon H, Lee M, Ryu J, Kang C, Kim S, Jung J, Kwon Y. Molecular origin of AuNPs-induced cytotoxicity and mechanistic study. *Sci Rep* 2019; **9**: 2494 [PMID: 30792478 DOI: 10.1038/s41598-019-39579-3]

193 **Harris ES**, Li F, Higgs HN. The mouse formin, FRLalpha, slows actin filament barbed end elongation, competes with capping protein, accelerates polymerization from monomers, and severs filaments. *J Biol Chem* 2004; **279**: 20076-20087 [PMID: 14990563 DOI: 10.1074/jbc.M312718200]

194 **Fraga S**, Brandão A, Soares ME, Morais T, Duarte JA, Pereira L, Soares L, Neves C, Pereira E, Bastos Mde L, Carmo H. Short- and long-term distribution and toxicity of gold nanoparticles in the rat after a single-dose intravenous administration. *Nanomedicine* 2014; **10**: 1757-1766 [PMID: 24941462 DOI: 10.1016/j.nano.2014.06.005]

195 **Pan Y**, Leifert A, Ruau D, Neuss S, Bornemann J, Schmid G, Brandau W, Simon U, Jahnen-Dechent W. Gold nanoparticles of diameter 1.4 nm trigger necrosis by oxidative stress and mitochondrial damage. *Small* 2009; **5**: 2067-2076 [PMID: 19642089 DOI: 10.1002/smll.200900466]

196 **Rosa S**, Connolly C, Schettino G, Butterworth KT, Prise KM. Biological mechanisms of gold nanoparticle radiosensitization. *Cancer Nanotechnol* 2017; **8**: 2 [PMID: 28217176 DOI: 10.1186/s12645-017-0026-0]

197 **Arnér ES**, Holmgren A. Physiological functions of thioredoxin and thioredoxin reductase. *Eur J Biochem* 2000; **267**: 6102-6109 [PMID: 11012661 DOI: 10.1046/j.1432-1327.2000.01701.x]

198 **Albrahim T**, Alonazi MA. Role of Beetroot (Beta vulgaris) Juice on Chronic Nanotoxicity of Silver Nanoparticle-Induced Hepatotoxicity in Male Rats. *Int J Nanomedicine* 2020; **15**: 3471-3482 [PMID: 32547008 DOI: 10.2147/IJN.S248078]

199 **Wang Z**, Xia T, Liu S. Mechanisms of nanosilver-induced toxicological effects: more attention should be paid to its sublethal effects. *Nanoscale* 2015; **7**: 7470-7481 [PMID: 25865054 DOI: 10.1039/c5nr01133g]

200 **Dong B**, Du S, Wang C, Fu H, Li Q, Xiao N, Yang J, Xue X, Cai W, Liu D. Reversible Self-Assembly of Nanoprobes in Live Cells for Dynamic Intracellular pH Imaging. *ACS Nano* 2019; **13**: 1421-1432 [PMID: 30730703 DOI: 10.1021/acsnano.8b07054]

201 **Xu M**, Yang Q, Xu L, Rao Z, Cao D, Gao M, Liu S. Protein target identification and toxicological mechanism investigation of silver nanoparticles-induced hepatotoxicity by integrating proteomic and metallomic strategies. *Part Fibre Toxicol* 2019; **16**: 46 [PMID: 31775802 DOI: 10.1186/s12989-019-0322-4]

202 **Almofti MR**, Ichikawa T, Yamashita K, Terada H, Shinohara Y. Silver ion induces a cyclosporine a-insensitive permeability transition in rat

liver mitochondria and release of apoptogenic cytochrome C. *J Biochem* 2003; **134**: 43-49 [PMID: 12944369 DOI: 10.1093/jb/mvg111]

203 **Costa CS**, Ronconi JV, Daufenbach JF, Gonçalves CL, Rezin GT, Streck EL, Paula MM. In vitro effects of silver nanoparticles on the mitochondrial respiratory chain. *Mol Cell Biochem* 2010; **342**: 51-56 [PMID: 20411305 DOI: 10.1007/s11010-010-0467-9]

204 **Assar DH**, Mokhbatly AA, Ghazy EW, Elbialy ZI, Gaber AA, Hassan AA, Nabil A, Asa SA. Silver nanoparticles induced hepatoxicity *via* the apoptotic/antiapoptotic pathway with activation of TGFβ-1 and α-SMA triggered liver fibrosis in Sprague Dawley rats. *Environ Sci Pollut Res Int* 2022; **29**: 80448-80465 [PMID: 35716303 DOI: 10.1007/s11356-022-21388-3]

205 **Matés JM**. Effects of antioxidant enzymes in the molecular control of reactive oxygen species toxicology. *Toxicology* 2000; **153**: 83-104 [PMID: 11090949 DOI: 10.1016/S0300-483X(00)00306-1]

206 **Srivastava M**, Singh S, Self WT. Exposure to silver nanoparticles inhibits selenoprotein synthesis and the activity of thioredoxin reductase. *Environ Health Perspect* 2012; **120**: 56-61 [PMID: 21965219 DOI: 10.1289/ehp.1103928]

207 **Ansar S**, Alshehri SM, Abudawood M, Hamed SS, Ahamad T. Antioxidant and hepatoprotective role of selenium against silver nanoparticles. *Int J Nanomedicine* 2017; **12**: 7789-7797 [PMID: 29123393 DOI: 10.2147/IJN.S136748]

208 **Piao MJ**, Kang KA, Lee IK, Kim HS, Kim S, Choi JY, Choi J, Hyun JW. Silver nanoparticles induce oxidative cell damage in human liver cells through inhibition of reduced glutathione and induction of mitochondria-involved apoptosis. *Toxicol Lett* 2011; **201**: 92-100 [PMID: 21182908 DOI: 10.1016/j.toxlet.2010.12.010]

209 **Adeyemi OS**, Adewumi I. Biochemical Evaluation of Silver Nanoparticles in Wistar Rats. *Int Sch Res Notices* 2014; **2014**: 196091 [PMID: 27350993 DOI: 10.1155/2014/196091]

210 **Sooklert K**, Wongjarupong A, Cherdchom S, Wongjarupong N, Jindatip D, Phungnoi Y, Rojanathanes R, Sereemaspun A. Molecular and Morphological Evidence of Hepatotoxicity after Silver Nanoparticle Exposure: A Systematic Review, In Silico, and Ultrastructure Investigation. *Toxicol Res* 2019; **35**: 257-270 [PMID: 31341555 DOI: 10.5487/TR.2019.35.3.257]

211 **Luedde T**, Duderstadt M, Streetz KL, Tacke F, Kubicka S, Manns MP, Trautwein C. C/EBP beta isoforms LIP and LAP modulate progression of the cell cycle in the regenerating mouse liver. *Hepatology* 2004; **40**: 356-365 [PMID: 15368440 DOI: 10.1002/hep.20333]

212 **Jiao ZH**, Li M, Feng YX, Shi JC, Zhang J, Shao B. Hormesis effects of silver nanoparticles at non-cytotoxic doses to human hepatoma cells. *PLoS One* 2014; **9**: e102564 [PMID: 25033410 DOI: 10.1371/journal.pone.0102564]

213 **Xin L**, Wang J, Wu Y, Guo S, Tong J. Increased oxidative stress and activated heat shock proteins in human cell lines by silver nanoparticles. *Hum Exp Toxicol* 2015; **34**: 315-323 [PMID: 24980441 DOI: 10.1177/0960327114538988]

214 **Fuchs Y**, Steller H. Live to die another way: modes of programmed cell death and the signals emanating from dying cells. *Nat Rev Mol Cell Biol* 2015; **16**: 329-344 [PMID: 25991373 DOI: 10.1038/nrm3999]

215 **Wen L**, Li M, Lin X, Li Y, Song H, Chen H. AgNPs Aggravated Hepatic Steatosis, Inflammation, Oxidative Stress, and Epigenetic Changes in Mice With NAFLD Induced by HFD. *Front Bioeng Biotechnol* 2022; **10**: 912178 [PMID: 35677306 DOI: 10.3389/fbioe.2022.912178]

216 **Recordati C**, De Maglie M, Bianchessi S, Argentiere S, Cella C, Mattiello S, Cubadda F, Aureli F, D'Amato M, Raggi A, Lenardi C, Milani P, Scanziani E. Tissue distribution and acute toxicity of silver after single intravenous administration in mice: nano-specific and size-dependent effects. *Part Fibre Toxicol* 2016; **13**: 12 [PMID: 26926244 DOI: 10.1186/s12989-016-0124-x]

217 **Kim YJ**, Rahman MM, Lee SM, Kim JM, Park K, Kang JH, Seo YR. Assessment of in vivo genotoxicity of citrated-coated silver nanoparticles *via* transcriptomic analysis of rabbit liver tissue. *Int J Nanomedicine* 2019; **14**: 393-405 [PMID: 30662263 DOI: 10.2147/IJN.S174515]

218 **Lee TY**, Liu MS, Huang LJ, Lue SI, Lin LC, Kwan AL, Yang RC. Bioenergetic failure correlates with autophagy and apoptosis in rat liver following silver nanoparticle intraperitoneal administration. *Part Fibre Toxicol* 2013; **10**: 40 [PMID: 23958063 DOI: 10.1186/1743-8977-10-40]

219 **Zhang J**, Liu S, Han J, Wang Z, Zhang S. On the developmental toxicity of silver nanoparticles. *Mater Des* 2021; **203**: 109611 [DOI: 10.1016/j.matdes.2021.109611]

220 **Tong Z**, Gao Y, Yang H, Wang W, Mao Z. Nanomaterials for cascade promoted catalytic cancer therapy. *View* 2021; **2**: 20200133 [DOI: 10.1002/VIW.20200133]

221 **Zeng C**, Hou X, Bohmer M, Dong Y. Advances of nanomaterials-based strategies for fighting against COVID-19. *View (Beijing)* 2021; **2**: 20200180 [PMID: 34766161 DOI: 10.1002/VIW.20200180]

222 **Xu M**, Song Y, Wang J, Li N. Anisotropic transition metal-based nanomaterials for biomedical applications. *View* 2021; **2**: 20200154 [DOI: 10.1002/VIW.20200154]

223 **Zheng D**, Yang K, Nie Z. Engineering heterogeneity of precision nanoparticles for biomedical delivery and therapy. *View* 2021; **2**: 20200067 [DOI: 10.1002/VIW.20200067]

Published by **Baishideng Publishing Group Inc**
7041 Koll Center Parkway, Suite 160, Pleasanton, CA 94566, USA
Telephone: +1-925-3991568
E-mail: office@baishideng.com
Help Desk: https://www.f6publishing.com/helpdesk
https://www.wjgnet.com

© 2024 Baishideng Publishing Group Inc. All rights reserved.